



<https://theses.gla.ac.uk/>

Theses Digitisation:

<https://www.gla.ac.uk/myglasgow/research/enlighten/theses/digitisation/>

This is a digitised version of the original print thesis.

Copyright and moral rights for this work are retained by the author

A copy can be downloaded for personal non-commercial research or study,
without prior permission or charge

This work cannot be reproduced or quoted extensively from without first
obtaining permission in writing from the author

The content must not be changed in any way or sold commercially in any
format or medium without the formal permission of the author

When referring to this work, full bibliographic details including the author,
title, awarding institution and date of the thesis must be given

Enlighten: Theses

<https://theses.gla.ac.uk/>
research-enlighten@glasgow.ac.uk

T H E S I S

submitted to

THE UNIVERSITY OF GLASGOW

in fulfilment of the
requirements for the

DEGREE OF DOCTOR OF PHILOSOPHY

by

Eric S. Beaton

Chemistry Department,
The Royal College of Science and Technology,
Glasgow.

MAY, 1960.

ProQuest Number: 10656306

All rights reserved

INFORMATION TO ALL USERS

The quality of this reproduction is dependent upon the quality of the copy submitted.

In the unlikely event that the author did not send a complete manuscript and there are missing pages, these will be noted. Also, if material had to be removed, a note will indicate the deletion.



ProQuest 10656306

Published by ProQuest LLC (2017). Copyright of the Dissertation is held by the Author.

All rights reserved.

This work is protected against unauthorized copying under Title 17, United States Code
Microform Edition © ProQuest LLC.

ProQuest LLC.
789 East Eisenhower Parkway
P.O. Box 1346
Ann Arbor, MI 48106 – 1346

74
GENERAL TITLE
=====

Studies of the decomposition of peroxy compounds.

A C K N O W L E D G M E N T S

The author wishes to express his appreciation to Professor F. S. Spring, F.R.S., and Professor P. L. Pauson for the privilege of working in their Department and also to Dr. A. B. Hart for his many helpful, stimulating and constructive suggestions.

Thanks are also extended to the Ministry of Supply and to Laporte Chemicals Ltd., for the provision of a Research Grant, receipt of which is gratefully acknowledged.

I N D E X

Index	(1)
Summary	(vi)
Form of Thesis	(xi)

PART I.

INTRODUCTION

General	1
Homogeneous Catalysis of H_2O_2	3
Heterogeneous Catalysis of H_2O_2	9
Electrochemical Studies	16
Plan of Present Investigation	23

EXPERIMENTAL

Introduction	29
Materials	29
Catalysts	30
Pretreatment of Catalysts	31
Equilibrium Potential Measurements	33
Apparatus	33
pH of H_2O_2 Solutions	34
Experimental Technique	35
Rate Studies	36

Current Flow Measurements	40
Apparatus	40
Procedure	40
Experiment to Illustrate the Existence of Small Permanent Currents on Electrode Surface	42
Apparatus and Procedure	43

RESULTS

Equilibrium Potentials	45
Silver Electrode Potentials	45
Reproducibility etc.	45
Variation with pH and $[H_2O_2]$	46
Variation with $[Ag^+]$	47
Effect of Temperature	48
Platinum Electrode Potentials	48
Other Metal Electrode Potentials	49
Rate of Oxygen evolution at a Silver Electrode	50
Reproducibility etc.	50
Dependence on $[H_2O_2]$	52
Variation with pH	53
Effect of Temperature	53
Effect of $[Ag^+]$	53
Current Flow	54
General	54
Reproducibility	55

Effect of $[H_2O_2]$ and pH	56
Determination of Exchange Currents	57
Variation of Exchange Current with pH and $[H_2O_2]$	58
Effect of Small Cathodic Currents on Rate of Decomposition	59
Effect of Added $[Ag^+]$	59
Existence of Anodic and Cathodic Areas.....	61

DISCUSSION

The Equilibrium Potentials	62
Rate of Catalysis at Silver Electrode	72
The Effect of Small Currents	74

PART II

Introduction	1
Experimental	3
Materials	3
Analysis of $NaBO_3 \cdot 4H_2O$	4
Estimation of Iron	7
Estimation of Copper	8
Decomposition Studies	9
Solid $NaBO_3 \cdot 4H_2O$	9
Fused $NaBO_3 \cdot 4H_2O$	16
Dilute Solutions of $NaBO_3 \cdot 4H_2O$	17

RESULTS

Decomposition of Solid $\text{NaBO}_3 \cdot 4\text{H}_2\text{O}$	20
At Atmospheric Pressure.	20
Under Vacuum	21
Sealed and Open Tests	22
Tensimetric Studies	22
Softening of Perborate	25
Single Crystal Observations	27
Decomposition in the Melt	28
Kinetics	28
Effect of Surface or Light	29
Effect of Iron and Copper Catalysts	29
Addition of Magnesium	31
Effect of H_3BO_3	32
Decomposition of Dilute Solutions	34
Effect of Added Copper	35
Effect of Added Iron	36
Stabilisation of Dilute Solutions	37
pH of Perborate Metaborate Solutions	38

DISCUSSION

Nature of $\text{NaBO}_3 \cdot 4\text{H}_2\text{O}$	40
Loss of Oxygen from Solid $\text{NaBO}_3 \cdot 4\text{H}_2\text{O}$	43
Fusion of the Tetrahydrate	46
Decomposition of Fused Tetrahydrate	48

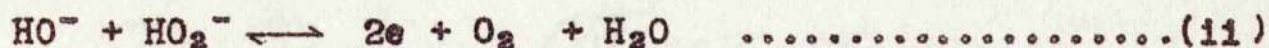
Catalysis in the Fused State49
Stabilisation in the Fused State50
Decomposition in Dilute Solutions52
Mechanism of Decomposition53
General Conclusions58

SUMMARY

In Part I a detailed study is described of the electrode kinetics of a silver electrode in the presence of H_2O_2 solutions from 0.0003 to 33M and in the pH range 1-13. Special attention is paid to the equilibrium potentials and to their dependence on pH and $[H_2O_2]$. At high pH the results of Berl⁵³ for carbon electrodes are found to apply and the electrode potential is both pH and $[H_2O_2]$ dependent and is given by the equation:

$$E = 0.91 - 0.059 \text{ pH} - 0.03 \log_{10} [H_2O_2] \quad \dots\dots\dots(1)$$

which, following Berl, is consistent with the following reversible electrode reaction



There is always catalysis even in the absence of current flow and this can be explained by breaking down equation (i) into 1-electron steps with HO_2 radicals as intermediates:



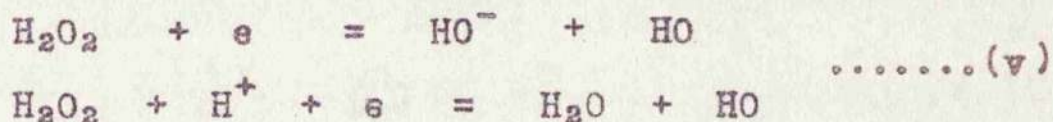
Reaction between HO_2 and H_2O_2 could produce decomposition cycles. At low pH (<6) the e.m.f. becomes independent of $[H_2O_2]$ and is then given by

$$E = 0.85 - 0.059 \text{ pH} \quad \dots\dots\dots(iv)$$

which is the result found by Bockris and Oldfield⁵⁴ for platinum and gold.

Other metals, viz., Cu, Ni, Mn and Fe give identical potentials and it is concluded that the metal plays no direct part in maintaining the steady potential.

A possible scheme is based on one put forward on a wide range of electrode kinetic evidence for platinum by Gerischer and Gerischer.⁵⁵ In the silver case it becomes



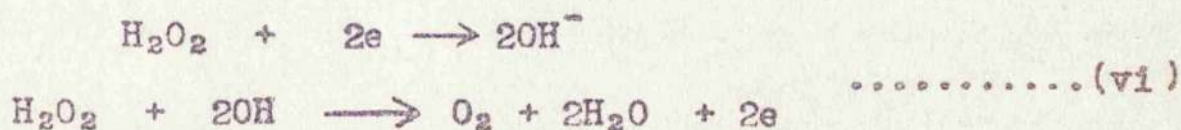
the HO radicals reacting further



or as centres for catalysis.

It is found that, at $[\text{H}_2\text{O}_2]$'s above 1 to 2 M and in the pH range 3-9, an $[\text{H}_2\text{O}_2]$ dependence occurs. This is explained in terms of a separation of anodic and cathodic areas. The anodic areas, once formed, are perpetuated by the fact that a p-n junction would be created at the metal metal oxide boundary and would permit current flow in one direction only. A proposal is made which on this basis links the potential in this zone to $[\text{H}_2\text{O}_2]$.

Experiments with flowing currents introduce the requirement that the anodic and cathodic reactions are 2-electron step processes involving 2 transition complexes per H_2O_2 molecule. Such a process would be written



and the transition complex would indicate that the rate determining step must involve an adsorbed OH radical or ion. Finally we show how these facts can be fitted in a general way to the Hoar⁷¹ scheme for the oxygen electrode. The scheme fits in also with a second order $[H_2O_2]$ dependence found for the rate of decomposition.

Part II describes a detailed account of the kinetics of the loss of oxygen from $NaBO_3 \cdot 4H_2O$ in the solid state, fused state and in dilution solutions, with and without added iron and copper catalysts, and also of the subsequent inhibition by magnesium and zinc compounds.

For the study of the first one per cent of loss of oxygen from the solid perborate a differential tensimetric technique was adopted.

Results obtained from decomposition of the solid perborate showed that a least partial liquefaction must occur before decomposition commences - heating the perborate at $60^\circ C$ in vacuo showed no loss of oxygen at all.

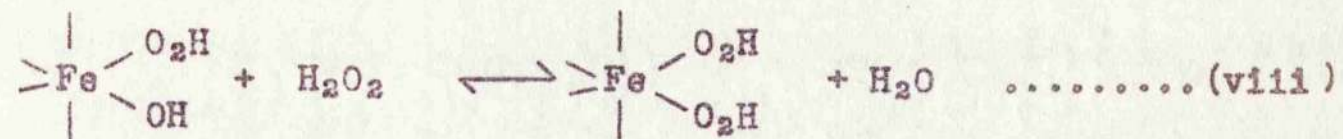
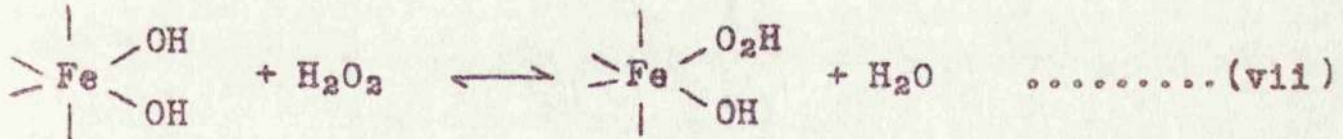
The results obtained from studies of the decomposition in the fused state indicated that the decomposition was entirely due to catalysis and that there was no inherent decomposition in pure perborate. This was confirmed from experiments on a few very pure perborate crystals.

Stabilisation of the fused material by the addition of

magnesium sulphate yielded a relationship with the $[BO_2']$ present, viz., at the onset of inhibition, the product $[Mg^{++}][BO_2'] = \text{constant}$.

Studies in dilute solutions showed clearly that the overall kinetics for the decomposition were identical with those for the fused state, and from the results it was concluded that the decomposition was indeed catalytic and due to iron.

The suggested mechanism which complied with the kinetics of the system studied is as follows.



i.e. a fixed concentration of catalyst forming addition compounds with H_2O_2 , the only essential being that it should be possible to exchange two-OH groups, attached to the iron, and therefore within range of electron transfer — with H_2O_2

From (vii) and (viii) we obtain $r = \frac{kK_2K_2c^2}{1 + K_1c + K_1K_2c^2}$

which gives in the limit $1 \gg (K_1c + K_1K_2c^2)$ second order kinetics and at higher $[H_2O_2]$ where $K_1K_2c^2 \gg (1 + K_1c)$ zero order kinetics apply. These equations agree exactly with the observed experimental results.

Stabilisation is explained in terms of the formation of an insoluble salt $(Mg)(BO_2)(BO_3)$ which both prevents formation of the liquid phase and, at the same time, inhibits the catalysts.

Consideration is also given as to the nature and structure of the metaborate and perborate ions.

FORM OF THESIS

The thesis deals with the catalytic decomposition of two peroxy compounds, viz., H_2O_2 and $\text{NaBO}_3 \cdot 4\text{H}_2\text{O}$.

Part I concerns a detailed electrochemical and rate study of the heterogeneous catalytic system $\text{Ag}/\text{H}_2\text{O}_2$ together with a less full account of results obtained from an electrochemical study of the $\text{Pt}/\text{H}_2\text{O}_2$ system. The purpose of including the latter system was to test the general applicability of the conclusions drawn on the $\text{Ag}/\text{H}_2\text{O}_2$ system and because of the conflicting results previously obtained from electrochemical studies of the $\text{Pt}/\text{H}_2\text{O}_2$ system.

Part II of the thesis concerns a detailed examination of the kinetics of the decomposition of $\text{NaBO}_3 \cdot 4\text{H}_2\text{O}$ with and without, added iron and copper catalysts, and of the subsequent stabilisation by the addition of zinc and magnesium compounds.

In the general introduction with historical background associated with homogeneous and heterogeneous catalysis of H_2O_2 is reviewed and attention directed to the rather sparse treatment, from an electrochemical viewpoint, of the heterogeneous catalysis of aqueous H_2O_2 by metals.

The experimental sections describe the apparatus, techniques and materials used for the investigations of the above mentioned systems. These sections are followed by their respective results sections and discussions.

PART I

An electrochemical study of the silver catalysed
decomposition of hydrogen peroxide.

INTRODUCTION

General.

The study of H_2O_2 has been of great interest to chemists since its discovery by Louis Jaques Thénard¹ until the present day. The ubiquity of its occurrence in the atmosphere, in animals and plants, in corrosion of metals and oxidation of organic systems, in photochemical reactions and radiochemical reactions - has ensured that its preparation, properties, stability and decomposition, and the part it plays in the mechanism of other reactions, should be the subject of continuous investigation.

In industry it has been widely used for its oxidising and bleaching properties and in organic chemical preparations. It is commonly handled industrially as a 30% solution concentrated from a more dilute solution (3%) prepared by anodic oxidation of bisulphate solutions at Pt electrodes. These solutions were rather impure and unless inhibitors were added they exhibited an inconveniently high rate of decomposition. The mechanism of the decomposition and the role of catalysts and stabilisers has been much studied but little progress made towards a satisfactory interpretation until recent years (cf. Wynne-Jones et al.²).

In recent years a more pure solution has been commercially prepared by distillation at low pressure and this has become increasingly available at concentrations

up to 90% w.w. A major impetus to the development was the use of the concentrated solution as an oxygen or high pressure gas source for rocket propulsion. In many of these applications the H_2O_2 had to be decomposed with great speed and efficiency by a catalyst, preferably a solid catalyst. This gave rise to a renewed interest in a topic, never much neglected, namely the heterogeneous decomposition of H_2O_2 . Ad hoc experiments with catalytic solids led to the adoption of silver metal (in wire or gauze form) as the ideal catalyst for decomposing the concentrated H_2O_2 (80-90%). The great effectiveness of Ag metal as a catalyst was first reported by Thénard³ in 1832 and had been recognised and studied by many later workers, e.g. Brodie⁴ in 1850, Bredig⁵ in 1899, Wiegel⁶ in 1929 and Maggs⁷ in 1954, as will be discussed later, but the new application drew attention to the need for further studies of specific questions and it was out of this, particularly out of design and development work at the Royal Aircraft Establishment, Rocket Propulsion Department, at Westcott, Bucks., that arose one aspect of the present work, namely the electrochemical investigation of the mechanism of the Ag catalysed decomposition of H_2O_2 in aqueous solution.

Another industrial use of H_2O_2 which has assumed an increasing importance in recent times is in inorganic peroxy compounds, in particular sodium perborate tetrahydrate as an ingredient of washing powders. Great interest centred on

the suppression of oxygen loss from this compound during storage and on the mechanism of the stabilisation achieved by the addition of magnesium compounds.

The second part of this thesis describes studies arising out of this technological problem with a view to elucidating the mechanisms of the decomposition of the solid perborate and of the mode of action of the stabiliser.

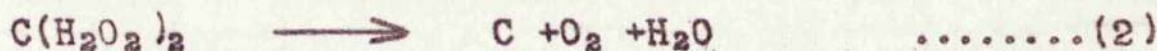
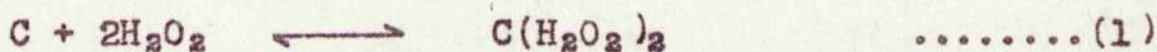
Homogeneous Catalysis of H_2O_2 .

H_2O_2 is now recognised in liquid, solution or vapour phase, as a comparatively stable molecule requiring the rupture of an O-O bond before it can pass to the thermodynamically more stable arrangement of the atoms of H_2O and O_2 . There have been few studies of the thermal, i.e. uncatalysed decomposition of H_2O_2 in the vapour phase owing to the difficulty of excluding the heterogeneous process even when working with clean glass and quartz surfaces, but these difficulties have been overcome recently by McLane⁸, Satterfield and Stein⁹ and Giguère and Liu¹⁰. The results of these workers, although in general agreement that homogeneous catalysis predominated above 400-425 °C., showed inconsistencies with respect to order of reaction and activation energy. However a very recent study by Hoare, Protheroe and Walsh¹¹, using a flow technique with several different carriers, confirmed that homogeneous catalysis predominated above 420 °C. They also reassessed

the results of the above workers and showed that their corrected activation energies were in good agreement with their own value of 50 kcal.

In the decomposition of aqueous H_2O_2 solutions the basic mechanism of the early 20th century was the "intermediate product" theory, where an unstable intermediate unstable peroxidic compound is formed which subsequently decomposes regenerating the original catalyst and liberating oxygen.

This may be represented as follows:

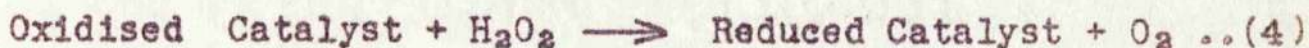


where C represents the catalyst (Spitalsky,¹² 1926).

The second significant theory to account for the homogeneous catalysis of H_2O_2 , gaining support from Abel¹³ and Bray,¹⁴ depended upon the facts:

- (a) Catalysts generally can exist in more than one valency state.
- (b) H_2O_2 can act both as an oxidising and as a reducing agent.

Hence the following type of reaction cycle occurs:

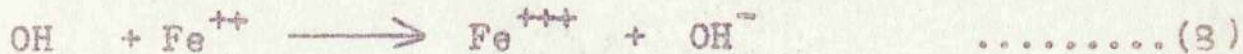


These two basic theories have been each applied sometimes exclusively to various catalysts but recently there has been a tendency to use a combination of the two theories.

In 1931, a major development in the theory of the mechanism occurred by the suggestion, by Haber and Willstätter,¹⁵ of the participation of free radicals in the decomposition of H₂O₂. Thus the oxidation-reduction mechanism would be seen to be more elaborate.

This suggestion was accepted and extended by Haber and Weiss¹⁶ to what is now considered to be the classical approach in explaining the homogeneous catalysis of dilute solutions of H₂O₂ by iron ions.

For the catalytic decomposition by Fe⁺⁺ ions shown by the fact that under certain conditions more H₂O₂ was destroyed than could be explained by a simple oxidation Fe⁺⁺⁺ + $\frac{1}{2}$ H₂O₂ → Fe⁺⁺ + OH⁻ the proposed reaction scheme was as follows:



where equation (5) represents the initiation.

equations(6) and (7) represent the propagation of a chain,

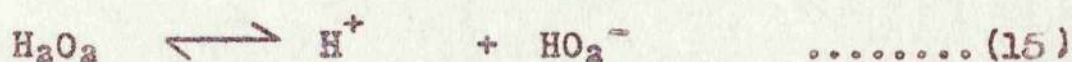
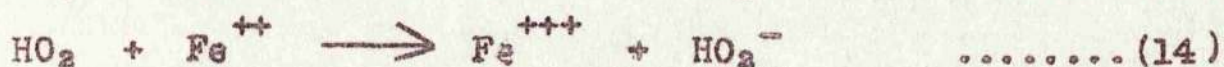
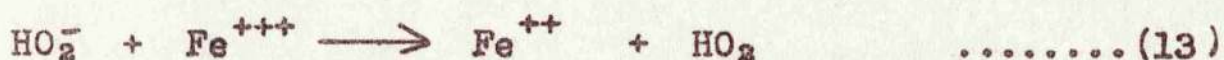
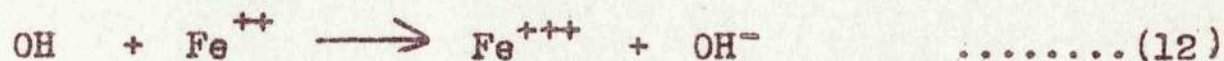
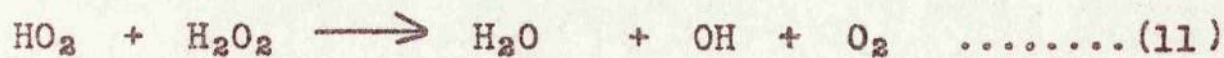
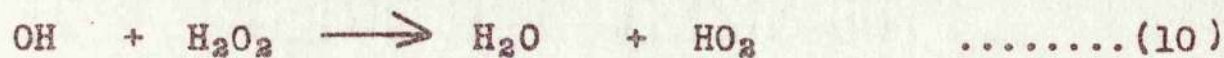
and equation (8) represents its termination.

The novelty of such a scheme was the formation of free OH and HO₂ radicals and their subsequent participation in a chain reaction. Also of importance was the simple electron

transfer steps, as seen in equations (5) and (8).

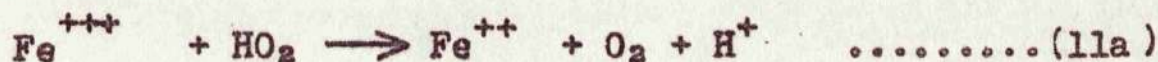
Confirmation of the occurrence of OH radicals in the $\text{Fe}^{++}/\text{H}_2\text{O}_2$ system was obtained by Evans et al.¹⁷ who showed that, using the above system, vinyl type polymerisation could be initiated and the OH radicals inducing the initiation recognised by infrared analysis in the polymer formed. Evidence for the occurrence of the HO_2 radical has not been easy to obtain in a direct form, but its participation seems beyond doubt in the decomposition of pure H_2O_2 initiated photochemically and radiochemically. Thus Dainton and Rowbottom¹⁸ were able to assign a half life to the HO_2 radical in very pure H_2O_2 solutions irradiated with γ -rays.

Although the above scheme only considers the catalysis by Fe^{++} ions, Haber and Weiss actually postulated a complete scheme for the catalysis by Fe^{++} and Fe^{+++} ions. Later Weiss¹⁹ revised and improved the mechanism in the light of extended experiments criticisms and the following mechanism, combining Fe^{++} and Fe^{+++} catalysis was proposed

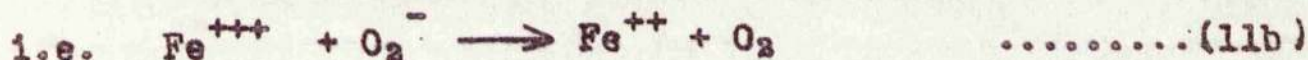


Catalysis by Fe^{++} is represented as before by equations (9), (10), (11), and (12). Catalysis by Fe^{+++} is given by (11), (12), (13) and (14) in addition to (15).

A later modification by Barb et al.²⁰ resulted in the following equation for the production of oxygen rather than (11) above.



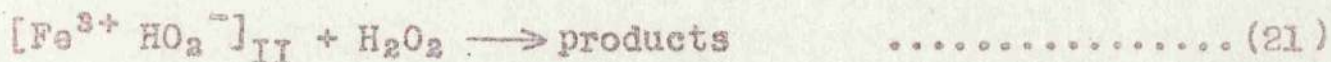
a view which Weiss and Humphrey²¹ supported with the additional modification that it was the anion O_2^- , rather than the undissociated HO_2 radical that reacted



Thus, from the above comprehensive investigations carried out on the iron ions/ H_2O_2 system, general principles were evolved that could be applied to many homogeneous systems, these principles being:

- (1) Decomposition was initiated by a single electron transfer step.
- (2) Free OH and HO_2 radicals were formed and gave rise to a reaction cycle.
- (3) The reaction steps were all bimolecular.

A very recent paper by Wynne-Jones et al.²² again provides some new ideas on the homogeneous Fe H_2O_2 system. Using $\text{Fe}(\text{ClO}_4)_3$ as catalyst, over a very wide range of $[\text{H}_2\text{O}_2]$, he shows that catalysis can be explained by the formation and subsequent dissociation of mono- and bi-peroxy iron complexes. His results show that rate of



i.e. again, through the formation and dissociation of iron complexes the catalysis of H_2O_2 is explained.

In principle the schemes of these authors are similar in regarding the HO_2 and OH radicals as not existing free in the solution, but anchored in an iron complex. The schemes are very similar to those earlier envisaged for decomposition by catalase (Chance²⁴) and synthetic complexed iron compounds (Wang²⁵) and represent a partial combination of the intermediate complex and compensated oxidation-reduction mechanisms.

Heterogeneous Catalysis.

The action of any solid catalyst must involve as an initial step, chemi-sorption, which may be regarded as the attachment of the reacting molecule to "anchored free radicals" on the surface.

The study of heterogeneous decomposition in the vapour phase has been of little importance in elucidating the mechanism. It has been confined mostly to decomposition on inactive catalysts, e.g. Baker and Oullet²⁶ on glass and silica, MacKenzie and Ritchie²⁷ on quartz, Giguère²⁸ on

pyrex, alumina and tin. Recent work in this laboratory by Hart and McFadyen²⁹, Hart and Ross³⁰, Hart and Taylor³¹ has covered a wide range of oxide catalysts, especially the p-type oxides Cu_2O , MnO_2 , CoO , PbO , Ag_2O and NiO and some n-type oxides ZnO , CuO , CdO , Al_2O_3 .

They have shown broadly, but with certain significant differences, the same considerations apply to gas phase heterogeneous catalysis as to the solution phase.

The earliest study of the heterogeneous catalysis of liquid H_2O_2 was the observations made by Thénard³ on the action of Ag , Ag_2O , Pt and Fe on pure H_2O_2 . He made the important observation that, during the decomposition, there was a lack of chemical reaction. Also, at this early stage, it was observed how much more efficiently Ag acted as a catalyst than other metals tried.

During 1850-60 Brodie^{4,32} published a very long series of papers on the action of such oxides as Ag_2O , MnO_2 and Cr_2O_3 on H_2O_2 . From his results Brodie showed:

- (a) For different oxides, widely differing rates of catalysis were obtained.
- (b) The efficiency of a given oxide was dependent upon its mode of preparation.

Berthelot³³, who also investigated the $\text{Ag}_2\text{O}/\text{H}_2\text{O}_2$ system, postulated the formation of higher Ag oxides and

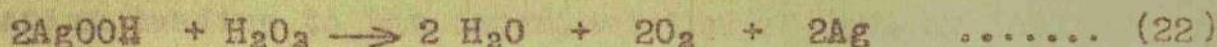
their subsequent decomposition and remarked on the large amount of decomposition effected by a small amount of the Ag_2O catalyst.

The greatest advancement of the nineteenth century knowledge, however, was due to the comprehensive investigations by Bredig et al.^{5,34} using colloidal Pt and Au as catalysts. This series of papers was entitled "Inorganic Ferments", as Bredig recognised this metal sol type of catalysis as being analogous in action to the organic enzyme, catalase. The results obtained from Pt and Au were similar, the outstanding features being:

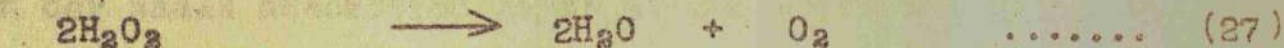
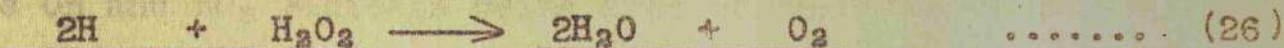
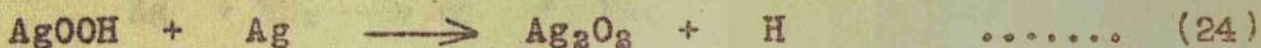
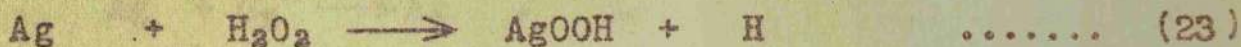
1. Rate of catalysis increases as $[\text{OH}']$ increases, up to and optimum $[\text{OH}']$, at $\text{pH} = 12$, then the rate falls off.
2. The action of Cl' , CN' , S'' and P''' inhibit catalysis
3. At the low $[\text{H}_2\text{O}_2]$ studied first order reaction kinetics prevail.

These results were later confirmed in 1940 by Teletof.³⁵

In 1929 Wiegel⁶ studied the relation of added Ag and alkali required to saturate dilute H_2O_2 solutions, the point of saturation being characterised by a rapid increase in the rate of catalysis. From his results Wiegel postulated that the factor controlling rapid catalysis was the solubility product $[\text{Ag}^+][\text{HO}_2']$, thereafter decomposition proceeded as follows:



The metallic Ag thus produced redissolved and a cyclic process ensued:

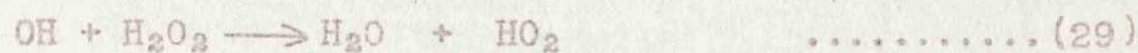
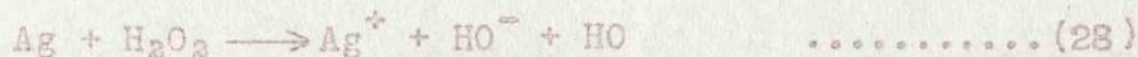


The postulated occurrence of H atoms as intermediates would now be considered as unacceptable on energetic grounds.

Wentworth³⁶ in 1951, on the other hand, while investigating the same relationship in solutions of H₂O₂ up to 20% w.w., proposed that it was the solubility product of Ag(OH)₂ that was the controlling factor. However some recent work by Maggs,⁷ and Maggs and Sutton^{37,38} on solubility, pH and conductivity measurements involving both Ag⁺ dissolved from a Ag catalyst and Ag⁺ added as AgNO₃ and working with H₂O₂ solutions ranging from 15-36% w.w., suggests this "catalysis point", i.e. the point of saturation, is controlled by the [Ag⁺][HO₂⁻] solubility product. Indeed Wentworth's experimental results, which were quite scattered, could, with reasonable agreement, support the same argument.

In 1935, Weiss³⁹ reinterpreted Wiegels data on the basis of his classical single electron transfer type of

mechanism leading to the decomposition of H₂O₂ as follows:

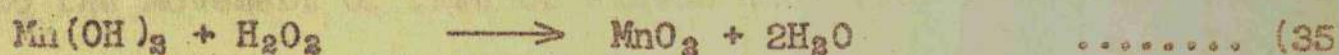
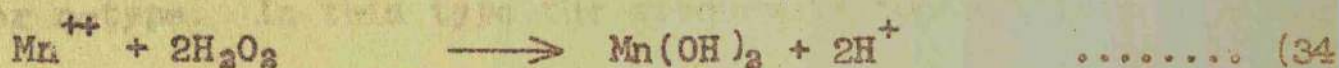
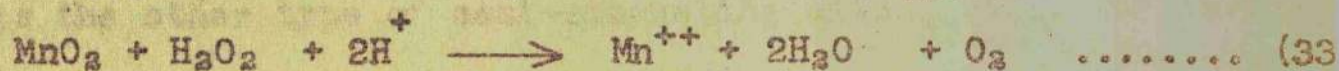


the OH and HO₂ radicals being free in solution or in the Van der Waals adsorption layer at the surface. Here the metal can be considered the source of and sink for electrons. However before an electron can be removed from a metal it must be able to overcome a potential energy barrier, i.e. the work function. Weiss, by applying a negative potential, decreased the work function of certain metals and discovered a corresponding increase in their catalytic activity, a fact that would be in agreement with his electron transfer theory. Further support was received for his theory when Dowden and Reynolds,⁴⁰ from their study of the Ni-Cu alloy H₂O₂ system, showed that the rate of decomposition decreased as the Cu metal atom d-band was progressively filled by addition of Ni i.e. as the electron availability decreased.

According to Pauling,⁴¹ and increase in the 'd' character of metals means that more 'd' electrons are employed in intermetallic atom bonds in the crystal lattice structure, and less electrons are available for chemisorption, resulting in a decrease in catalytic activity.

In catalysis by metals it was considered by Dowden and Reynolds that the thin oxide film on the surface, which is of the order 20-50 Å. in the case of Cu exposed to air at room temperature, takes no part in the catalysis and is transparent to electrons, i.e. the catalysis being controlled completely by the nature of the underlying metal.

Relatively little investigation has been carried out on the mechanism of catalysis of H₂O₂ solutions by oxides. The MnO₂/H₂O₂ system was studied by Broughton *et al.*⁴², who held that the solubility of the Mn(OH)₂ governed the decomposition of H₂O₂. The following mechanism was suggested:



However Broughton *et al.*⁴³, were unable to find parallel confirmation of this effect on a cobalt oxide/peroxide system

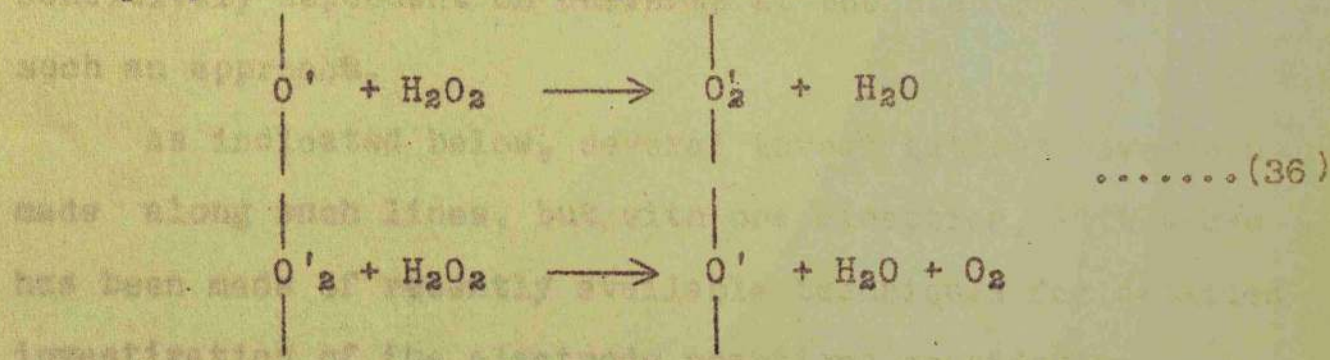
Voltz and Weller,⁴⁴ in a recent investigation of chromia and chromia/alumina oxides on H₂O₂ solutions, showed that the catalytic activity was related to the surface oxidation state. The catalysts were pretreated at 500°C in H₂ or O₂ and the oxidised catalysts were found to be six to eight times more active.

Earlier, a major contribution to the understanding of heterogeneous catalysis and also to the enhancement of the knowledge of the solid state, was made by Garner, Grey and

Stone.⁴⁵ They showed that oxygen was adsorbed on Cu₂O in an active form, considered to be either O' or O₂' ions. A feature of this work was the attention which it drew to the relevance of the defect structures of the oxide, i.e. the oxide as a semi-conductor, to its catalytic action.

The more active semi-conducting oxide catalysts are the p-type oxides, i.e. where the electronic conductivity in the solid state is due to positive holes in the crystal lattice.

Not quite so active, in terms of catalytic activity, is the other type of semi-conducting oxide, viz., the normal or n-type. In this type the electronic conductivity is due to the movement of free or excess electrons inside the crystal. A very recent investigation by Weir⁴⁶ on the decomposition of dilute H₂O₂ solutions by the p-type semi-conducting oxide Cu₂O in a flow system confirms the above postulation by Garner et al. From a kinetic study of the Cu₂O/H₂O₂ system, Weir proposes that the catalysis is represented by:



i.e. that the surface concentration of the free radical ions O⁻ or O₂⁻ was responsible for catalysis. Weir referred briefly to electrode potentials on Cu₂O in H₂O₂ solutions

and showed that the electrode potential, which he interpreted as an indication of the surface activity of adsorbed oxygen in the free radical state, was sensitively related to the efficiency of the catalyst.

Studies of electrodes in H_2O_2 solutions have been the subject of several important reports which will now be considered.

Electrochemical Studies and Catalysis.

(1) General.

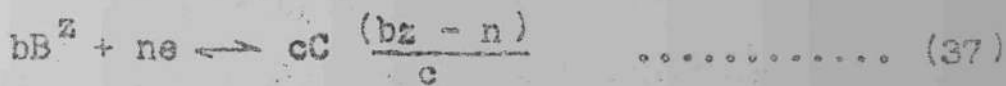
Various considerations, particularly the apparent similarity between the anodic evolution of oxygen from aqueous solution at a metal or metal oxide electrode and the evolution of oxygen from H_2O_2 solutions at metal or metal oxide surfaces, suggest an electrochemical study,

The facts that the electrode potentials are controlled by the H_2O_2 during catalysis (and not by the chemical nature of the catalyst) and that the rate of decomposition is sensitively dependent on currents at the electrode support such an approach.

As indicated below, several investigations have been made along such lines, but, with one exception, little use has been made of recently available techniques for detailed investigation of the electrode reactions considering catalysis to involve a flow of electrons to and fro between the metal and the H_2O_2 or H_2O_2 derived species which are at

the surface during the sequence of reactions leading to oxygen evolution. Most have based discussion on the equilibrium potentials, which are assumed to result from a single electrode reaction just as in the case of a metal in a solution of its ions.

For such a reaction, e.g.



the equilibrium potential may best, for the purpose of this thesis, be considered kinetically as the balance between a cathodic process, where electrons leave the metal and pass into the solution phase molecules and an anodic when this process is reversed. Some aspects of Parson's⁴⁷ general treatment of electrode processes may be followed here. The result of the reversible electrode potential of equation (37) is given by:

$$E = E_0 - \frac{RT}{nF} \ln \frac{a_c^c \left(\frac{b}{c} - n\right)}{a_B^b} \dots\dots (38)$$

(European Convention)

and in the case of



the potential would be given by:-

$$E = E_0 - \frac{RT}{F} \ln a_{OH^-} \dots\dots (40)$$

Displacement of the reversible potential value would produce a change in the equilibrium concentrations of the species on and near the electrode surface, and reaction would

occur, the rate of reaction depending to some extent on the displacement of the equilibrium value and also to some extent on such factors as diffusion of reactants and products in the vicinity of the electrode, or possibly on the relatively slow reaction of intermediately formed species. Consequently a study of the electrode equilibrium potentials of silver in aqueous H₂O₂ solutions and subsequent displacement of these reversible potential values may yield interesting details of the complex reaction mechanism involved.

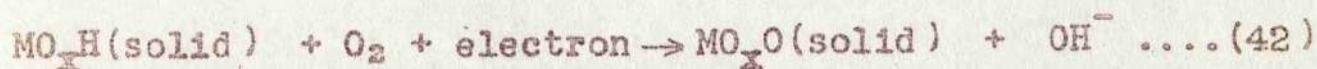
(11) Study of electrodes in H₂O₂ solutions.

The earliest known observation on electrodes in H₂O₂ solutions was made by Thénard,⁴⁸ in 1830, who observed an increase of O₂ evolution on passing a small current at a Pt electrode. Further limited studies on the electrolysis of H₂O₂ were made by Schöne⁴⁹ in 1879 and Tanatar⁵⁰ in 1903.

An early paper by Bornemann⁵¹ in 1903 may be particularly noted. Using Pt and Au electrodes in acid solutions of H₂O₂, he found a steady electrode potential value.

$$E = 0.66 \pm 0.03 \text{ volts} \dots\dots\dots (41)$$

(this electrode potential, as are all subsequent potentials in this thesis, is referred to the standard hydrogen electrode). This potential was explained by Bornemann in terms of an oxide equilibrium of the type:

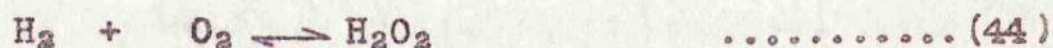


the oxide MO_xO being formed by the H_2O_2 . However Bornemann neither varied pH nor $[\text{H}_2\text{O}_2]$.

Later, in 1933, Wolff^{5a} conducted a systematic investigation using Pt electrodes and varying the pH of a H_2O_2 solution from 1.25 to 11.34. From his results the following relationship was found:

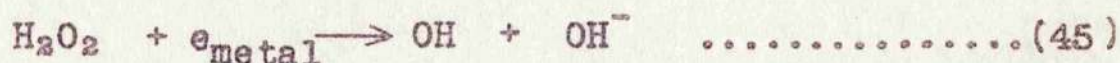
$$E = E_0 - 0.059 \text{ pH v. at } 25^\circ\text{C} \dots (43)$$

where $E_0 = 0.80 \text{ v.}$ Wolff explained this value of 0.80 v. in terms of a hydrogen electrode, the hydrogen pressure being controlled by the equilibrium:



However Wolff only worked at one $[\text{H}_2\text{O}_2]$ and was unable to test this hypothesis.

In 1935, Weiss³⁹ observed the effect of anodic or cathodic polarisation on the rate of catalysis of H_2O_2 by a Pt catalyst and found the results obtained supported his earlier postulation that the initiating step in catalysis at a metal surface is given by the equation



The first detailed attempt to investigate the H_2O_2 electrode system at equilibrium was carried out by Berl⁵³, in 1943, using alkaline solutions, $[\text{KOH}] = 0.1 \text{ to } 11\text{M}$, where $[\text{KOH}] \gg [\text{H}_2\text{O}_2]$ generally. Alkali and H_2O_2 concentrations were varied separately and the electrode potential at equilibrium on a porous carbon electrode, stirred by oxygen

bubbling through the carbon, was given by the expression:

$$e = 0.042 - 0.03 \log_{10} a_{OH^-} a_{HO_2^-} \quad \text{at } 27^\circ\text{C} \quad \dots\dots\dots (46)$$

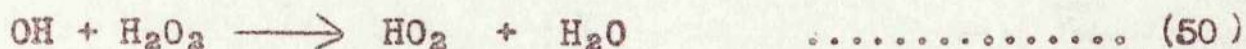
This relationship is consistent with the following reaction:



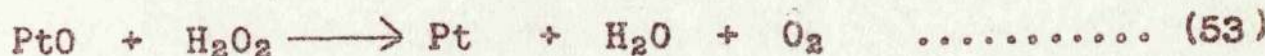
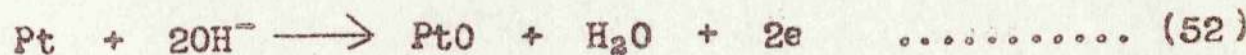
In 1951, Hickling and Wilson⁵⁴ made a comprehensive study of the anodic decomposition of H₂O₂ in alkaline, neutral and acid solutions at the relatively inert Pt, Au, Ni and graphite electrodes. They studied the equilibrium electrode potentials and attributed the results at all electrodes in alkaline solutions to:



which takes place at a low potential, but in acid and neutral solutions a higher potential is required for anodic decomposition and the reaction is then said to occur through the discharge of an OH radical.



The Pt electrodes behave in an anomalous fashion in neutral and acid solutions and this was explained by the participation of platinum oxides introducing the electrode reaction:



Hickling and Wilson did not attempt a detailed interpretation of the kinetics of the electrode reactions which these experiments seem to have made possible. Indeed, their discussion seems to rest rather heavily on measurements of electrode potentials, i.e. with zero current, and on earlier work, particularly by Berl.⁵³

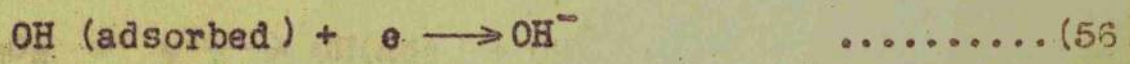
The electrode potentials of the Pt and Au electrodes H₂O₂ system were subjected to an even more detailed treatment by Bockris and Oldfield⁵⁴ in 1955. Using buffers they varied the pH between 1 and 12.55 while using a concentration range of H₂O₂ between 5 x 10⁻⁵M and 5M. Within this range they observed that neither [H₂O₂] nor oxygen pressure had any effect on the steady equilibrium potentials recorded.

From their results the following expressions were obtained:

$$E = 0.835 - 0.059 \text{ pH v. at } 25^\circ\text{C for Pt} \dots\dots\dots(54)$$

$$E = 0.842 - 0.059 \text{ pH v. at } 25^\circ\text{C for Au} \dots\dots\dots(55)$$

The fact that neither O₂ pressure nor [H₂O₂] (and therefore HO₂⁻) affected the e.m.f. led Bockris and Oldfield to suggest that the electrode reaction is as follows



the OH(ads) being provided by the dissociative adsorption of H₂O₂. The small differences between the E₀ values in

the equation was regarded as a measure of the role the metal plays in modifying this free energy of the radical by adsorption.

The most recent contribution to the field was made by Gerischer and Gerischer⁵⁵ in 1956 who studied Pt electrodes in a very limited [H₂O₂] range, viz., 0-0.1M, varying the pH from 1 to 10.5. They found, for pH < 5, the expression:

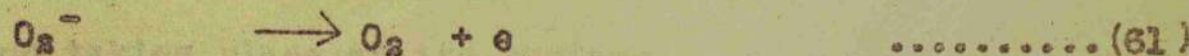
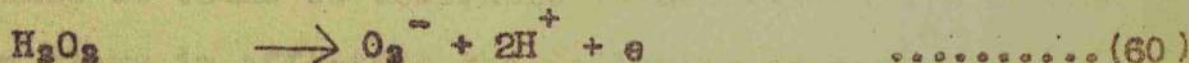
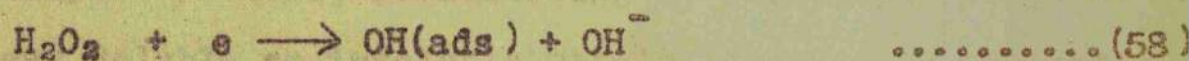
$$E = 0.832 - 0.059 \text{ pH v.} \quad \text{at } 25^\circ\text{C} \quad \dots\dots (57)$$

or

$$E = 0.898 - 0.059 \text{ pH v.}$$

for two different experiments. Correspondingly they found for pH > 7.5 the respective E₀ values were 1.372 v. and 1.442 v. Gerischer and Gerischer potential values were obtained instantly on immersion in H₂O₂ solution, as opposed to Bockris and Oldfield potential values which were obtained after several hours immersion.

Using their stationary potential results in conjunction with current potential studies Gerischer and Gerischer interpreted the decomposition of H₂O₂ at a Pt surface as occurring through a Weiss type electron transfer process as follows:



Plan of Present Investigation.

According to Schumb, Satterfield and Wentworth,⁵⁶ the two best metal catalysts for decomposing H_2O_2 are Pb and Ag respectively. Appreciating the mechanical shortcomings of Pb, then the obvious choice of a metal catalyst in a technical decomposer would be Ag. Hart⁵⁷ observed that when concentrated H_2O_2 solutions meet a Ag surface, there are three stages in the reaction, viz.,

(I) A quiescent period, the duration depending upon the nature of the Ag surface.

(II) A period of vigorous catalysis

(III) A period of noisy ebullient catalysis, associated with vapour binding and an elevated temperature at the catalyst surface.

It would be obviously desirable that the mechanism of the processes occurring at the silver surface under such conditions should be understood.

Of the solid catalysts mentioned in the preceding introduction Ag differs markedly in that it dissolves to an appreciable extent during the catalytic decomposition of H_2O_2 . The dissociation of the Ag catalyst appears to be linked with the catalytic process, facilitating it perhaps, as compared with less soluble or insoluble metals like Pt, Au, Ni and Cu. Thus it would be desirable to observe what role the Ag^+ ion plays in affecting the following stages of the reaction taking place at its surface.

- (1) Diffusion of H_2O_2 to the Ag surface.
- (2) Adsorption of H_2O_2 on the Ag surface.
- (3) Reaction on the surface.
- (4) Desorption of products from the surface.
- (5) Diffusion of products from the surface.

The knowledge gleaned from a study of the effect of $[Ag^+]$ would be greatly enhanced by the detailed study of the effect of small positive or negative currents.

Hart and Aitken⁵⁸ made some preliminary equilibrium potential measurements with a solid silver catalyst immersed in H_2O_2 solutions in a static system. They observed that above a critical $[H_2O_2]$ at acid and neutral pH values, deviations from the Bockris and Oldfield⁵⁴ relationship, viz.

$$E = 0.84 - 0.59 \text{ pH v. at } 25^\circ\text{C} \quad \dots\dots\dots(62)$$

occurred, the potential becoming independent of pH. They also observed that equilibrium potential values were dependent on the condition of the electrode, especially in neutral or slightly alkaline solutions. In very acid or alkaline solutions the effect was less marked. The two types of electrode used were:

(a) Silver wire sealed into soda glass, then cleaned by refluxing with petroleum ether.

(b) Same as (a) with additional treatment of violently etching in 33M H_2O_2 .

These different types of catalysts gave different rates of evolution of oxygen, neither type of catalyst however yielding reproducible results.

Initially the purpose of the present investigation was to obtain a Ag catalyst that would produce consistent rate values and consistent equilibrium potential measurements.

Then it was proposed to survey the equilibrium potentials of Ag in H_2O_2 , ranging from very dilute to very concentrated solutions over the entire pH range. It is obvious that in the highly alkaline region the $[H_2O_2]$ range available for study is limited as concentrated solutions will become self-heating on the immersion of a Ag catalyst. The effect of added $[Ag^+]$ on the potential values would also be observed.

A parallel investigation of the reaction kinetics of the system under equilibrium conditions, varying $[H_2O_2]$, pH and $[Ag^+]$ was also indicated.

From these experiments, coupled with the knowledge obtained from an investigation of the effect of anodic and cathodic polarisation of the catalyst electrode on

(a) equilibrium potential values and

(b) rates of loss of oxygen

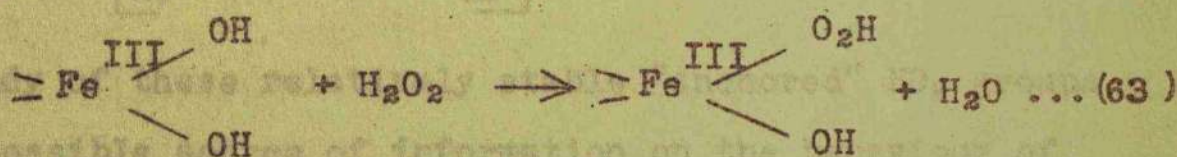
varying $[Ag^+]$, pH and $[H_2O_2]$, it was hoped to determine the detailed mechanism of the decomposition of H_2O_2 at a solid

silver surface and to determine precisely what factors rendered silver so effective. Even although a moderate number of studies had been carried out on the Ag/H₂O₂ system, most of them had involved colloidal Ag catalysts and consequently the results and conclusions could not be extended without reserve to a solid Ag catalyst H₂O₂ system.

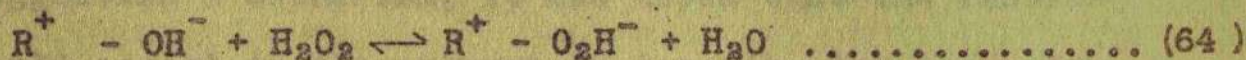
It was also proposed, in the light of the conflicting equilibrium potential results, of Hart and Aitken on Ag/H₂O₂ and of Brockris and Oldfield on the Pt/H₂O₂ system, to conduct an examination of the equilibrium potentials of Pt in H₂O₂ solution over a wide concentration range.

Over the last 30 years most investigators have agreed that the decomposition of H₂O₂ must involve the OH or O₂H radicals either in the free state, adsorbed at surfaces or combined in complex ions.

Investigation of the detailed reactions of the radicals, when adsorbed at surfaces, is usually difficult and rests on kinetic evidence, usually of an indirect nature. This is the case for enzyme or complexed iron catalysts where the process is usually explained as first involving the exchange.



In an earlier investigation in this laboratory an attempt was made by Graham⁵⁹ to examine the role of the exchange with anion exchange resins. Graham showed that the resin surface could be largely covered with O_2H^-

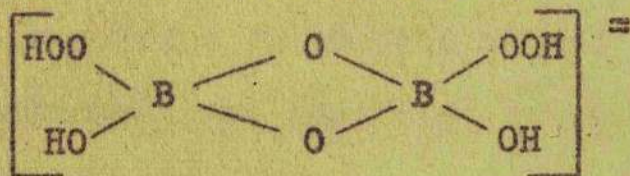


with the equilibrium constant for this exchange of 380, and that catalysis was governed by the kinetic equation

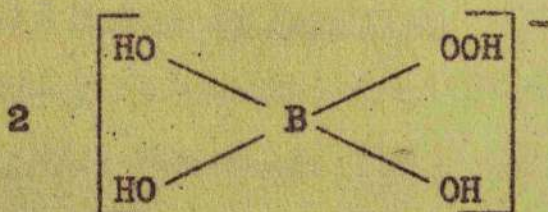
$$\begin{aligned} \text{rate} &= k_1\theta [H_2O_2] \text{ at high } [H_2O_2] \\ &\text{or} = k_2\theta \quad \quad \quad \text{at low } [H_2O_2] \end{aligned}$$

which indicated the importance of the adsorbed HO_2^- .

As a development of this it seemed interesting to study the reported slow decomposition of the solid sodium perborate. It seemed from the work of Menzel⁶⁰ and Partington and Fathallah⁶¹ that this compound contained in the crystal state the peroxide in the form of a complex ion containing two boron atoms and HO_2 groups, i.e. the dimeric ion



and in solution



Study of these relatively stable "anchored" HO_2 groups was a possible source of information on the behaviour of the same type of adsorbed species at more active metal oxide catalysts. Thus, while the primary object in the

Investigation of the decomposition of sodium perborate crystals and solution was an exploratory one with the aim of describing the nature of this process itself and suggesting a mechanism, it was hoped that the results would assist in the attempt to describe the mechanism at the silver surface during catalysis.

to the electrode potential, the nature of the electrode surface, the rate of deposition of the metal, and the nature of the solution.

The experiments are described under three main headings, viz: equilibrium potentials; rate of decomposition; current flow.

The silver electrode used eventually in all cases was a thick silver wire, but other forms were tested. The pretreatment of the metal was found to be important and some experiments were carried out before a satisfactory procedure was found which gave satisfactory reproducibility. These experiments are described.

3. Materials.

(1) Sodium peroxide.

25% a.s. unstabilised high test peroxide was obtained from Laporte Chemicals Ltd., in polythene containers, in which the material was kept until required. Confirmation as to the purity of this peroxide was obtained when it was observed that silver catalysed decomposition of several redistilled hydrocarbons gave

EXPERIMENTAL

1. Introduction.

The object of the experiments was to elucidate the conditions at a catalysing silver surface in aqueous H_2O_2 solutions by means of current-potential and equilibrium potential measurements and to relate the rate of catalysis to the electrode potential, the nature of the electrode surface, the rate of corrosion of the metal, and the nature of the solution.

The experiments are described under these main headings, viz: equilibrium potentials; rate of decomposition; current flow.

The silver electrode used eventually in all cases was a thick silver wire, but other forms were tested. The pretreatment of the metal was found to be important and many experiments were carried out before a satisfactory annealing procedure was found which gave satisfactory reproducibility. These experiments are described.

2. Materials.

(1) Hydrogen Peroxide.

36% m.m. unstabilised high test peroxide was obtained from Laporte Chemicals Ltd., in polythene containers, in which the material was kept until required. Confirmation as to the purity of this peroxide was obtained when it was observed that silver catalysed decomposition measurements on several redistilled batches gave results identical with those

on the peroxide as received. A careful check was made on each batch on arrival to test for the presence of any trace of unintended stabiliser, e.g. sodium stannate which, even in small traces, seriously affected rate measurement.

Solutions for use were obtained by dilution of the 36% peroxide and concentrations were determined by titration against standard $KMnO_4$. The pH values were adjusted by the addition of calculated amounts of solutions of Analar $NaOH$ or $HClO_4$ and checked by a pH meter previously calibrated for use in H_2O_2 solutions, by the method of Hart and von Döhren⁶² or Wynne-Jones and Mitchell.⁶³ The ionic strength of the solutions was controlled by the addition of $NaClO_4$. This reagent could not be obtained commercially quite free from chloride and several recrystallisations had to be carried out from redistilled water until the chloride was removed. It may be noted in respect of the use of $NaClO_4$ that the mobilities of the Na^+ and ClO_4^- ions alter only slightly over the entire range of $H_2O_2-H_2O$ compositions (Wynne-Jones⁶⁴).

(ii) Catalysts.

The silver and platinum catalysts used in the subsequent measurements were obtained from Johnson, Matthey and Co., in the form of 28S.W.G. These wires had been extruded from spectroscopically standardised rods containing the following maximum impurities in parts per million

- Fe,3; Pb,1; Cd,1; Cu, Li, Mn and Mg all < 1.

Pretreatment of Catalysts.

Background to the work.

During preliminary electrode potential measurements on a catalysing silver electrode in aqueous H_2O_2 solutions it was evident that the steady or equilibrium potential value of the silver electrode was dependent on the condition of the catalyst. In those experiments the electrodes employed were either "inert", i.e. polished as extruded and left in air, or "active", i.e. silver wires etched by immersion in a concentrated H_2O_2 solution. These electrodes were sealed into lengths of drawn soda glass tubing using a hot flame.

Differences of 0.05 to 0.1v in the steady potential values of the two types of electrodes were found in aqueous H_2O_2 solutions over the entire pH range and variations up to $\pm 0.05v$ in the steady potential values of different types of inert electrodes were also recorded. No consistency between detailed treatment and the potential was obtained except that an "inert" electrode was less stable than a thoroughly activated one.

Also during initial studies of evolution of oxygen from aqueous H_2O_2 solutions at a silver surface, large differences in rates were observed, even when the silver wire catalysts were taken from the same roll of wire and cleaned and/or etched in the same fashion. Indeed quite often a three-fold range in values was obtained.

The conclusion drawn at that stage was that the flame employed during the sealing of the silver wire catalysts into the glass was causing the formation of active zones in the different catalysts. However, it was shown that this could not be the complete answer when inconsistent rate and potential values were obtained from an annealed silver ring catalyst screwed on to a stainless steel shaft covered by a teflon holder, because, with this type of catalyst, no sealing process was required.

In an attempt to eliminate heterogeneity, several catalysts, after being sealed into glass, were immersed in a 33M H_2O_2 solution for 1 minute. The violent evolution of oxygen and considerable etching which occurred were considered likely to impart equal degrees of heterogeneity to the surface of the catalyst. However, no better agreement in potential or rate values were obtained.

A low temperature surface annealing process was then attempted. The catalysts, after sealing in glass, were placed in alundum combustion boats which were inserted in an impervious aluminous porcelain tube in a tubular muffle furnace. The catalysts were heated to 200 °C, held at that temperature for 1 hour, then allowed to cool. During the entire process the catalysts were held in an atmosphere of

nitrogen or oxygen, which was passed continuously through the tube, and after removal from the furnace the catalysts were stored in a pure atmosphere of N_2 or O_2 in air-tight containers. Experiments with these catalysts showed that no good agreement in results had been yet attained.

Finally a high temperature, bulk annealing process, at $500^\circ C$ was employed, the general procedure being the same as above, and it was then discovered that all anomalies were eliminated and both reproducible rate and potential measurements were obtained.

The Pt electrodes were treated in the same fashion.

3. Equilibrium Potential Measurements.

Apparatus.

(i) Cell arrangement.

The apparatus was shown in Fig.1. The peroxide solution was contained in a cell with two limbs. One limb contained the electrode and connected to this limb was a side arm through which N_2 could be passed for stirring purposes. The other limb, separated from the first by a G.4 porous sinter to minimise mixing by diffusion, was used to connect the cell via an agar/saturated NH_4NO_3 salt bridge to a saturated calomel half cell. Preliminary experiments utilised a Hg/HgO $[NaOH] = 0.1$ half cell to ensure exclusion of chloride ions, but the above cell arrangement

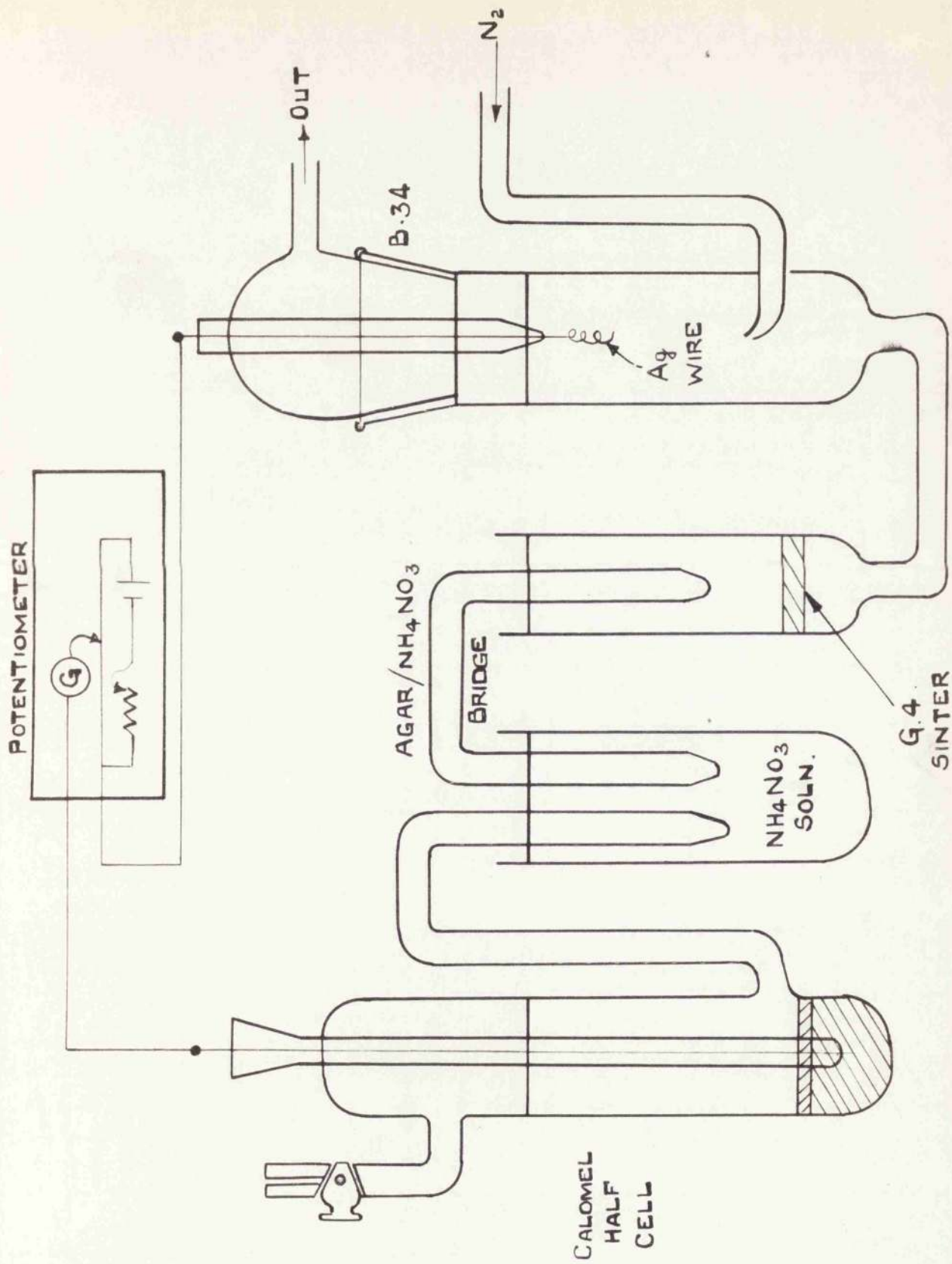


FIG. I. CELL ARRANGEMENT FOR ELECTRODE
POTENTIAL MEASUREMENTS.

appeared to ensure this with the use of the more convenient saturated calomel reference electrode.

For measurements at $25^{\circ}\text{C} \pm 0.1^{\circ}\text{C}$ the apparatus was placed in a thermostatically controlled water bath

(ii) Electrical apparatus.

The e.m.f.'s were measured with a Muirhead 4-figure potentiometer in conjunction with either a Cambridge unipivot galvanometer, or a Cossor cathode ray oscilloscope and preamplifier, as a null point indicator. The oscilloscope method was used to obtain measurements quickly, e.g. immediately after immersion.

(iii) pH of H_2O_2 solutions.

For pH values up to 10.5 pH measurements were made with an Alki glass electrode in conjunction with a saturated calomel half cell. The pH reading obtained was corrected for the effect of the H_2O_2 on the asymmetry potential of the glass electrode from a calibration curve constructed by the author from $\text{HClO}_4/\text{H}_2\text{O}_2$ and $\text{NaOH}/\text{H}_2\text{O}_2$ mixtures according to the method of Hart and von Döhren⁶² and Wynne-Jones and Mitchell⁶³.

In the pH range 4-10 reliance was placed upon the measured pH value, but in the more acid and more alkaline solutions the pH was calculated, as well as the concentration of H_2O_2 and HO_2^- in the solutions. On the alkaline side the H_2O_2 buffer equation was used:

$$\text{pH} = \text{pK} - \text{pHO}_2^- + \text{pH}_2\text{O}_2 \dots\dots\dots (65)$$

where $pK = -\log_{10}K = 11.55$, K being the dissociation constant of H_2O_2 . The value of K was taken from Joyner⁶⁴ in 1912, viz., 2.4×10^{-12} at $25^\circ C$. pHO_2^- and pH_2O_2 are the negative logarithms of the activities of the species. The calculations have been simplified by:-

(a) Using concentrations. However allowances were made for the errors this introduced by assuming $f_{O_2H^-} = f_{OH^-}$ in solutions of equal ionic strength.

(b) By assuming

(1) when $[NaOH]$ exceeds $[H_2O_2 \text{ added}]$

$$pHO_2^- = -\log_{10} [H_2O_2 \text{ added}] \dots\dots\dots(66)$$

$$\text{and } pH = 14 - pOH^- \dots\dots\dots(67)$$

$$\text{where } pOH^- = \log_{10} ([NaOH] - [H_2O_2 \text{ added}]) \dots\dots\dots(68)$$

(2) where $[H_2O_2 \text{ added}]$ exceeds $[NaOH]$

$$pHO_2^- = -\log_{10} [NaOH] \dots\dots\dots(69)$$

$$\text{and } pH_2O_2 = -\log_{10} ([H_2O_2 \text{ added}] - [NaOH]) \dots\dots\dots(70)$$

(iv) Experimental technique.

The solution under test, with an ionic strength of 0.05, was placed in the cell in the thermostat. The electrode, which had been previously connected to the potentiometer etc. was then inserted and the e.m.f. of the assembly measured immediately and for some time afterwards.

It was discovered that stirring was not generally required as the oxygen evolved from the electrode proved

an effective stirrer. However the nitrogen was employed to sweep the apparatus clear of air when work was being carried out at the critical $\text{pH} = 6$ zone where CO_2 would affect the pH of the solution. This procedure was repeated for different values of the following parameters:-

- (a) $[\text{H}_2\text{O}_2]$, (b) pH , (c) $[\text{Ag}^+]$ in the bulk solution,
- (d) temperature.

Variation of the ionic strength did not affect the measured potential values.

Equilibrium Potentials on a Pt catalyst in H_2O_2 .

A similar set of experiments on the equilibrium potential values of a Pt electrode were conducted at 25°C , varying (a) and (b).

Electrode Potentials of Various Metals, catalytic and non-catalytic, in H_2O_2 .

For one $[\text{H}_2\text{O}_2]$, 1.5M, at $\text{pH} = 3.00$, the equilibrium potentials of Ag, Pt, Fe, Cu, Ni, Al and Sn were found by the above method for purposes of comparison.

4. Rate Studies.

A series of measurements was made on the rate of oxygen evolution at a silver electrode under conditions of steady potential to see how this was related to $[\text{H}_2\text{O}_2]$, $[\text{Ag}^+]$, and pH . When these measurements were made the potential behaviour of the metal in the given solution had

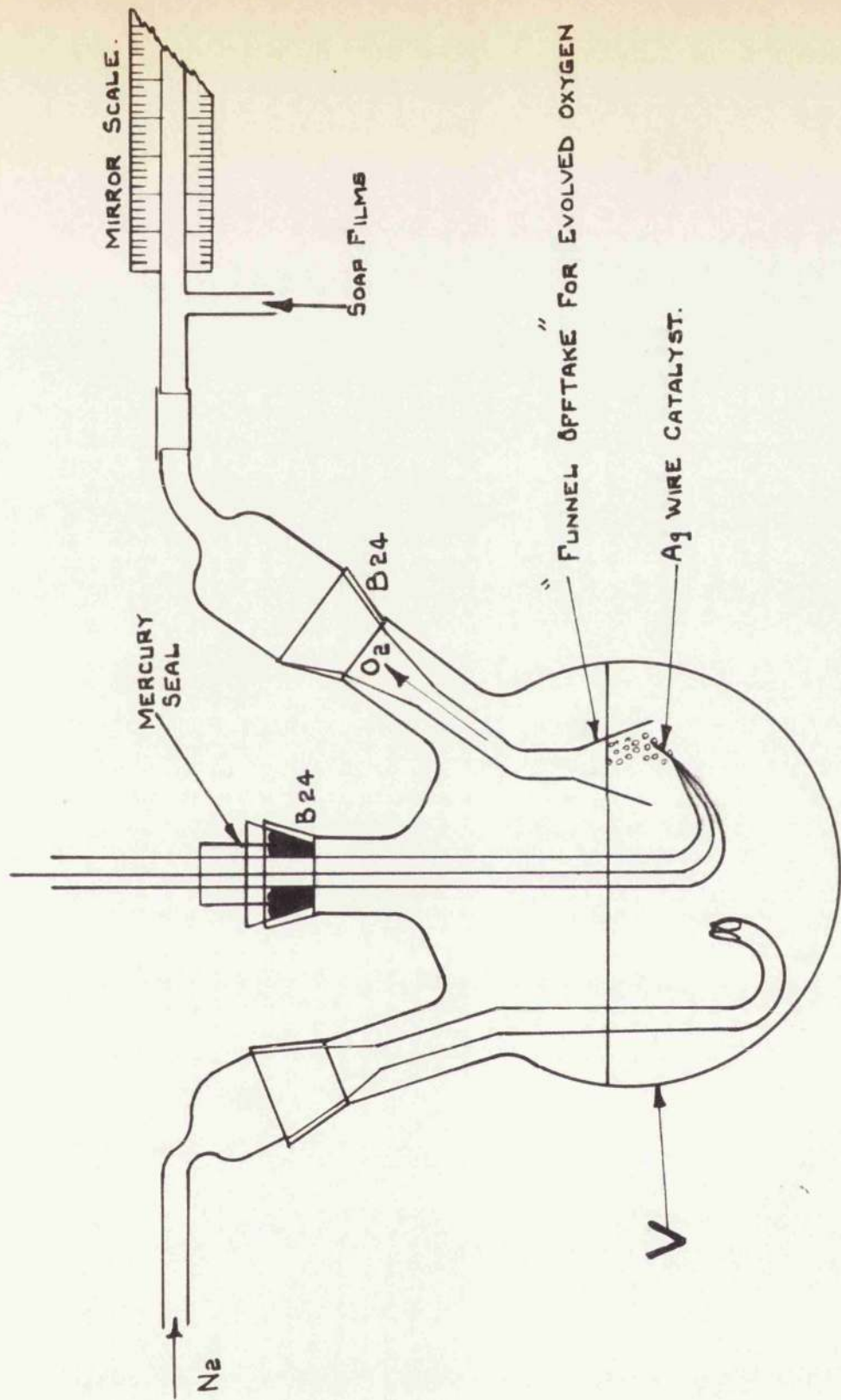


FIG 2. APPARATUS USED FOR RATE STUDY MEASUREMENTS

considered to represent the absolute amount of oxygen evolved at the temperature and pressure of the tube.

The volumes were corrected to N.T.P. The procedure was as follows:-

400 ml. of the test solution was placed in the reaction vessel which in turn, was inserted in the thermostat at the reaction temperature and allowed to attain equilibrium conditions. The flow meter apparatus was cleaned and washed with a dilute soap solution.

The catalyst, in the form of a small length of 28 S.W.G. silver wire sealed into a drawn soda glass tube, then annealed, was immersed in the solution.

Rates of gas evolution were recorded every half minute until a steady rate of catalysis was attained. The pH was again checked to see whether dissolution of Ag had appreciably altered the pH ($2\text{Ag} + \text{H}_2\text{O}_2 = 2\text{Ag}^+ + 2\text{OH}^-$). Generally the change in pH was kept small of the order of 0.01 pH units this being accomplished by limiting the size of the catalyst in accord with the volume of H_2O_2 employed during the experiment.

The surface area of the catalyst exposed to the H_2O_2 solution was generally within the range 2×10^{-2} to $8.5 \times 10^{-2} \text{cm}^2$.

Some preliminary rate measurements were carried out on the effect of ionic strength of the rate of decomposition, the electrolyte used was NaClO_4 . Table I shows the results.

Table I

$[\text{H}_2\text{O}_2] = 0.8\text{M}$	$\text{pH} = 4.00$
$[\text{NaClO}_4]$ Gm.mol. litre ⁻¹	Rate of Catalysis M.l.s. O ₂ min. ⁻¹
0.00	1.02×10^{-2}
0.01	1.00×10^{-2}
0.05	0.92×10^{-2}
0.10	0.71×10^{-2}
1.00	0.24×10^{-2}

In conjunction with the preliminary experiments conducted in the following experimental section, an ionic strength of 0.05 was selected for the rate measurements. From the above results it is seen that for an ionic strength of 0.05 there was about 10% reduction in the rate of catalysis of H_2O_2 , above this value the rate of catalysis was quite sharply diminished. This agrees with the observations by Wynne-Jones²² on the effect of NaClO_4 on the rate of decomposition with ferric perchlorate catalyst.

The Experiments were conducted varying (a) $[\text{H}_2\text{O}_2]$, (b) pH, (c) temperature and (d) $[\text{Ag}^+]$ in the bulk solution.

5. Passage of Small Currents at Catalysing Silver Electrodes.

(1) Cell Arrangement.

The apparatus shown in Fig.3 consisted of two limbs. The larger limb had three necks, one holding the silver electrode, one connected to an agar/NaClO₄ salt bridge terminating in a Luggin capillary about 0.2 mm. from the surface of the Ag catalyst. The other neck led to the soap film flow meter. Provision was also made for stirring with N₂ if required.

The smaller limb contained the Pt electrode and was connected to the larger limb via a G.4 sinter in order to prevent any escape of oxygen into the wrong limb. The half cell employed, connected by the salt bridge to the peroxide solution, was of the saturated calomel type.

The Ag and Pt electrodes were prepared by sealing 28 S.W.G. wires into glass and annealing at 500°C in the manner described above.

(ii) Electrical Apparatus.

Constant currents were drawn from a 120v. Drydex H.T. dry battery supply through a resistance selector, which contained resistances ranging from 10^a ohms. to 10^b ohms. The currents were read on a Sangamo Weston d.c. milliammeter.

(iii) Procedure.

The solution under test was placed in the reaction vessel which was inserted in the controlled water bath at 25°C

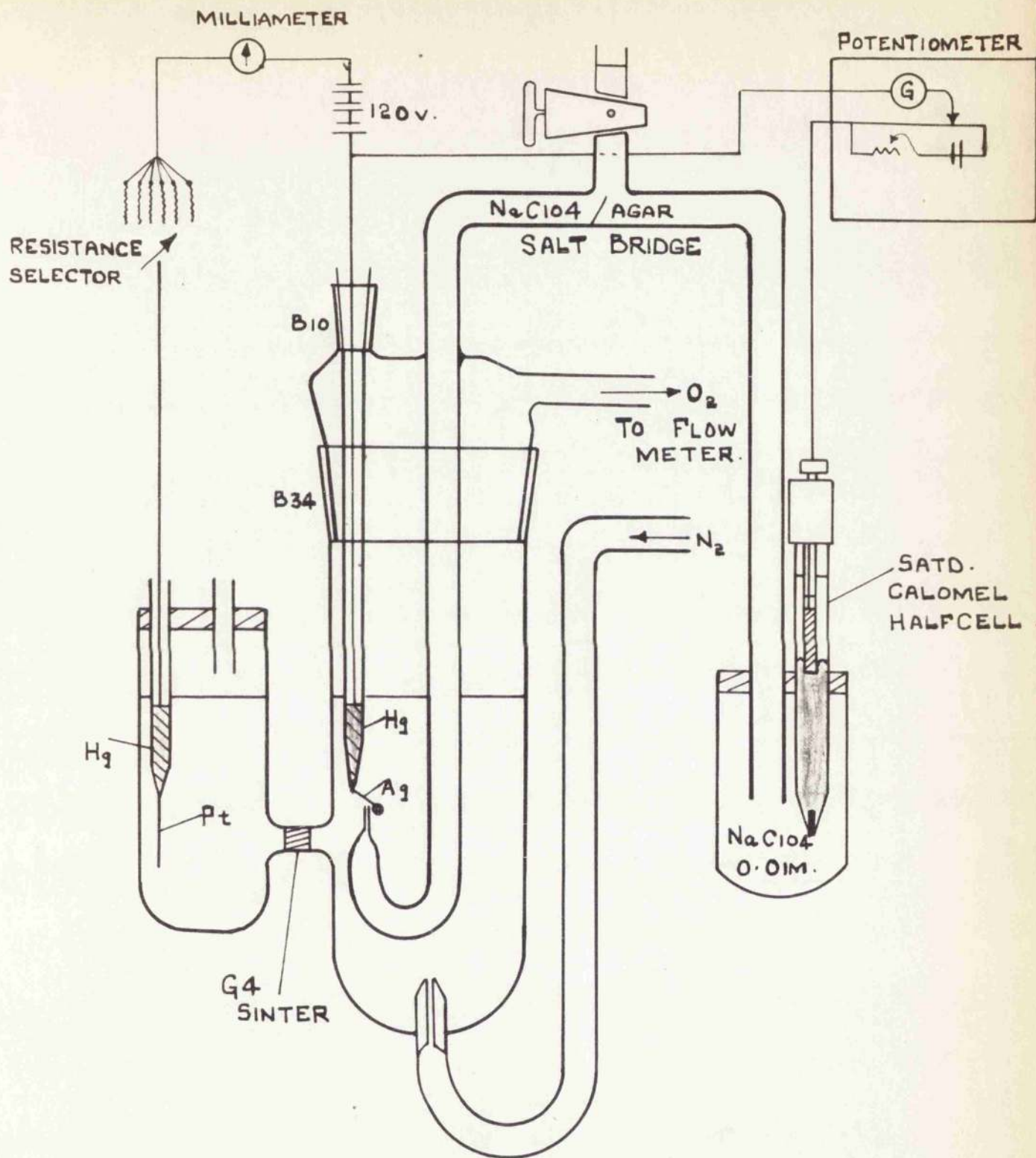


FIG. 3 APPARATUS USED FOR
CURRENT - POTENTIAL - RATE
MEASUREMENTS

$\pm .1C^\circ$ and allowed to attain equilibrium conditions. The Ag catalyst was then inserted. When equilibrium conditions had been attained i.e. steady rate of evolution of oxygen and steady e.m.f. value, these values were recorded.

With the Ag electrode connected to the positive terminal of the battery, i.e. making Ag the anode, a small positive current was passed and the corresponding steady rate and e.m.f. values were noted. Progressively larger currents were subsequently passed, and the rate and e.m.f. for each current determined. The range of current densities used was 1×10^{-3} to 1×10^{-1} m A. cm.⁻² On removal of the current the e.m.f. of the cell always returned rapidly to the original 'no current' steady value.

The same procedure was then repeated with the Ag electrode connected to the negative terminal of the battery i.e. a series of small negative currents were passed, and their corresponding steady rates and e.m.f.'s obtained.

A preliminary set of experiments were conducted varying the ionic strength of the solution from 0.01 to 1.00. The results are shown in Table II for one particular $[H_2O_2]$ and pH.

Table II.

Ionic Strength	E.M.F. at various current densities (m A. cm. ⁻²).		
	0	1×10^{-2}	1×10^{-1}
0.01	0.6040	0.5892	0.5488
0.05	0.6030	0.6021	0.5990
0.10	0.6034	0.6022	0.5997
1.00	0.6042	0.6036	0.6002

In the subsequent experiments an ionic strength of 0.05 was used in the H₂O₂ solutions under test, as it is apparent from these results that this successfully eliminated any IR potential in the solution gap between the electrode surface and the Luggin capillary during the passage of small currents.

6. Illustrating the existence of small permanent currents between adjacent anodic and cathodic type areas on the surface of a catalysing silver electrode.

It was observed, on removal of an Ag catalyst from H₂O₂ solutions of concentrations greater than 1 Molar that there were macroscopic variations in the appearance of the surface of the Ag. Two different types of areas were discernable, these areas being adjacent to each other and between them, completely covering the entire surface. One type of area was very

highly polished and smooth while the other consisted of brown discoloured etched patches. The former type of area was more deeply pitted than the latter.

This type of differentiation of electrode surface is not uncommon in the field of electro-polishing, the highly polished areas corresponding to thin anodic oxide films and the etched areas corresponding to the cathodic metal.

This has been reported by Hoar.⁶⁵

The following experiment was conducted to investigate these differing areas on the surface of a silver catalyst with a view to determining whether or not these adjacent areas were anodic and cathodic to each other.

Apparatus and Procedure.

The apparatus consisted of a reaction vessel with three necks, two to incorporate electrodes and the other for evolution of oxygen. The electrodes consisted of Ag wires, 1 cm. length of 28 S.W.G., sealed into soda glass. One electrode was treated by etching for one minute in 33M H₂O₂. The other electrode was first reduced in a muffle surface, by heating in H₂ at 250°C then anodised to a layer of Ag₂O about 246Å thick in N.NaOH by passing 1μA for 30 minutes. The calculation is as follows:-

$$\begin{aligned} Q &= I \times t = 1 \times 10^{-6} \times 30 \times 60 \text{ coulombs} \\ &= 1.8 \times 10^{-3} \text{ coulombs.} \end{aligned}$$

However 9.65×10^4 coulombs deposit 116 gms. Ag_2O .

°. 1.8×10^{-3} coulombs deposit 2.16×10^{-6} gms Ag_2O .

Density of Ag_2O = 7.27 gm. c.c.

°. Volume deposited = 2.96×10^{-7} c.c.

Area of electrode = 1.2×10^{-1} cm.²

°. Thickness of Ag_2O film = 2.46×10^{-6} cm.

Length of unit cell of Ag_2O = 4.72×10^{-8} cm. (66)

°. No. of layers = 50 (approx.)

These two electrodes were inserted in a 3M H_2O_2 solution in the reaction vessel and connected via a Weston d.c. microammeter. Readings commenced immediately and continued for some time afterwards. The oxide film electrode was positive. It was observed that most of the oxygen evolved was from the cathode.

In all cases it was found that silver was the positive electrode in cell C. In the above representation of the cells the double line denotes the elimination of liquid junction potentials between the Ag_2O solution and the reference half cell. The salt bridge is assumed to have effected this.

(b) Reproducibility, effect of time and stirring.

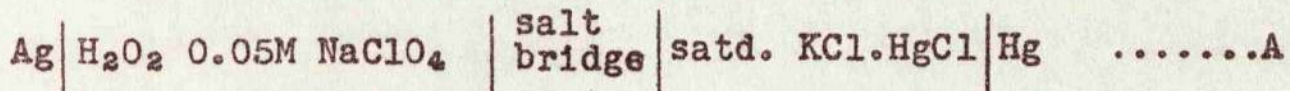
An annealed silver electrode in H_2O_2 solutions gave an easily established, well defined steady potential value within

RESULTS

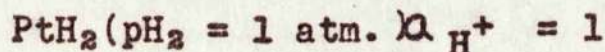
1. Equilibrium Potentials.

(a) Silver electrode equilibrium potentials.

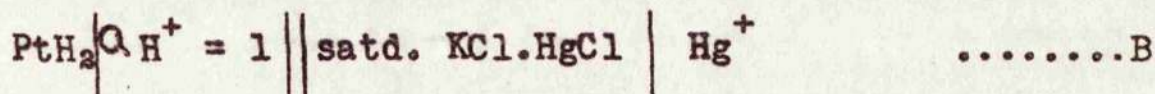
The measured e.m.f.'s refer to the cell



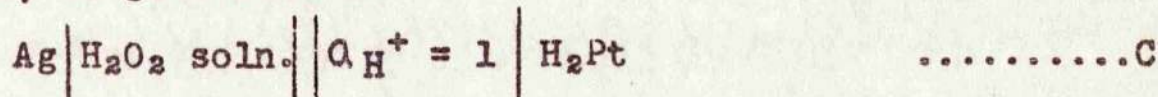
and except in the most alkaline solutions the silver electrode was the positive one. The e.m.f's were recorded in the conventional manner, as referred to the standard hydrogen electrode, viz:



Thus cell A was combined with cell B:



which has an e.m.f. of 0.242 v. at 25°C with the signs as indicated, to give cell C.



the e.m.f's of which were referred to as the electrode potentials at the silver electrode.

In all cases it was found that silver was the positive electrode in cell C. In the above representation of the cells the double line denotes the elimination of liquid junction potentials between the H₂O₂ solution and the reference half cell. The salt bridge is assumed to have effected this.

(b) Reproducibility, effect of time and stirring.

An annealed silver electrode in H₂O₂ solutions gave an easily established, well defined steady potential value within

two or three minutes of immersion. This value was reproducible to within 0.01v. A typical result is shown in Fig.4. Under these conditions steady gas evolution took place in all but very dilute solutions and this provided stirring; further stirring by bubbling N_2 through the solution did not change the potential. The initial "settling down" period depended to a certain extent on such variables as $[H_2O_2]$, pH and $[Ag^+ \text{ bulk}]$.

(c) Variation of e.m.f. with pH and $[H_2O_2]$.

The equilibrium potential results are graphed in Figs. 5 and 6. Fig. 5 shows the results obtained in the alkaline region, pH 11-14, and it is clear from the graph that the e.m.f. was sensitive to H_2O_2 in this region. The results obeyed

$$E = 0.91 - 0.059 \text{ pH} - 0.03 \log_{10} [H_2O_2]. \quad \dots\dots\dots(71)$$

as was shown from the plot of $E + 0.03 \log_{10} [H_2O_2]$ against pH. The maximum $[H_2O_2]$ used in this region was 1.6M.

Fig.6 shows a much sharper potential change with pH, for the pH region 11 to about 8.5. From pH8.5-5.5 for very dilute H_2O_2 solutions and from about pH7-1 for very high $[H_2O_2]$'s there was a virtually pH independent zone. Here the potential was very strongly dependent on $[H_2O_2]$, moving to a more positive or more highly oxidised value with increase in $[H_2O_2]$ of solutions. It is to be observed however that, even with very concentrated H_2O_2 solutions, the

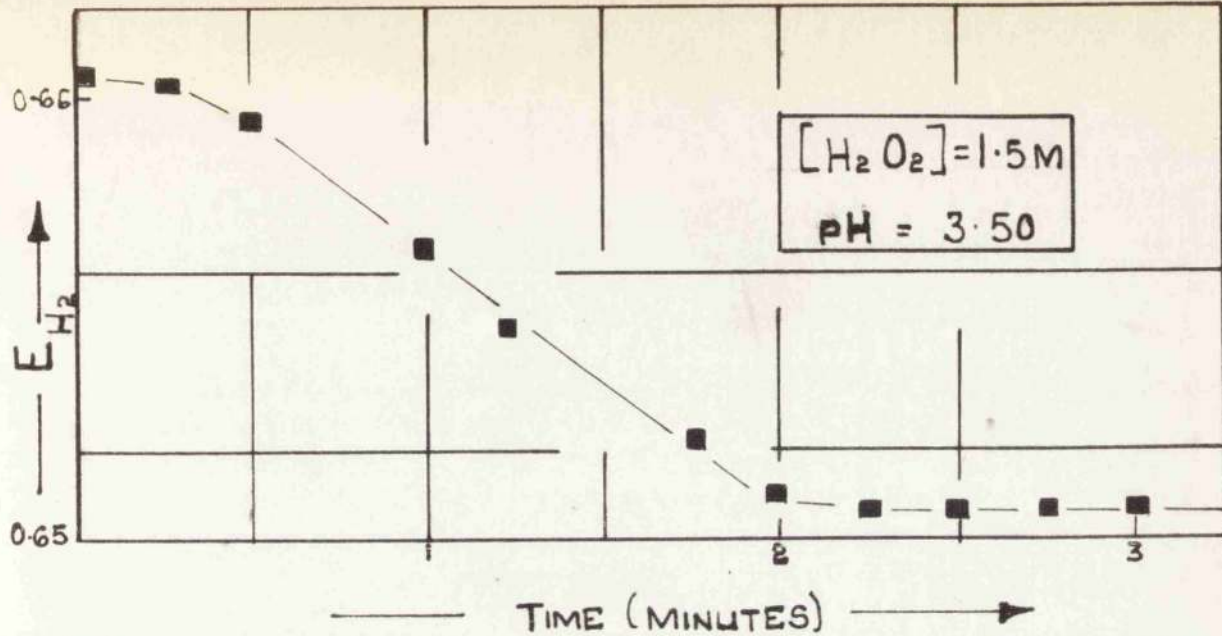


FIG. 4. SHOWING A TYPICAL CHANGE OF E.M.F. WITH TIME TO A STEADY VALUE AT 25°C.

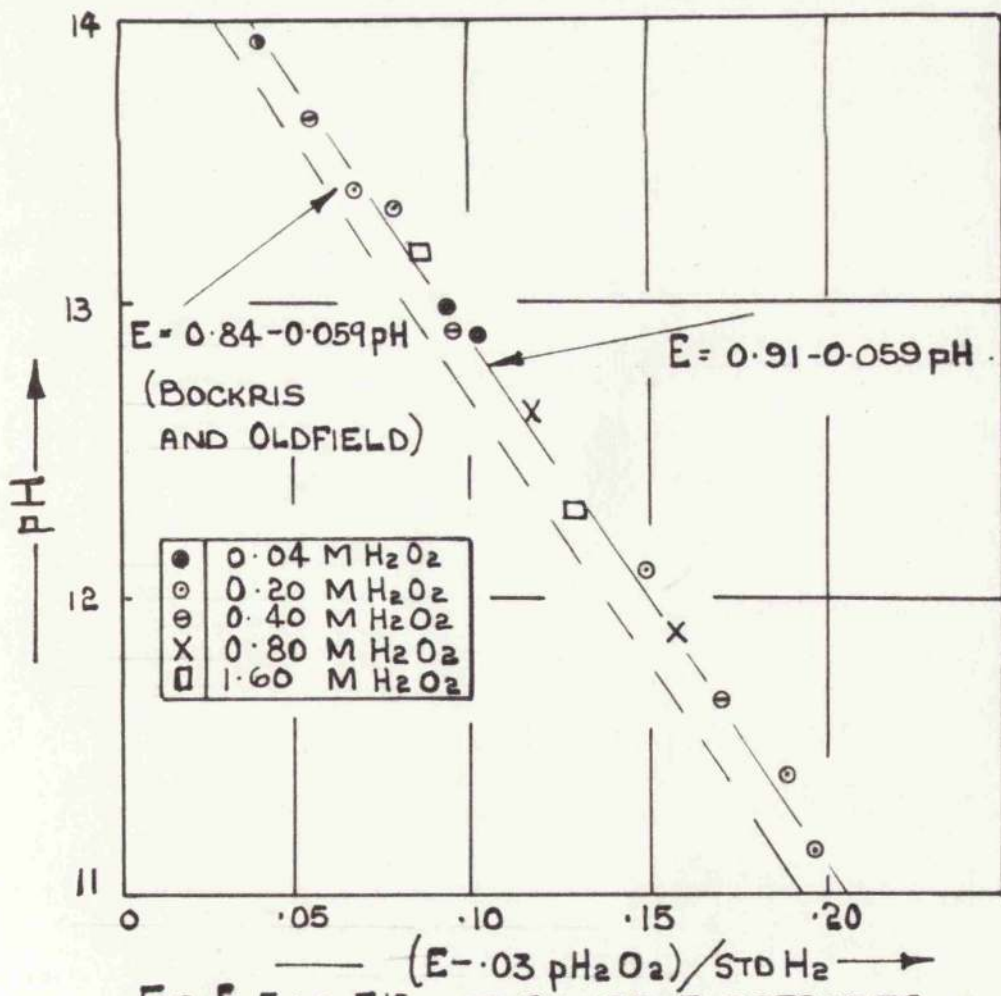


FIG. 5. E.M.F.'S AT SILVER ELECTRODES IN ALKALINE SOLUTIONS AT 25°C, ALLOWANCE BEING MADE FOR $[H_2O_2]$

THIS DEMONSTRATES ARRANGEMENT OF THE RESULTS WITH THE EQUATION

$$E = E_0 - 0.059 pH - 0.03 \text{ LOG}_{10} [H_2O_2]$$

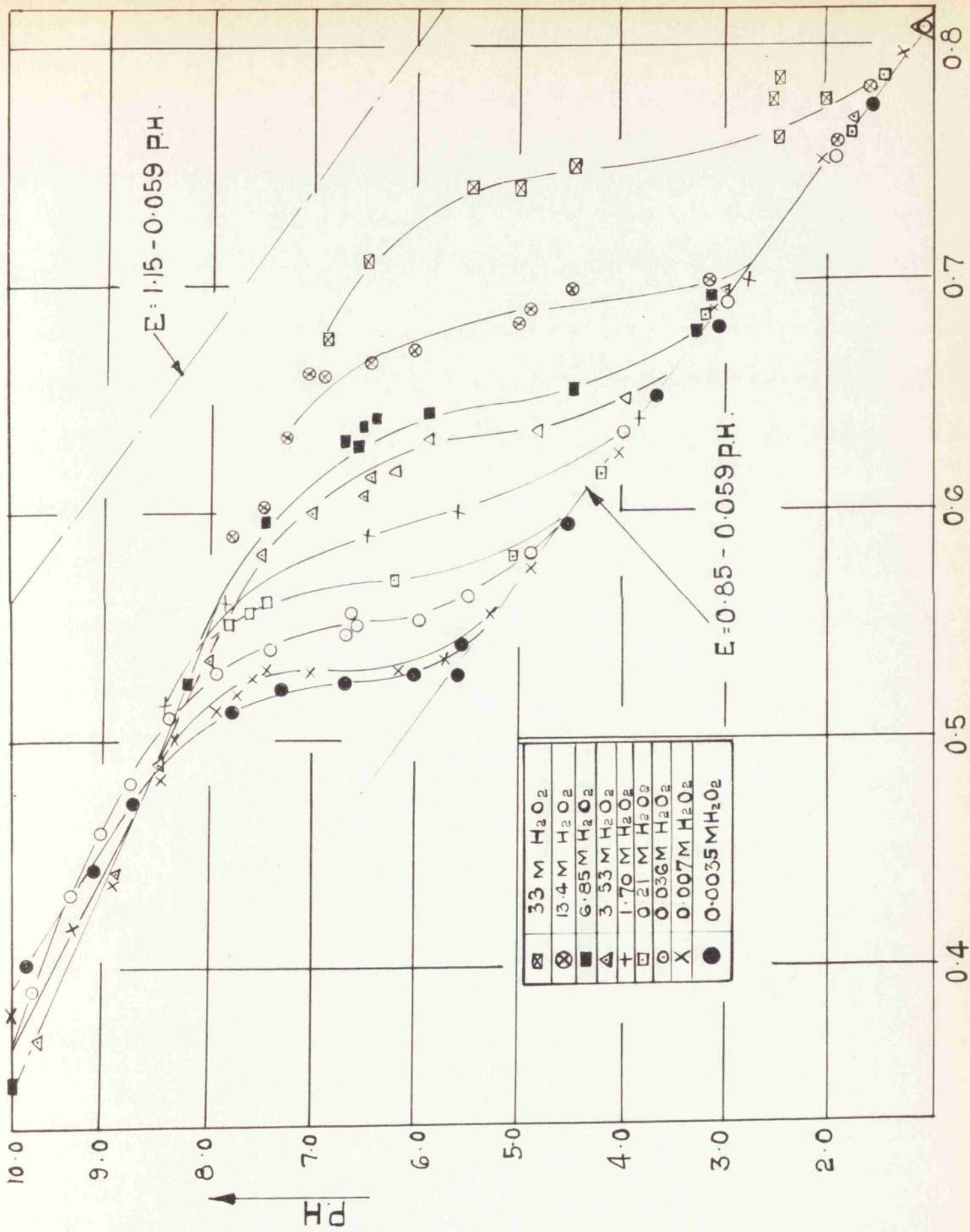


FIG. 6 SHOWING THE EQUILIBRIUM POTENTIALS OF A SILVER ELECTRODE IN H₂O₂ SOLUTIONS AT 25°C

potential never attained that value corresponding to the $\text{Ag}/\text{Ag}_2\text{O}\cdot\text{OH}^-$ equilibrium in aqueous solution. That relationship is given by

$$E = 1.15 - 0.059 \text{ pH v. at } 25^\circ\text{C} \quad (\text{Latimer}^{68}) \dots (72)$$

At pH values < 5.5 the potential / pH relationship is given by the expression:-

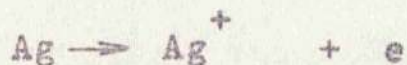
$$E = 0.85 - 0.059 \text{ pH v. at } 25^\circ\text{C}. \dots\dots\dots (73)$$

this relationship only existing if the $[\text{H}_2\text{O}_2]$ was below a certain value dependent on pH value.

(d) Variation of e.m.f. with $[\text{Ag}^+]$.

Fig. 7 shows the effect of adding silver ion, in the form of AgNO_3 , to hydrogen peroxide solutions at pH's 3.3, 5.2, and 9.25.

Small additions of Ag^+ affected the measured potential only slightly, changing it to a more positive value, but above a certain limit the effect was much more marked and the potential then became controlled by the silver electrode reaction.



whose potential is related approximately to $[\text{Ag}^+]$ by

$$E = 0.799 + 0.059 \log_{10}[\text{Ag}^+] \text{ v. at } 25^\circ\text{C} \dots\dots\dots (74)$$

From this equation one can calculate the $[\text{Ag}^+]$ corresponding with the equilibrium potential at the catalyst electrode in the absence of added Ag^+ , and this calculated value must be

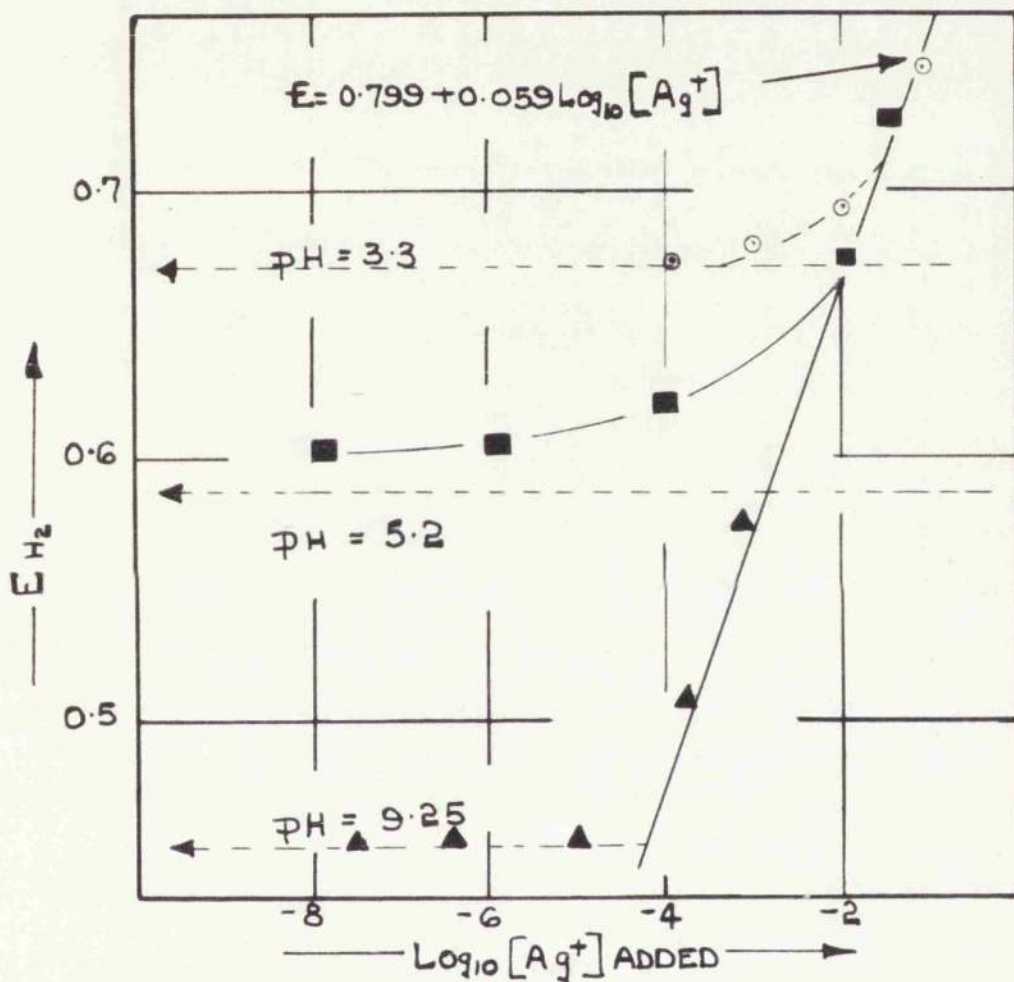


FIG 7 THE EFFECT OF ADDED Ag^+ ON EQUILIBRIUM POTENTIALS AT CONSTANT pH VALUES AT 25 C.

interpreted as the $[Ag^+]$ at the electrode surface resulting from the tendency of the metal to pass into solution during the catalytic action. It is noted that it is this value of the bulk $[Ag^+]$ which must be exceeded before the electrode potential is markedly raised.

(e) Effect of temperature on e.m.f. at silver electrodes.

Experiments were conducted at 25°C and 0°C. The results at 25°C are as shown in Figs. 5 and 6. In Fig. 8 the results at 0°C for 0.48M solution are shown or it is seen that the "step" in results obtained at higher temperatures was almost eliminated, the relationship between potential and pH being given by

$$E = 0.81 - 0.054pH \quad \dots\dots\dots(75)$$

The rate of evolution of oxygen was very much lower at 0°C.

(f) Electrode potential measurements on platinum

An annealed Pt electrode gave a steady potential value, reproducible to $\pm 0.02v$. after approximately 10-15 minutes in solution. Stirring was found to be necessary to prevent drift.

The results are shown in Fig. 9, for a $[H_2O_2]$ range from $3 \times 10^{-6}M$ to 33M, and over a pH range from 0-9.5. Generally the features are the same as those obtained on silver but the "step" is less pronounced and the rate of evolution of oxygen is much less.

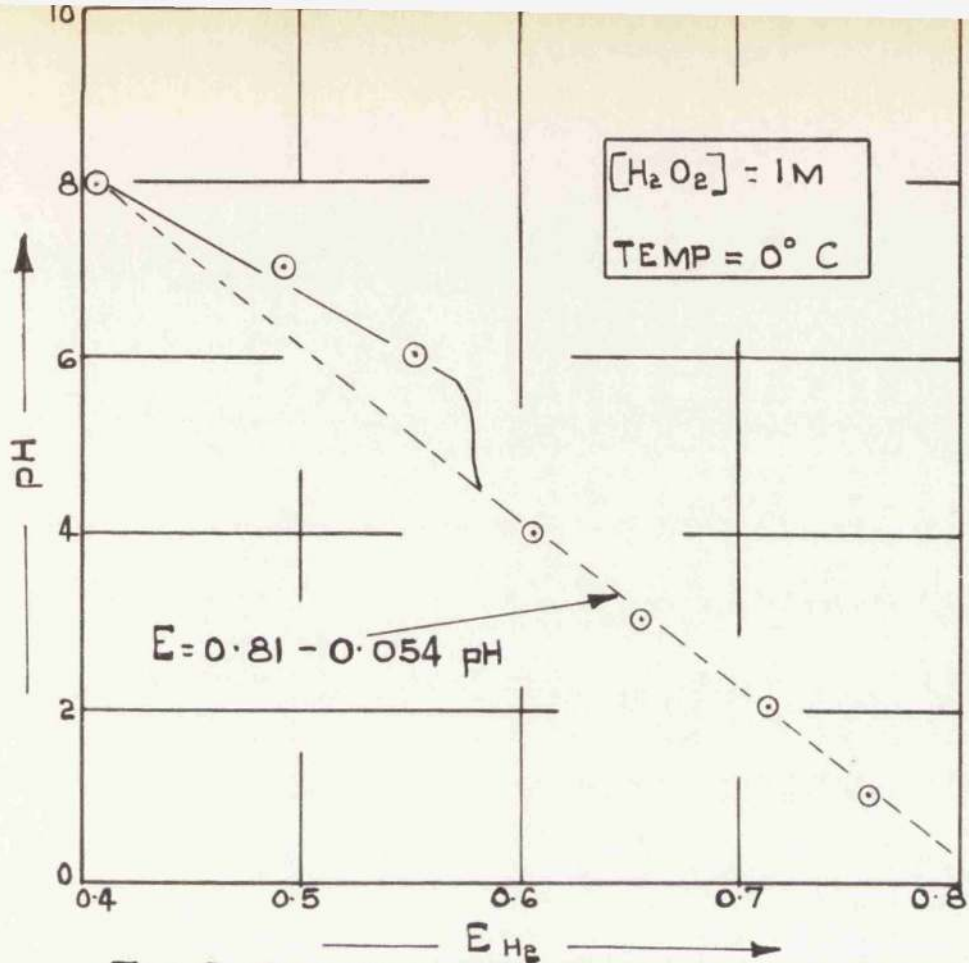


FIG. 8 THE EQUILIBRIUM POTENTIAL VALUES OF A SILVER ELECTRODE IN H_2O_2 AT 0°C.

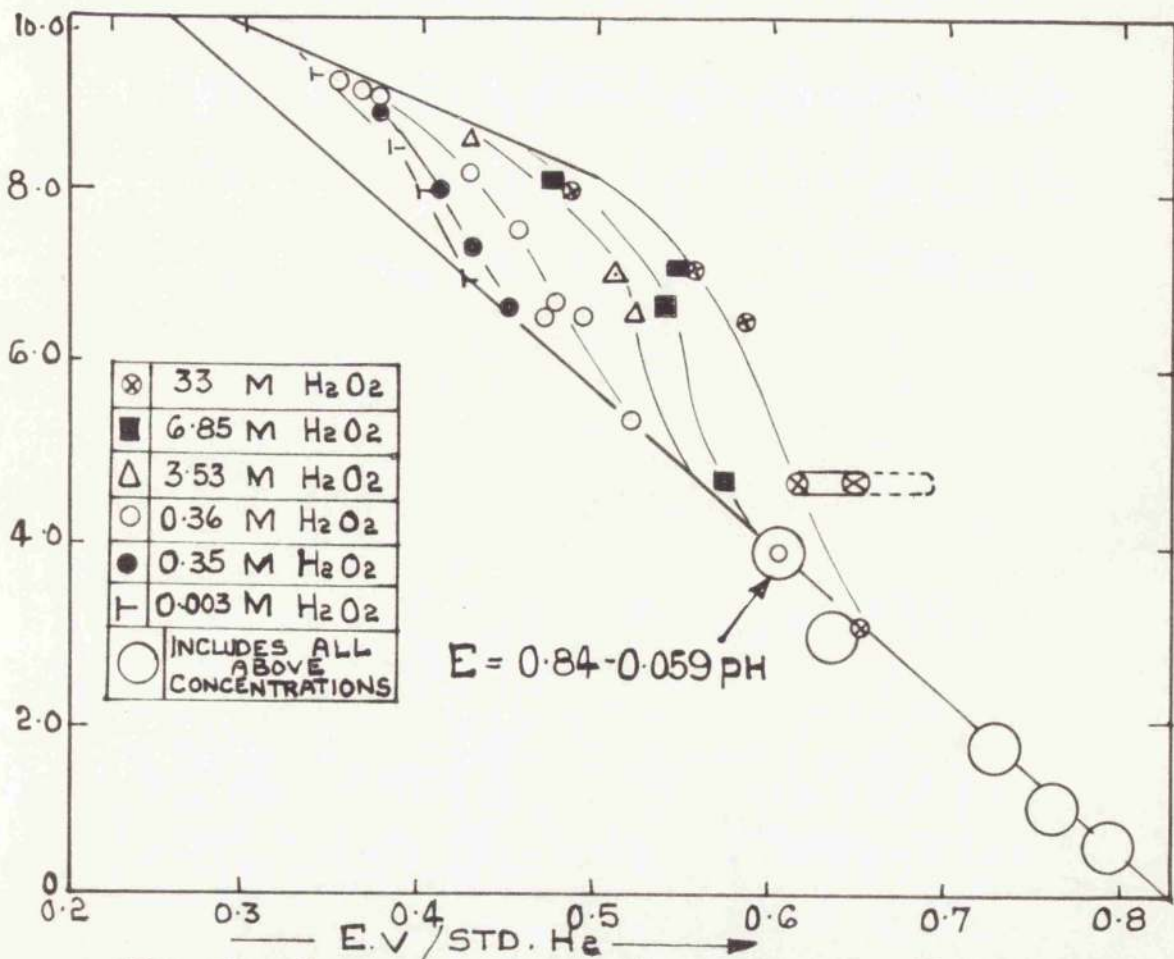


FIG. 9. SHOWING THE ELECTRODE POTENTIALS OF A PLATINUM ELECTRODE IN H_2O_2 SOLUTIONS AT 25°C.

In the pH range 0-6.5, the following $[H_2O_2]$ independent relationship was found

$$E = 0.84 - 0.059pH \text{ v. at } 25^\circ\text{C} \dots\dots\dots (76)$$

i.e. when the $[H_2O_2]$ is below a critical value which varies with pH.

In the pH regions 9.7-6.5, for very dilute H_2O_2 , and 3-3, for very concentrated H_2O_2 solutions, the same type of "step" in potential values was recorded as was observed with Ag electrodes, but with Pt there was still a definite pH dependence even in this region especially with dilute H_2O_2 solutions.

(g) Comparison of electrode potentials of metals in H_2O_2

The results of the equilibrium potential measurements on the catalytic metals Ag, Pt, Cu, Au and Ni and those of the non-catalytic metals Al and Sn are shown in Table 1 below.

TABLE 1.

$[H_2O_2] = 2M$ $pH = 3.00$ $Temp. = 25^\circ\text{C}.$		
Metal	Steady Potential in volts.	Remarks.
Silver	0.68	Vigorous Catalysis.
Platinum	0.67	Moderately rapidly reached
Gold	0.67	Moderately rapidly reached
Copper	0.70	Moderately rapidly reached
Iron	0.71	Moderately rapidly reached
Nickel	0.68	Slowly reached
Aluminium	-0.02	Slowly reached
Tin	0.25 0.44	Freshly immersed Sn became blackened showing evidence of impurities in this case.

From the above results it is apparent that any catalytic metal, although differing greatly in catalytic activity, yielded electrode potential values of the same order of magnitude. The truly non-catalytic metals, such as Al and Sn did not permit a similar steady potential value to be reached but gave unsteady metal-dependent values, showing that a more reducing condition was being maintained.

2. Rate of Oxygen Evolution at a Silver Electrode

Throughout the rate studies the rate of decomposition has been taken as the rate of loss of oxygen from the H_2O_2 whereas in fact:

$$\frac{-d[H_2O_2]}{dt} = r_1 + r_2$$

where $r_1 = do_2/dt$ i.e. rate of evolution of oxygen and

$r_2 = r_{Ag}$, the rate of solution of silver. This point will be discussed later, but for the present one may note that $r_1 \gg r_2$ in all cases met with in this work. For this reason r_2 has been ignored when considering the rate of decomposition or have regarded r_1 as a sufficient measure of it.

(a) Reproducibility, effect of stirring, routes to steady rate of catalysis.

Steady rate measurements on silver catalysts annealed in a pure atmosphere at $500^\circ C$, etc., then immersed in H_2O_2 solutions, showed an excellent degree of reproducibility and generally stirring had no effect on the rate of catalysis,

except in very dilute solutions, as the evolved oxygen bubbles appeared to act as effective stirring agents.

Generally 20-30 minutes elapsed since the moment of immersion to the commencement of a steady rate of catalysis, although with higher $[H_2O_2]$'s and at highly acid pH values, this period was reduced to 5-10 minutes.

A striking feature of this series of measurements is illustrated by Fig. 11, which shows the various routes by which the steady state was attained. It may again be emphasised here that catalyst size and H_2O_2 volume were controlled such that there was only a negligible change in the pH value of the solution, even under fairly corrosive conditions, i.e. high $[H_2O_2]$ and low pH values.

From Fig.11 it is observed that four possible routes to equilibrium conditions were detected. These are enumerated as follows:

- (i) Route A:- here the initial rate value gradually increased to the steady rate value. This was observed generally for H_2O_2 solutions of concentrations $< 3M$ and $pH < 7$.
- (ii) Route B:- the initial rate value gradually decreased to the steady rate. This was observed for $[H_2O_2] > 0.2M$ and $pH > 7$.

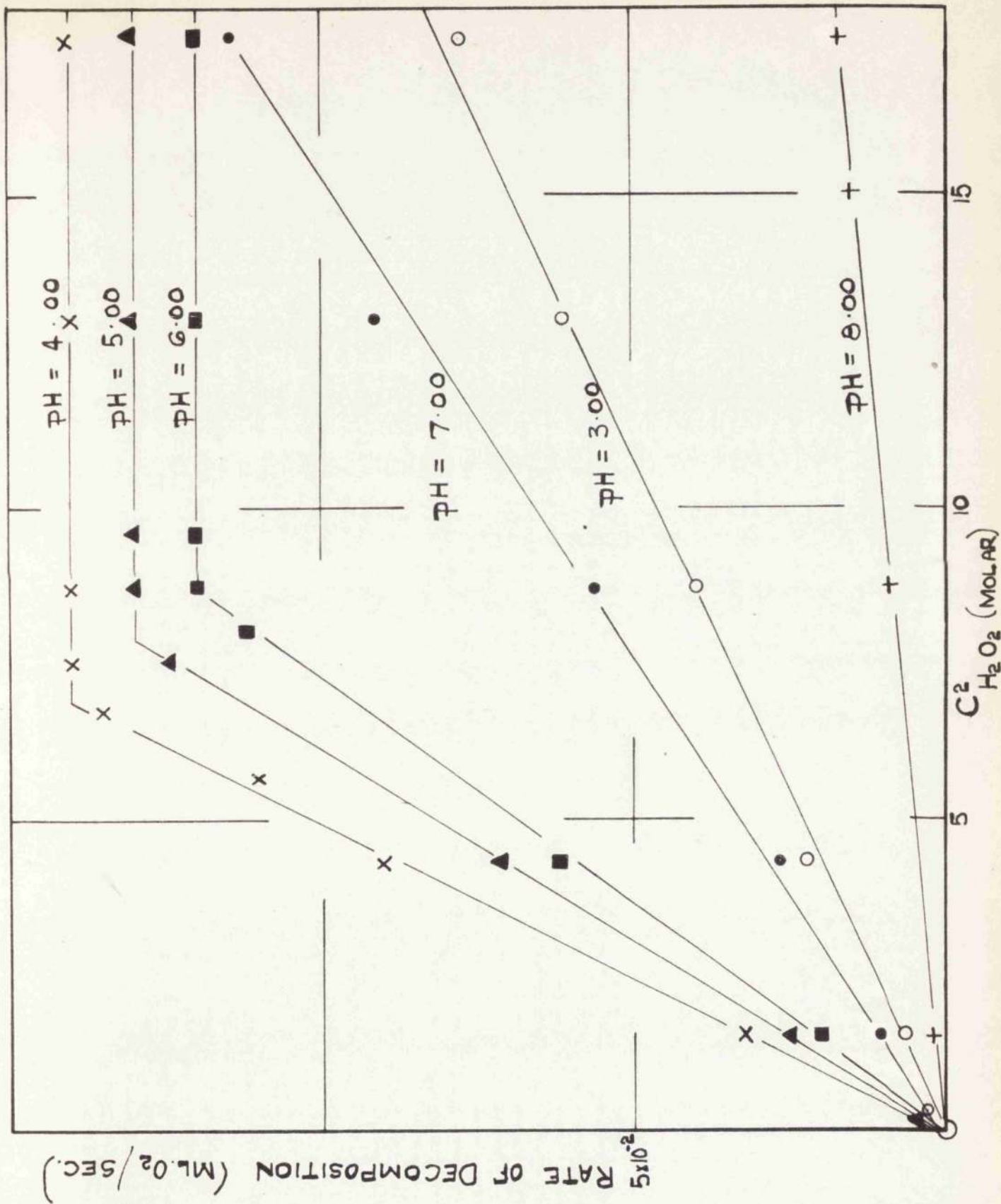


FIG 10 SHOWING THE KINETIC ORDERS OF REACTION AT 25°C

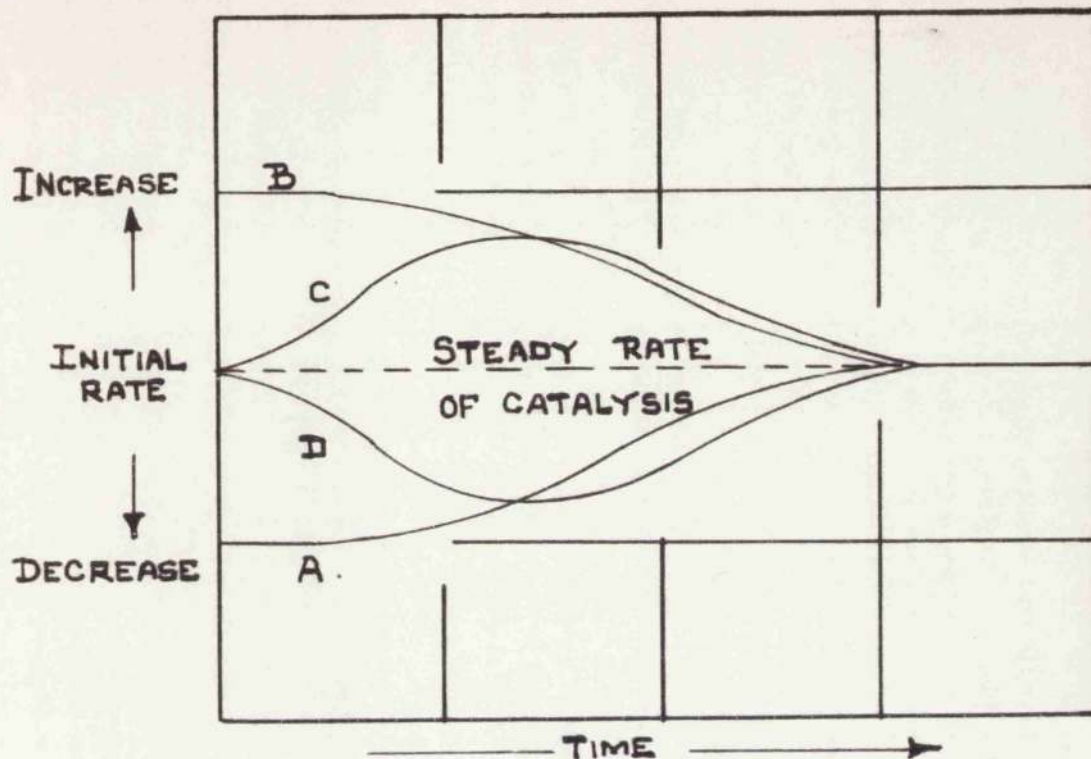


FIG. II. ILLUSTRATING POSSIBLE ROUTES TAKEN TO ATTAIN A STEADY RATE OF CATALYSIS.

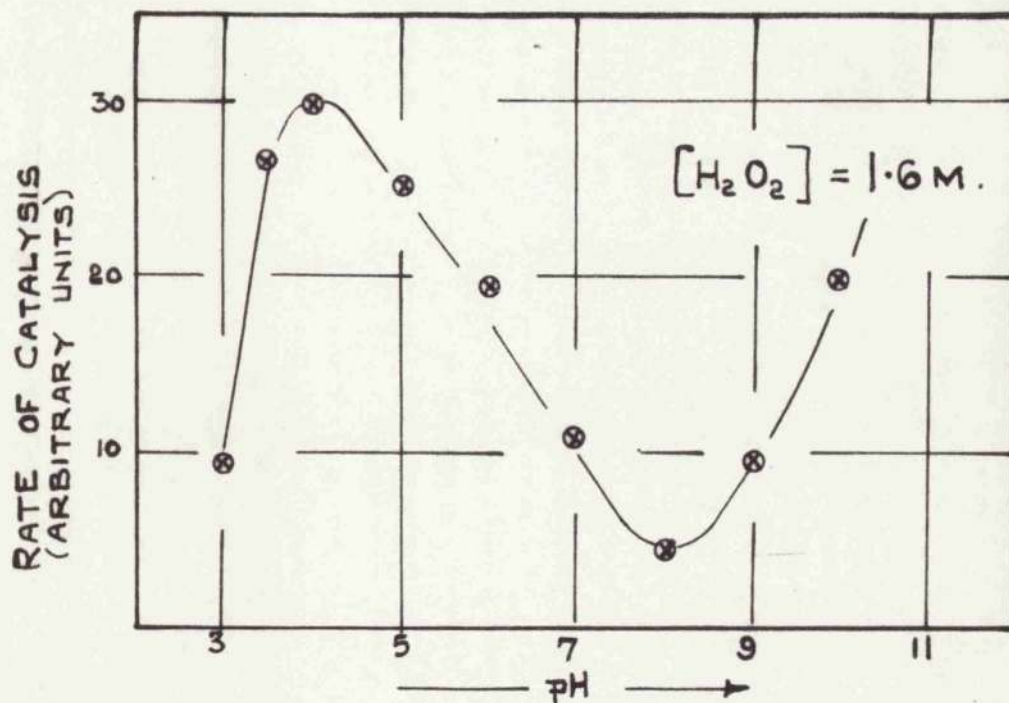


FIG. 12 SHOWING THE EFFECT OF $[H^+]$ ON STEADY RATES OF CATALYSIS.

(iii) Route C:- the initial rate increased for a period, then gradually decreased again to a steady value which was of the same order of magnitude as the initial value. This particularly occurred at pH = 3 for H_2O_2 concentrations between 0.2M and 1M.

(iv) Route D:- The initial rate decreased for a time then recovered to a steady value - the same relationship holding between initial and steady values as in (iii) above. This type happened particularly at pH 4-6 for $[H_2O_2] = 3M$.

(b) Dependence of rate on $[H_2O_2]$

It was observed that above a certain concentration of H_2O_2 in the medium acid range of pH values (4,5,6) the rate of O_2 evolution was independent of $[H_2O_2]$. i.e. the kinetic order of the process was zero. In both more acid and more alkaline solutions zero order range was not reached. At lower $[H_2O_2]$ in all solutions a very clear second order dependence on $[H_2O_2]$ was found. There was no range of first order dependence. This is shown in Fig.10 where the rate of oxygen evolution is plotted against $[H_2O_2]^2$ for pHs 3 to 8.

As the $[H_2O_2]$ was increased the rate rose slowly declined to an almost steady limiting rate value.

(c) Variation of rate of catalysis with pH.

Fig. 12 shows the effect of varying the $[H^+]$ of a 1.6M H_2O_2 solution on the corresponding steady rate of catalysis. The maximum rate was at a pH of approximately 4, and a minimum rate occurred at pH = 8 (approx.).

It is seen that there was a very sharp rise in rate of catalysis in changing from pH 3 to 4, the rate being actually trebled. After the maximum at pH = 4 a relatively slow, almost linear, decline occurred until the minimum value at pH = 8, the rate value then only being $\frac{1}{7}$ of that at pH = 4. After pH = 8 an increase in rate occurred and was of the same order as the decline immediately preceding it.

(d) Effect of temperature on rate of catalysis.

The effect of temperature on the rate of catalysis in the zero order range is seen in Fig. 13 (for a 4M solution at pH 4) where from an Arrhenius type plot of $\log_{10}(\text{rate})/1/T$, the energy of activation was calculated to be 19.5 kcal.mol.⁻¹. The temperature range covered was 10-25°C.

(e) Effect of $[Ag^+]$ on rate of catalysis.

Fig. 14 shows the effect of added Ag^+ in the solution in the form of $AgNO_3$, on the steady rates of catalysis at pH's 2, 3, and 4. For pH's 3 and 4 it is observed that on very small additions of Ag^+ , sharp depressions in rates occurred. As the $[Ag^+]$ was increased the rate more slowly declined to an almost steady limiting rate value.

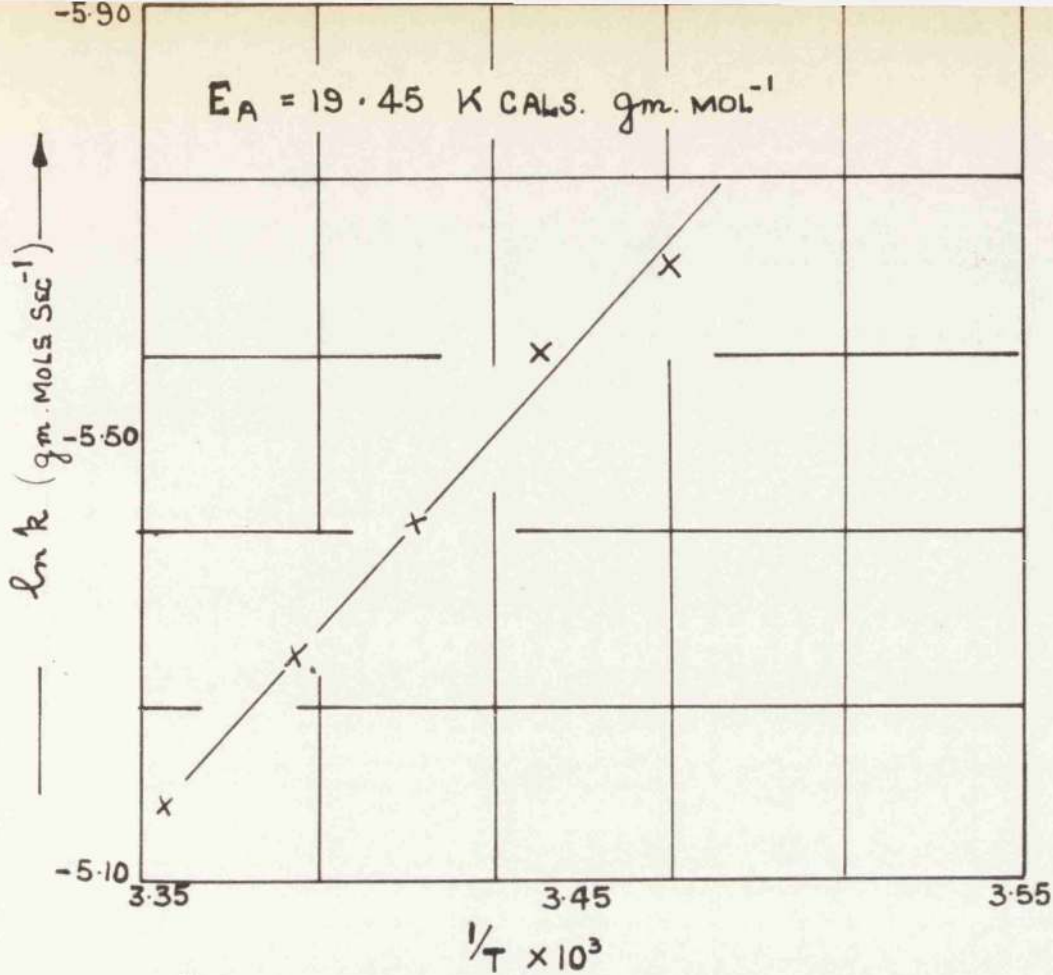


FIG. 13 SHOWING THE ARRHENIUS PLOT TO DETERMINE THE ACTIVATION ENERGY, OVER THE TEMPERATURE RANGE 10-25°C

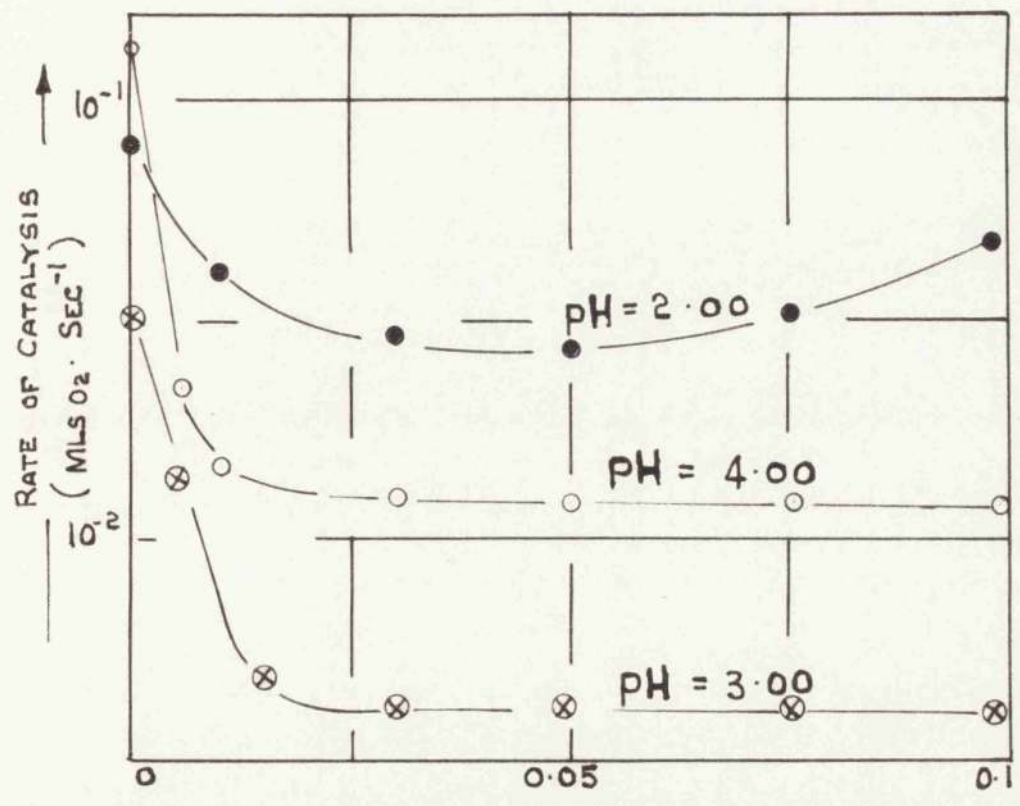


FIG 14 SHOWING THE EFFECT OF ADDED AG⁺ ON THE STEADY RATE OF CATALYSIS .

At pH = 2 the effect of a continued addition of Ag^+ after a critical $[\text{Ag}^+]$ was exceeded there was an increase in the rate of catalysis.

Generally, during catalysis of H_2O_2 by a solid silver catalyst, large oxygen bubbles are evolved from the catalyst surface, i.e. aggregates of many much smaller bubbles. However at pH = 2 when the increase in rate occurred, the mode of oxygen evolution changed and instead of single large spheres evolve, many tiny bubbles were very rapidly evolved.

The reason for investigating the effect of added $[\text{Ag}^+]$'s to bulk solutions of acid and not alkaline H_2O_2 solutions was that at pH = 6 and above homogeneous catalysis set in when $[\text{Ag}^+]$ in the bulk solution exceeded 1×10^{-3} gm. mols.litre⁻¹.

3. Effect of current flow on catalytic behaviour of silver electrodes.

(a) General.

The effect of small anodic or cathodic currents on the rate of catalysis at a silver electrode was usually quite marked. Fig.15 illustrates a typical example using 0.9M H_2O_2 (0.05M in NaClO_4) at pH6. Oxygen evolution is seen to be sharply increased by quite small anodic (i_a) current densities (electrons withdrawn from the metal electrode) while a small suppression of the rate of oxygen evolution is

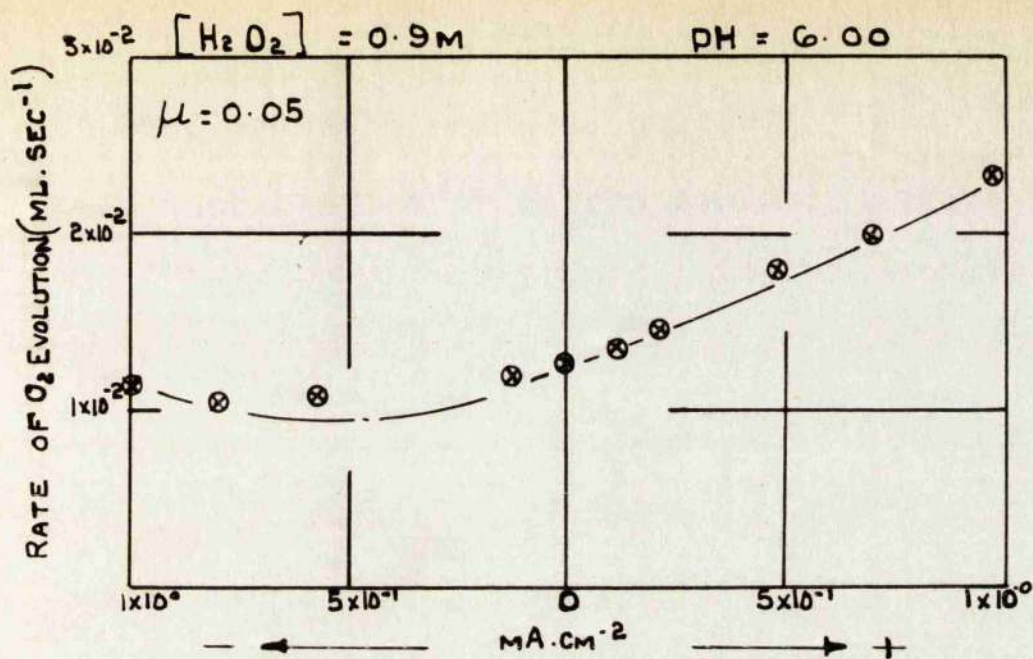


FIG. 15 THE EFFECT OF SMALL CURRENTS ON THE RATE OF EVOLUTION OF OXYGEN AT A SILVER CATALYST AT PH = 6.00 AT 25° C.

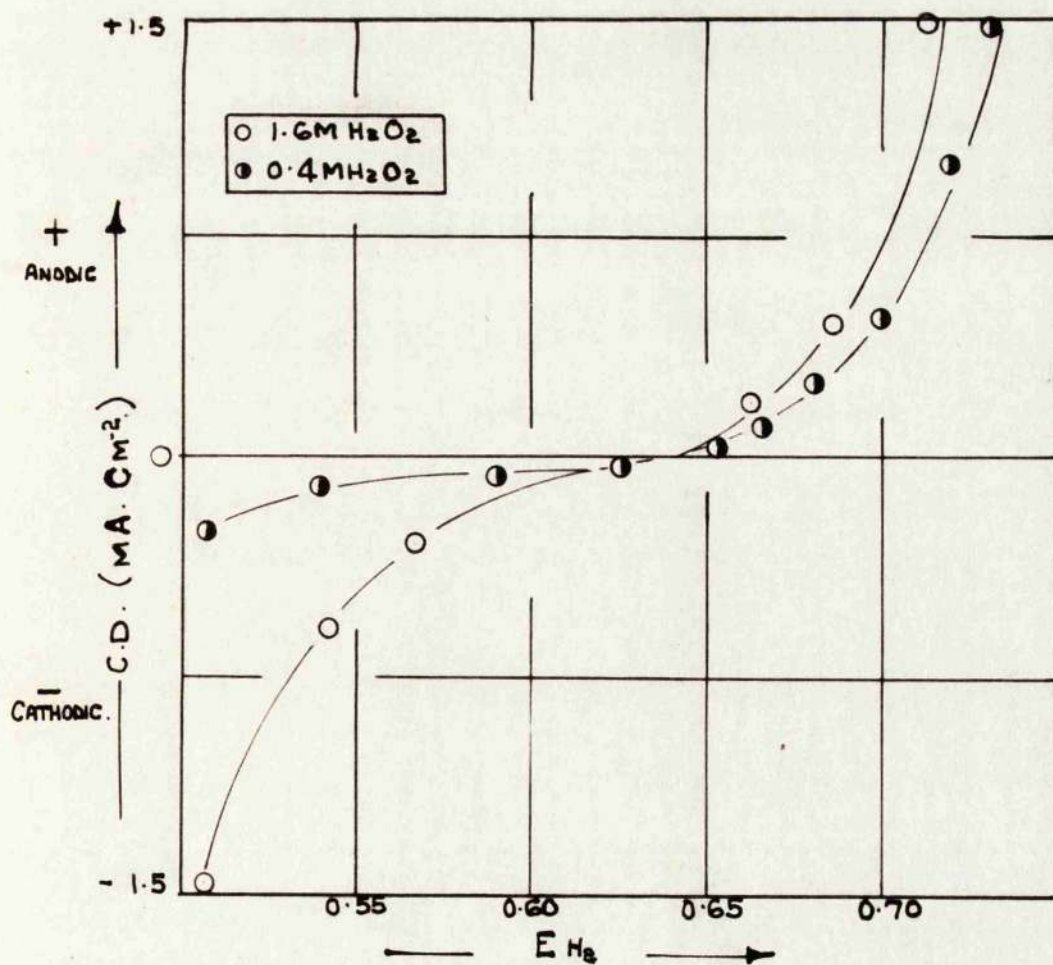


FIG. 16 CURRENT - POTENTIAL CURVES FOR TWO H_2O_2 CONCENTRATIONS AT PH = 4.00.

effected by small cathodic currents (i_c). Larger i_c cause acceleration of oxygen evolution again. Fig.16 shows the effect on the equilibrium electrode potential of small currents.

This section of the results describes experiments made with a view to using the measured effects of current flow on oxygen production, and also on other variables such as electrode potential and silver dissolution as a means of securing further evidence about the surface reaction.

(b) Reproducibility of small current behaviour.

On passing a small positive or negative current at a silver electrode, in dilute aqueous H_2O_2 solutions, the electrode potential immediately attained a well defined value corresponding to the magnitude of the current density and reproducible to within 0.02 v. Also, for a particular current density, the rate of evolution of oxygen yielded a consistently reproducible corresponding value.

On removal of the current, the electrode potential immediately recovered 70% of its original "no-current" equilibrium value and within 2-3 minutes had completely resumed it. Also the rate of oxygen loss resumed its original value, but more slowly taking 5-10 minutes to accomplish this.

These effects illustrate the non-permanent effect of small anodic or cathodic currents on a silver electrode.

Moreover, when passing a series of currents, the potential and rate values corresponding to a particular current density will always be attained whether or not that particular current is immediately assumed or reached after several intermediate currents have been passed.

(c) The effect of small anodic currents on the electrode potential with $[H_2O_2]$ and pH.

Fig.16 shows the effect of $[H_2O_2]$ on the current-potential curves at pH 4.00 for two solutions of 0.4 and 1.6M respectively. These curves are typical of results obtained in the pH range studied i.e. 2-7.

From the graph it is observed that the $[H_2O_2]$ affects the cathodic polarisation to a much greater extent than the anodic, although in both cases the potential-current change is greatest in the region of the equilibrium potential, i.e. the smallest currents produce the largest dE/di decrements or increments.

Fig. 17 shows the effect of pH on the current potential relationship for a 1.6M H_2O_2 solution at pH's 4, 5 and 6. As above the greater effects take place on the cathodic side. There appears to be almost no effect in the anodic regions. Also again the largest dE/di values take place in the region of the "no-current" potential value.

When considering figs.16 and 17 one must bear in mind that the potential - pH relationship given by

$$E = 0.085 - 0.059 \text{ pH} \quad \dots\dots\dots(73)$$

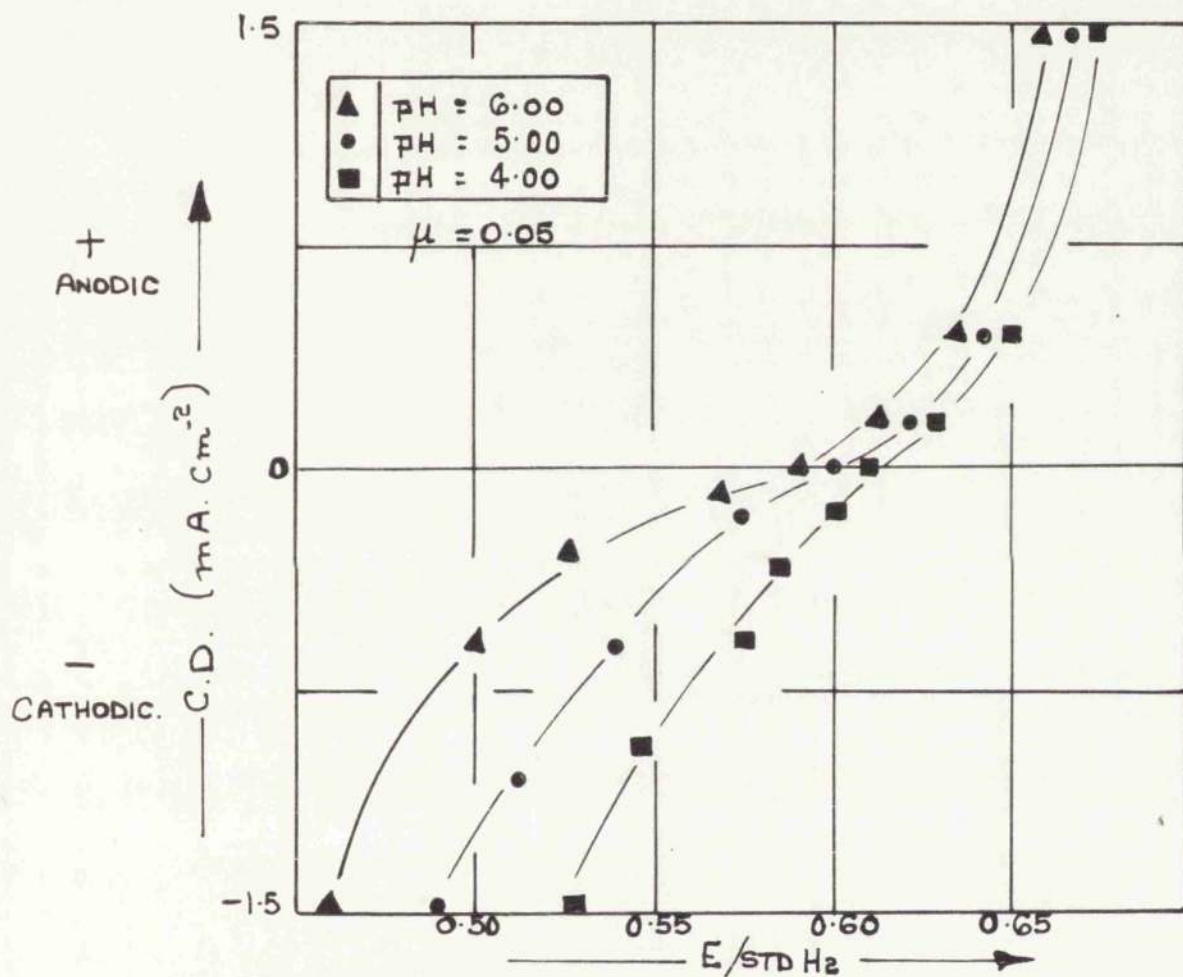


FIG. 17 THE EFFECT OF CURRENTS ON POTENTIAL
AT A SILVER ELECTRODE AT DIFFERENT pH VALUES
FOR A 1.6M H₂O₂ SOLUTION AT 25° C .

is generally not obeyed (cf. fig.6)

(d) Determination of exchange currents.

The exchange current at the electrode is defined as that corresponding to the equal and opposite velocities of the anodic and cathodic transformations going on simultaneously.^{6a} When there is no resultant (overall) cathodic or anodic flow of current at the electrode, clearly $i_r = 0$, $i_c = i_a = i_e$ where i_e is the exchange current and i_r is the resultant or measured current, zero in the equilibrium case, i.e. when the electrode potential is E' .

Strictly the definition given here ought to be applied to a single reversible electrode reaction, i.e. the reaction which controls the electrode potential at equilibrium but in the present sense in which it is being used the application extends to a polyelectrode in which there may be several separate anodic and cathodic transformations involving electrons. Thus we must consider the H_2O_2 process as well as the Ag/Ag^+ process to mention, at this stage, only two possible processes.

The total anodic currents are then determined by the electrode potential, thus

$$i_a = i_0' \exp. (\alpha' n' EF/RT) + i_0'' \exp. (\alpha'' n'' EF/RT) + \dots \quad (77)$$

where the primes refer to the different electrode transformations. This may be put in the form

$$i_a = \exp. \frac{EF}{RT} (\alpha' n' + k' + \alpha'' n'' + k'' + \dots) \dots\dots (78)$$

where the values of 'k' take account of the different i_0 values associated with the different processes. $k' = \ln i_0'$ etc.

$$\ln i_a = \frac{EF}{RT} (\alpha' n' + \alpha'' n'') + \ln i_0' + \ln i_0'' \dots\dots\dots (79)$$

and a graph of $\log_{10} i$ against E , when E is well on the anodic side, should have a slope of $\frac{2.3F}{RT} (\alpha' n' + \alpha'' n'' + \dots)$ and an intercept at $E = E'$ of $(\log_{10} i_0' + \log_{10} i_0'' + \dots)$.

For the sake of simplicity $\alpha' n' + \alpha'' n'' + \dots$ is referred to as αn , the resultant values and the sum of the current terms as $\log_{10} i_a$ where i_a is the resultant exchange current.

Similarly for cathodic conditions. For the cathodic process β is used instead of α as the asymmetry factor.

(e) Variation of the exchange current with pH and H_2O_2 .

Fig.13 shows the current potential results obtained over the pH range 2-7 for a 1.6M H_2O_2 solution at 25°C in the form of a graph of \log_{10} .C.D. against E.M.F. Intersection of the extrapolated linear portions of the anodic and cathodic controlled regions yields the exchange current value at each pH. From the graph it is observed that $dE/d \ln i$ is independent of pH over the range studied, although there is a fourfold increase in the exchange current values in passing from neutral or slightly acid solutions to the highly acid

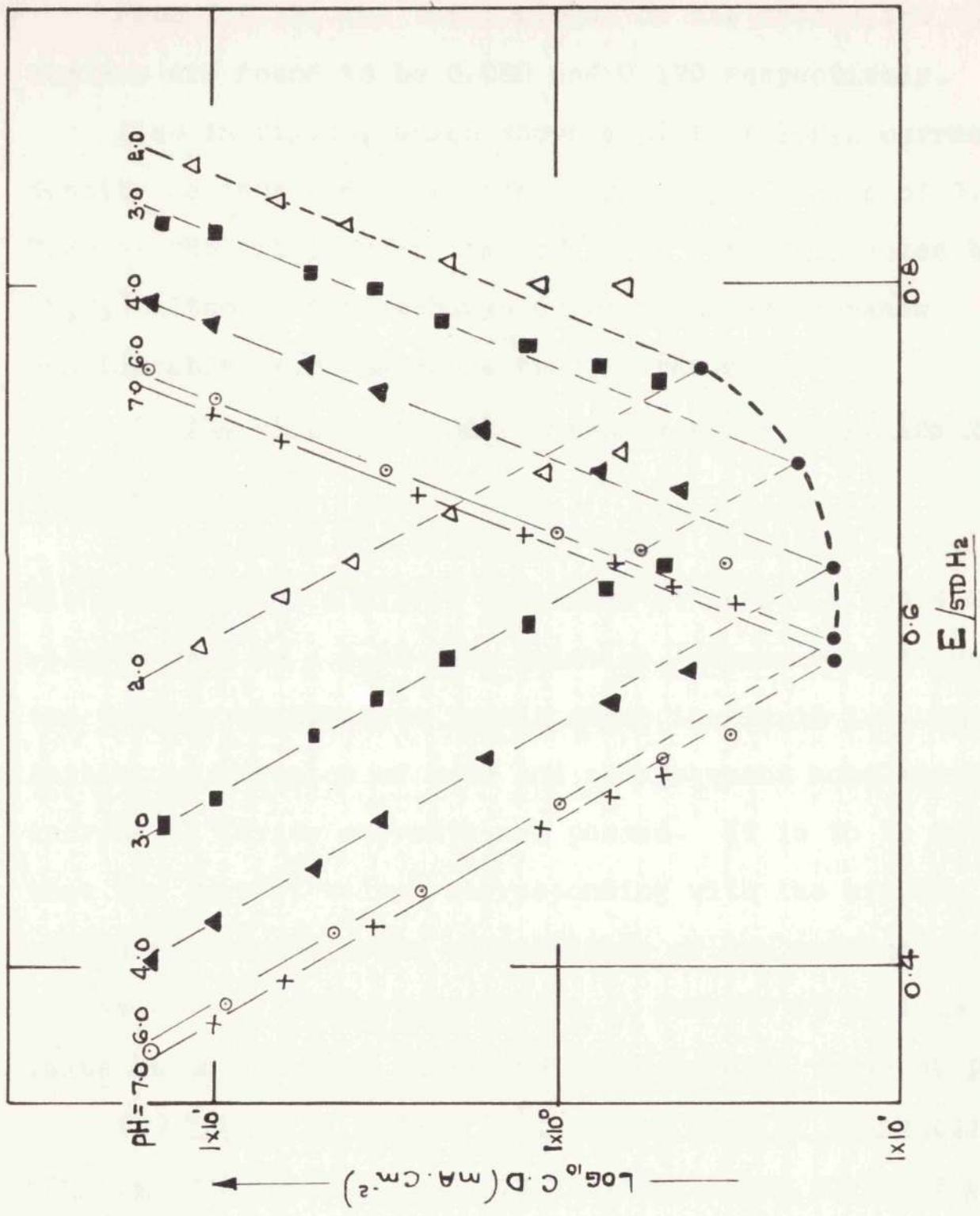


FIG 18 SHOWING THE VARIATION OF THE "EXCHANGE CURRENT VALUES WITH pH FOR A 1.6M H₂O₂ SOLUTION AT 25°C.

conditions at pH = 2.

From fig.18, the Tafel slopes of the anodic and cathodic regions are found to be 0.080 and 0.120 respectively.

Also in fig.19, which shows a plot of \log_{10} current density against over potential for a $[H_2O_2]$ range of 0.4 to 7.6M at pH6, it is seen that $dE/d\log_{10}i$ is unaffected by $[H_2O_2]$ although the exchange current values increase considerably over the concentration range.

(f) The effect of small negative currents on the rate of decomposition.

Fig.20 shows the results obtained on passing small cathodic currents and a silver electrode at pH's 1.8 and 4.0 respectively in a 0.5M H_2O_2 solution. These results confirm the earlier qualitative result shown in fig.15 i.e. immediate initial suppression of rate and a subsequent acceleration as increasing larger currents are passed. It is to be noted that the current values corresponding with the minimum rate values are of the order of magnitude of the exchange current values at the appropriate pH's i.e. current at minimum rate value at pH 1.8 3-4 times the corresponding value at pH4.

(g) Effect of added $[Ag^+]$ on the rate of decomposition and electrode potential, when small negative currents are flowing.

Fig.21 shows the effect of small negative currents on rate in a 2.45M H_2O_2 solution at pH3 with Ag^+ added to the solutions

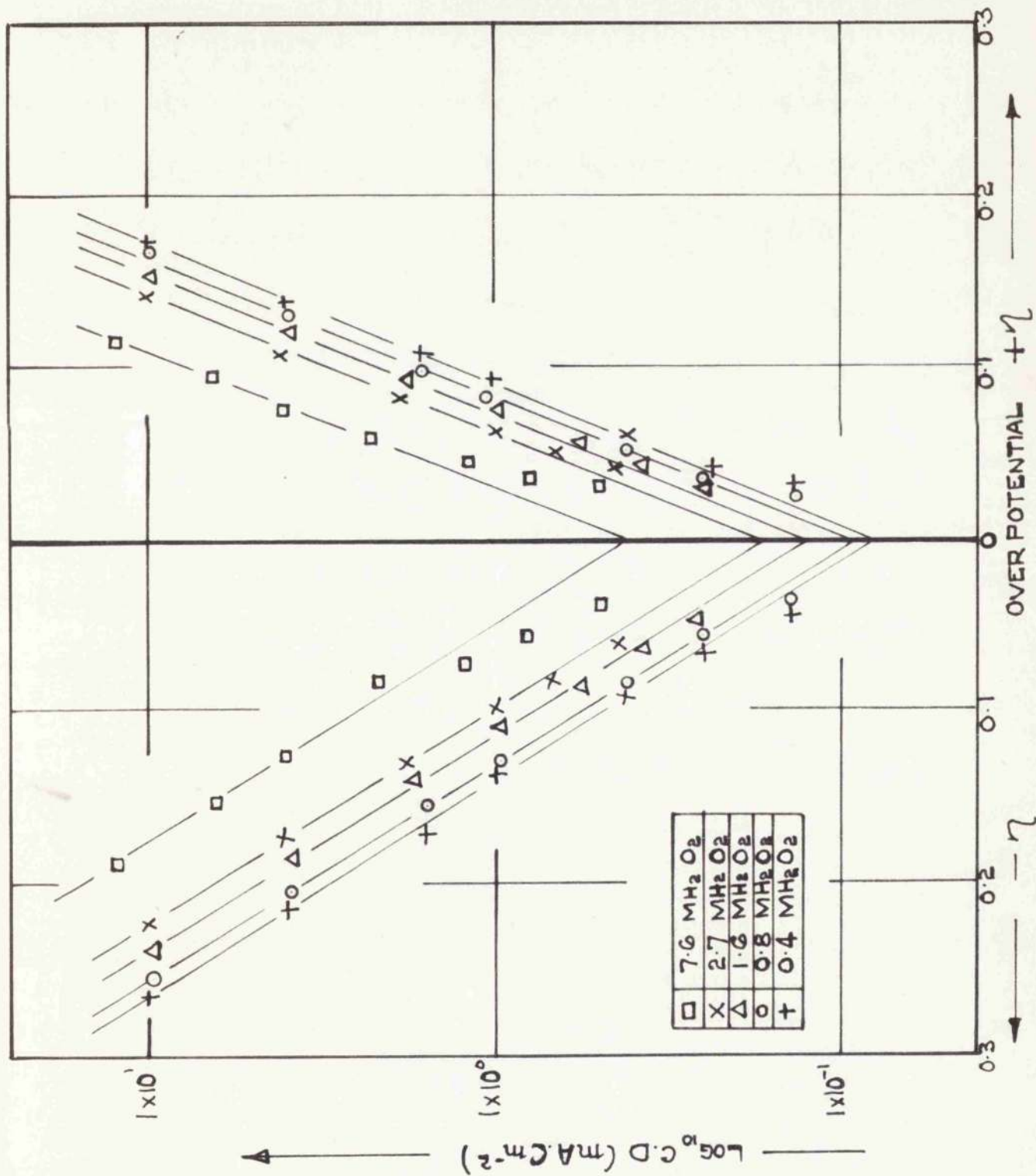


FIG. 19 THE DEPENDENCE OF THE EXCHANGE CURRENT VALUE ON $[\text{H}_2\text{O}_2]$

AT $\text{pH} = 6.00$.

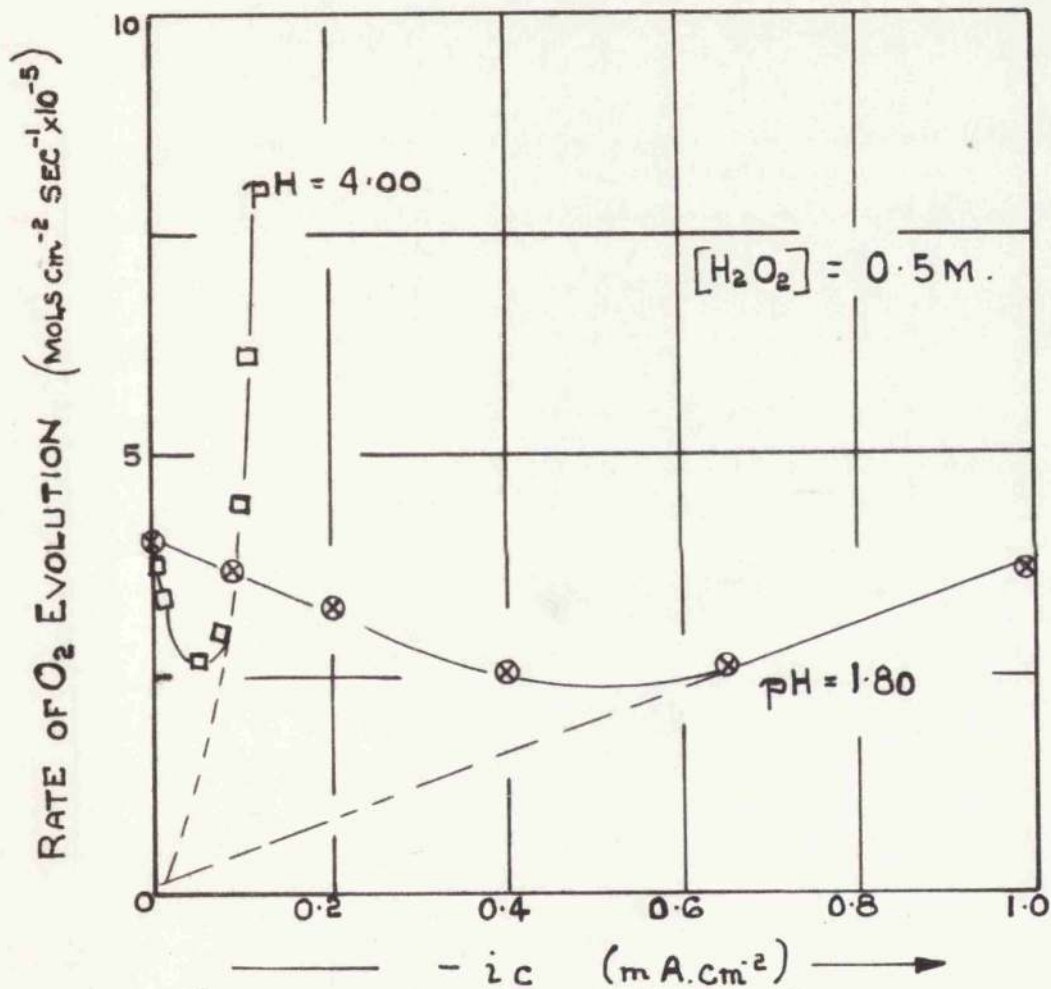


FIG. 20 THE EFFECT OF SMALL CATHODIC CURRENTS ON THE RATE OF DECOMPOSITION.

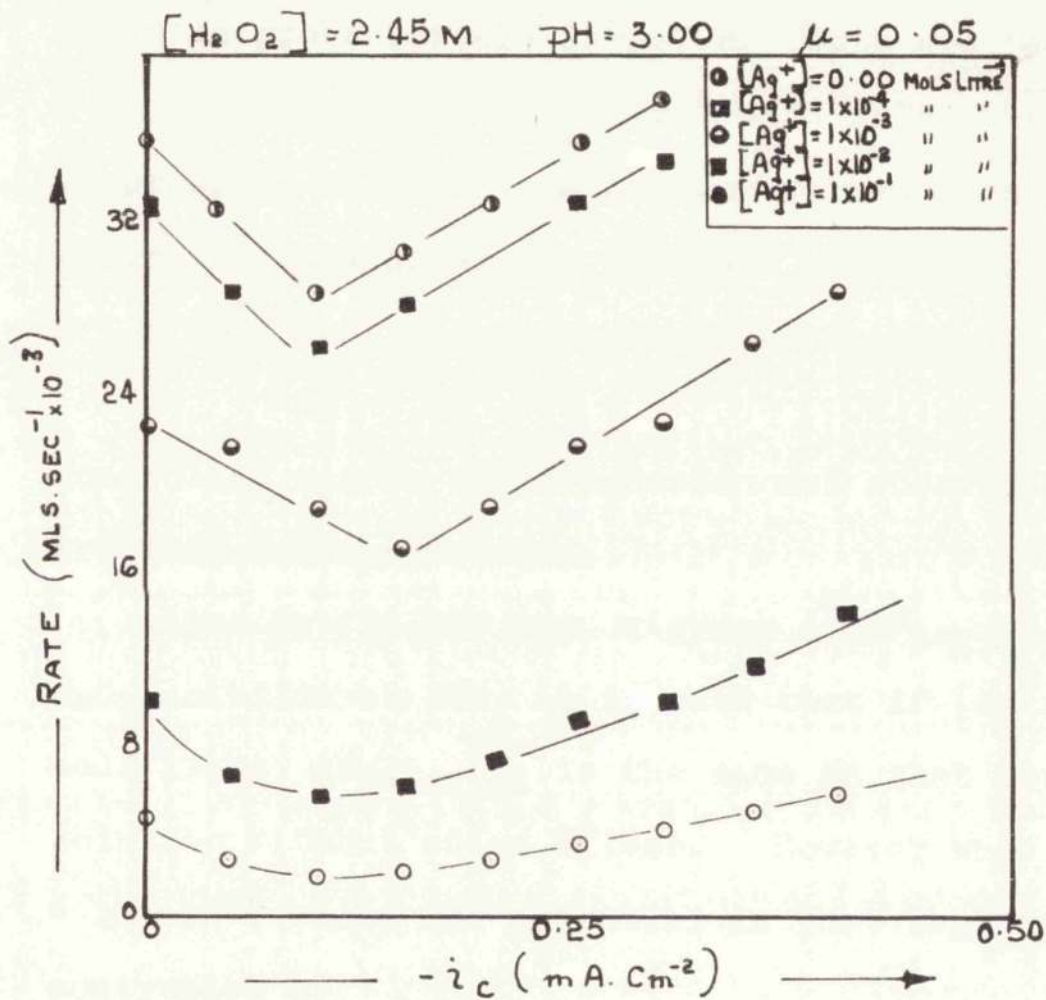
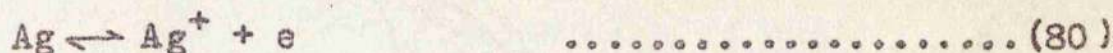


FIG. 21. THE EFFECT OF SMALL NEGATIVE CURRENTS
ON THE RATE OF CATALYSIS WITH VARIOUS SILVER
ION ADDITIONS

in the form of AgNO_3 . From the graph we see that in all cases the rate is initially lowered, then begins to accelerate again as progressively larger currents are passed.

For $[\text{Ag}^+]_{\text{added}} \leq 1 \times 10^{-3}$ mols/litre there is a sharp suppression of rate to a minimum value, then an equally sharp increase after the minimum. However, with $[\text{Ag}^+]_{\text{added}} \geq 1 \times 10^{-2}$ i.e. according to fig.7 in the



controlled region the depression and subsequent acceleration are much less pronounced.

Also in fig.22, i.e. a graph of $E/\log_{10}i$, for a 1.6M H_2O_2 solution at pH4, it is seen that if $[\text{Ag}^+]_{\text{added}} \leq 1 \times 10^{-6}$ mols/litre $dE/d\log_{10}i$ is the same as that for an H_2O_2 solution without added silver. However when $[\text{Ag}^+]_{\text{added}} = 1 \times 10^{-3}$ where the potential is just beginning to be controlled by

$$E = 0.8 + 0.059 \log_{10} [\text{Ag}^+] \quad \dots\dots\dots(74)$$

at the larger current densities, i.e. just in the boundary of the cathodically controlled region, $dE/d\log_{10}i$ becomes much smaller and does not tend toward the linear relationship obtained for solutions with either very little or no added Ag^+ . This is even more strikingly displayed for the curve corresponding to $[\text{Ag}^+]_{\text{added}} = 1 \times 10^{-1}$ where the electrode potential is definitely controlled by



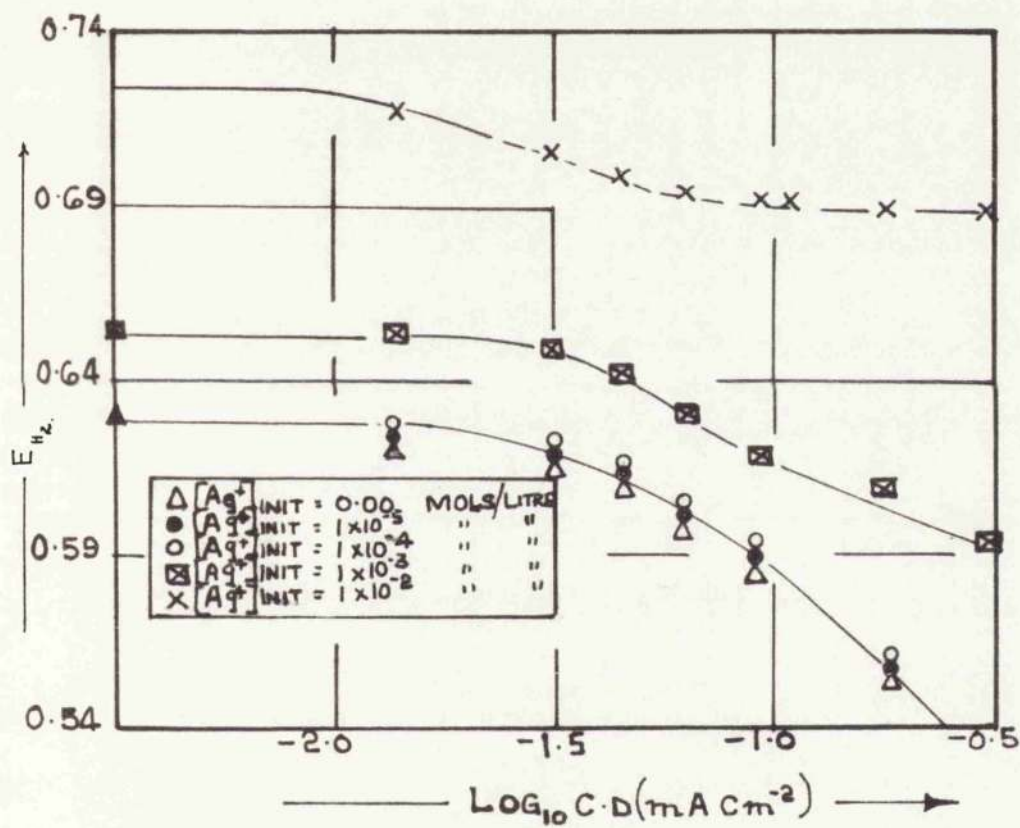


FIG. 22. THE EFFECT OF SMALL CATHODIC CURRENTS ON POTENTIAL IN 1.5M H₂O₂ SOLUTION WITH VARIOUS AMOUNTS OF ADDED SILVER AT 25° C AT pH = 4.00.

as the effect on potential on passing progressively larger currents has tended to zero.

4. Existence of anodic and cathodic areas on the electrode surface.

The attempt to separate the two types of areas was partially successful on combining the well etched and the oxidised electrode in a 3M H_2O_2 solution. Fig.23 shows the results of the experiment. While each electrode may itself have tended towards an equilibrium state, the oxidised electrode stayed positive to the other and a small steady current continued almost indefinitely to flow. The return current indicated initial electrochemical reduction of the oxide as the value fell from 3.5 microamps to a steady value of 0.4. Such a current in the reverse direction would form a monolayer in 10 seconds. From a rough estimate of the rate of solution of Ag_2O in peroxide it may be inferred that at most only one tenth of the anode remains covered during this experiment.

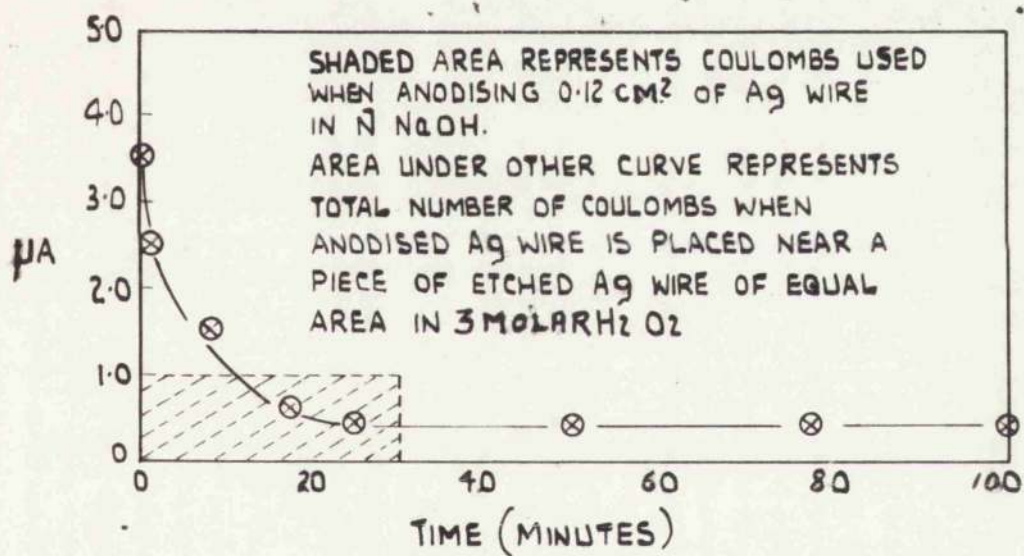


FIG.23.

DISCUSSION

1. The Equilibrium Potentials.

All potentially catalytic metals or metal oxide films on metals, e.g. Pt, Au, Ni, Cu, Pb, Mn, etc., as well as Ag, give stable electrode potentials with H_2O_2 solutions which, for a wide pH range, i.e. between pH 1-10, are represented, at 25°C, by

$$E = E_0 - 0.059 \text{ pH} \quad \dots\dots\dots (81)$$

E_0 is little, if at all, affected by the nature of the catalyst, and has the value, referred to the standard hydrogen electrode, of 0.83 - 0.85 v. At high $[H_2O_2]$ this equation no longer holds. The lowest $[H_2O_2]$ for which it holds varies with the nature of the metal; for Pt it is $10^{-5}m$, for Cu $10^{-2}m$. Non-catalytic metals like Al, Sn, or Zn, give much less oxidising potentials, i.e. more negative E_0 values which are however quite unstable and of no significance as far as the H_2O_2 solution is concerned. These facts suggest a link between the catalytic process and the potential determining one.

The basic requirement for a steady potential is, of course, that there should be a ready electron exchange between some solution species or surface adsorbed entities, and the metal itself. The above facts would therefore, support the widely held view that an electron exchange is a basic part of the catalytic process. The metals which do not allow the process to occur would then be those which form insulating (protective) oxide layers, while metals which do not form oxides (Pt or Au) or those whose oxides are readily dissolved

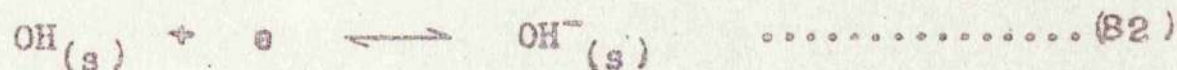
(Pb, Ag) or are semiconducting (Ni, Co, Mn) are all varyingly good catalysts.

The potential of the metal may be regarded as determined by the electron concentration maintained at its surface by the determining reaction, e.g.



In the case of the metal/metal ion equilibrium, or in the H₂O₂ case, by the cycle of catalytic processes. If we suppose the cycle to involve one or a series of labile molecules or ions, e.g. HQ, HO₂, O₂, etc. we could regard the electrode potential as being determined by any one of the labile species whose concentration would under steady state catalytic conditions be held constant by virtue of its being an intermediate in the cycle.

This is an alternative way of viewing the explanation of Bockris and Oldfield⁵⁴ when they give the potential controlling reaction:



with α_{OH} having a very small value to explain the very large difference between the experimental E_0 (i.e. 0.83 v) and the value expected for E_0 for the above reaction. This is given by Latimer⁵⁶ as 2.0 v (i.e. when $\alpha_{\text{OH}} = \alpha_{\text{OH}^-} = 1$) which compares with the Bockris and Oldfield value of 0.01 v when $\alpha_{\text{OH}} = 1$ for platinum in H₂O₂. The relevant value for

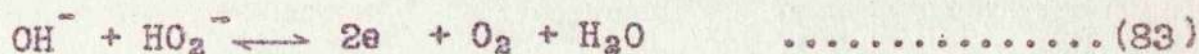
α_{OH} in the whole range of pH covered by Bockris and Oldfield can be calculated to be the constant one of $10^{-33.3}$

This very low value is explained in passing by Bockris and Oldfield as due to the surface absorption of the free OH; but a difficulty with this explanation is revealed in the case of silver. The state of the OH radical at its lowest free energy content at a silver surface would surely be a surface anchored OH^- ion. No more firmly bound OH could be envisaged. But the electrode potential of the $Ag/AgOH/OH^-$ electrode, which we may take as being identical with that of the $Ag/Ag_2O/OH^-$ electrode, is 0.34 v. when $\alpha_{OH^-} = 1$. Thus the H_2O_2 potential is 0.24 v. lower, i.e. more negative than this.

Fig.6 shows that for Ag with increasing $[H_2O_2]$ the electrode potentials never quite reach the Ag/Ag_2O value although these become more positive at the middle of the pH range.

We have for these reasons sought a catalytic process which is anchored to the metal by an electron exchange but which maintains an electron concentration independent of the metal and characteristic of H_2O_2 and the solution. Such an explanation is that of Gerischer and Gerischer⁵⁵ to which we have already referred.

Before dealing further with this scheme it will be profitable to consider the high pH results ($> \text{pH}10$) in which we have reproduced the findings of Berl⁵³ for carbon electrodes, and Hickling and Wilson⁵⁴, for platinum, as regards the dependence of the e.m.f. on pH and $[\text{H}_2\text{O}_2]$. This is seen clearly in Fig.5. We have not tested the finding of Berl that in this region the oxygen pressure affects the potential in a manner expected from the equation.



$$\text{i.e. } E = E_0 - \frac{RT}{2F} \ln Q_{\text{OH}^-} Q_{\text{O}_2} + \frac{RT}{2F} \ln p_{\text{O}_2} \quad \dots\dots\dots(84)$$

If we accept however that this reaction does control the potential in this pH range we may observe that it may be linked with a catalytic cycle if it is broken down into the steps.

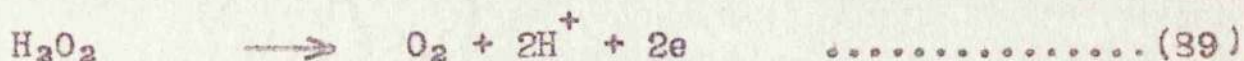
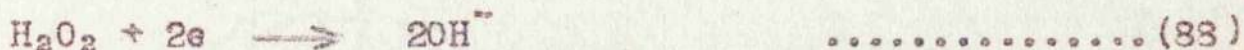


with the possibility of a side catalytic process based on the interaction of O_2^- or HO_2 with H_2O_2 in modified Haber-Weiss cycles.

We come now to the question, of how this process, involving an $[\text{H}_2\text{O}_2]$ influence on the potential merges at about pH 10-11, into an $[\text{H}_2\text{O}_2]$ independent range. The obvious suggestion which applies to any metal (or Carbon) electrodes is that the high pH scheme requires a high

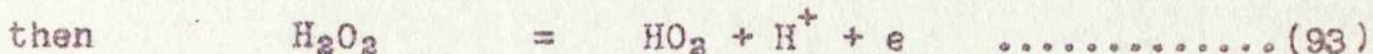
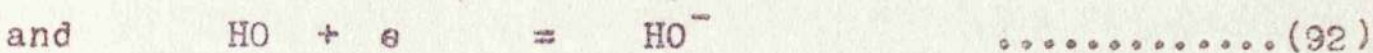
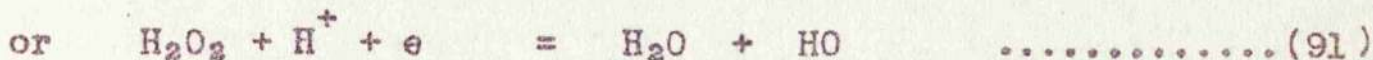
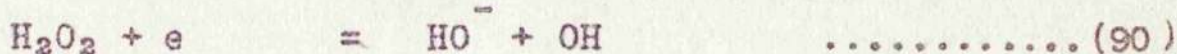
concentration of HO_2^- and that the H_2O_2 molecule in the undissociated form favours a different cycle because of its ability, which HO_2^- clearly lacks, to accept one or two electrons:

Thus the potential determining cycle could be written:



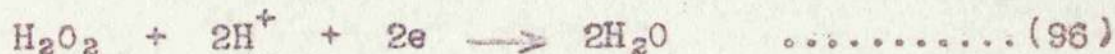
This type of potential determining process differs from the previous one in consisting of two balanced steps neither of which is itself an equilibrium process. The electron balance requires a forward reaction and an effective decomposition of H_2O_2 whereas the high pH scheme is overall quite reversible and is linked with the reversibility, in strongly alkaline solutions, of the O_2 electrode.

This process differs from that of Gerischer and Gerischer⁵⁵ in using two 2-electron steps. 1-Electron processes imply the occurrence of free radicals, e.g.

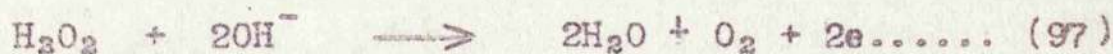


and Haber-Weiss cycles could occur by interaction with these free radicals.

We may now note that in either of these schemes since H_2O_2 acts as both donor and acceptor of electrons the potential is independent of $[H_2O_2]$. In the 2-electron process, however, there would be no pH dependence although that could be readily introduced by rewriting the first equation.



or the second



Following Parson's⁴⁷ we may write the rate of the process as

$$rate_1 = c_{H_2O_2} c_{H^+}^2 K_1 \frac{kT}{h} \exp. \left(\frac{-\Delta G^\ddagger + 2\beta_1 EF}{RT} \right) \dots(98)$$

and of the corresponding reverse process

$$rate_2 = c_{H_2O_2} K_2 \frac{kT}{h} \exp. - \left(\frac{\Delta G^\ddagger + 2(\beta_2 - 1)EF}{RT} \right) \dots\dots\dots(99)$$

At potential equilibrium the rates will be equal and one has to simplify, for this, these equations by assuming the transmission coefficients K_1 and K_2 are equal and that the symmetry coefficients β_1 and β_2 for the potential energy barriers, about the activated state, are equal to 0.5 (or that $\beta_1 = \beta_2$). Then,

$$E = E_0 + \frac{RT}{F} \ln c_{H^+} \quad \dots\dots\dots(100)$$

which is the same as (31)

The 1-electron process gives a similar equation if

similar assumptions are made. It may be noted that if β_1 and β_2 are not equal to 0.5 the coefficient of $\ln c_{H^+}$ is changed.

Then,

$$E = \frac{E_0}{(\beta_1 - \beta_2 - 1)} + \frac{RT}{(\beta_1 - \beta_2 - 1)F} \ln c_{H^+} \dots\dots\dots (101)$$

which would give a possible explanation of deviations of E from the values of the simpler equation at increasing $[H_2O_2]$ if the assumption is made that the high $[H_2O_2]$ would distort the potential field at the electrode boundary and cause β_1 and β_2 to differ from the symmetrical 0.5. This would not however explain either the pH independent zone or the dependence on $[H_2O_2]$ which occurs in this zone.

Gerischer and Gerischer's⁵⁵ explanation of the deviations of E from the line given by equations (81) seems for these reasons inadequate.

Other explanations of this behaviour in the central region of fig.6 may now be considered. First, may be considered, the possibility that it is due to increasing $[Ag^+]$ at the electrode surface caused by dissolutions of the electrode material. As fig.7 shows, increasing the bulk $[Ag^+]$ has little effect on the potential until it rises above a value given by the Ag/Ag^+ equilibrium potential value.

$$E = 0.799 + \frac{RT}{F} \ln [Ag^+] \dots\dots\dots (102)$$

In these experiments the bulk $[Ag^+]$ certainly does not rise to measurable values but at the potentials of pH4-9 the

Ag^+ concentrations required to be exceeded to raise the electrode potential are quite small - from 10^{-4} to 10^{-2}M

This explanation does not extend, of course to Pt with which we confirm the findings of Gerischer and Gerischer⁸⁵ are that the same type of deviations occur at high $[\text{H}_2\text{O}_2]$. Bockris and Oldfield,⁵⁴ however, did not find such effects up to $5\text{M H}_2\text{O}_2$. This is a discrepancy which we cannot adequately explain.

With silver, however, it appears that the $[\text{Ag}^+]$ found at the electrode surface is maintained as a result of the electrode potential and does not cause it.

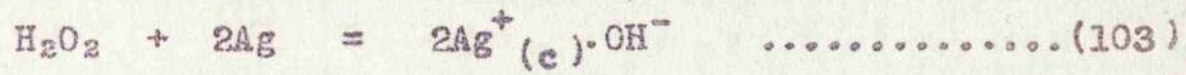
Another possibility linked with this is that the surface pH is in fact very different from that in the bulk, but on examination the effect is seen to require a much lower surface pH. Thus the experimental potential on fig.6 could be explained if the true surface pH was much lower (pH2-3 in the case of the more concentrated H_2O_2), whereas as a result of the enhancement of the Ag dissolution caused by increasing the $[\text{H}_2\text{O}_2]$, the actual pH at the electrode surface will be higher than the bulk value.

Thus we are left to explain the effect as due entirely to the H_2O_2 itself. However, at this stage, note must be made of the fact that the region of the more positive potential is the region where electrode condition effects most markedly the potential. In this region annealed, etched and polished

silver electrodes give results differing as much as 0.1 to 0.15 v. The same instability occurs with Pt in this zone and it is only by the most careful annealing that reproducible values can be obtained.

This is linked with the observation that the silver surface can take up macroscopic differences of colour and tone which, as the experiment of fig.23 shows, are to be associated with definite anodic and cathodic zones at which we may regard the processes of (96) and (97) as separately predominating with an electron current passing through.

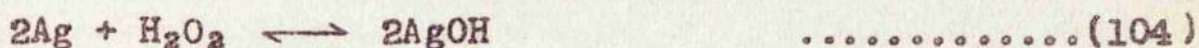
We regard the anodic area as being covered by a thin Ag₂O oxide layer which is formed by the process



Once a layer of the Ag⁺.OH⁻ (or Ag₂O with OH⁻ at the solution surface) is formed it would provide a rectifying p-n junction with the metal and electron could only pass through it in the direction from metal to boundary. Thus (97) could carry on at the surface of the oxide with electrons coming from (96) occurring elsewhere at a bare (or etched) metal.

In this situation the potential of the electrode will behave as if it were two electrically connected electrodes, one being the Ag/Ag₂O/OH⁻ electrode and the other the metal/H₂O₂/OH⁻ electrode which is given by equation (81). We may express the inevitable polarisation effect which will

control the measured potential as electrode resistances and further we may regard the actual value of this as inversely proportional to the fraction of the whole electrode surface devoted to the particular type. Thus for the anodic area of fraction α the resistance = $r_a \alpha$ and the cathodic $r_c (1 - \alpha)$, r_a and r_c being characteristic constants. Then if the two areas are related by the reversible equation:



i.e. (cathodic area) $\times \frac{1}{2} \text{H}_2\text{O}_2 =$ (anodic area)

$$K_1 = \frac{\alpha}{(1 - \alpha) \alpha^{1/2} \text{H}_2\text{O}_2} \quad \dots\dots\dots(105)$$

$$\text{i.e. } \frac{1}{\alpha} = 1 + \frac{1}{K_1 \alpha^{1/2} \text{H}_2\text{O}_2} \quad \dots\dots\dots(106)$$

Then if ΔE is defined as follows:

$$\Delta E = E_{\text{measured}} - E_{\text{cathodic}} \quad \dots\dots\dots(107)$$

E_{cathodic} being given by equation (72) for dilute solutions as already mentioned, we obtain

$$\frac{\Delta E}{E_{\text{anodic}} - E_{\text{cathodic}}} = \alpha \quad \dots\dots\dots(108)$$

$$\text{and } \frac{1}{\Delta E} = \text{const.}^1 + \frac{\text{const.}^2}{(\alpha \text{H}_2\text{O}_2)^{1/2}} \quad \dots\dots\dots(109)$$

Fig. 24 shows, at pH6, the graph of $1/\Delta E$ against $1/(\alpha \text{H}_2\text{O}_2)^{1/2}$, the values of $\alpha \text{H}_2\text{O}_2$ being calculated from Kavanagh, Scatchard and Ticknor.⁶⁹

Very satisfactory linearity is found over the range of $[\text{H}_2\text{O}_2]$ from 1-86% w.w.

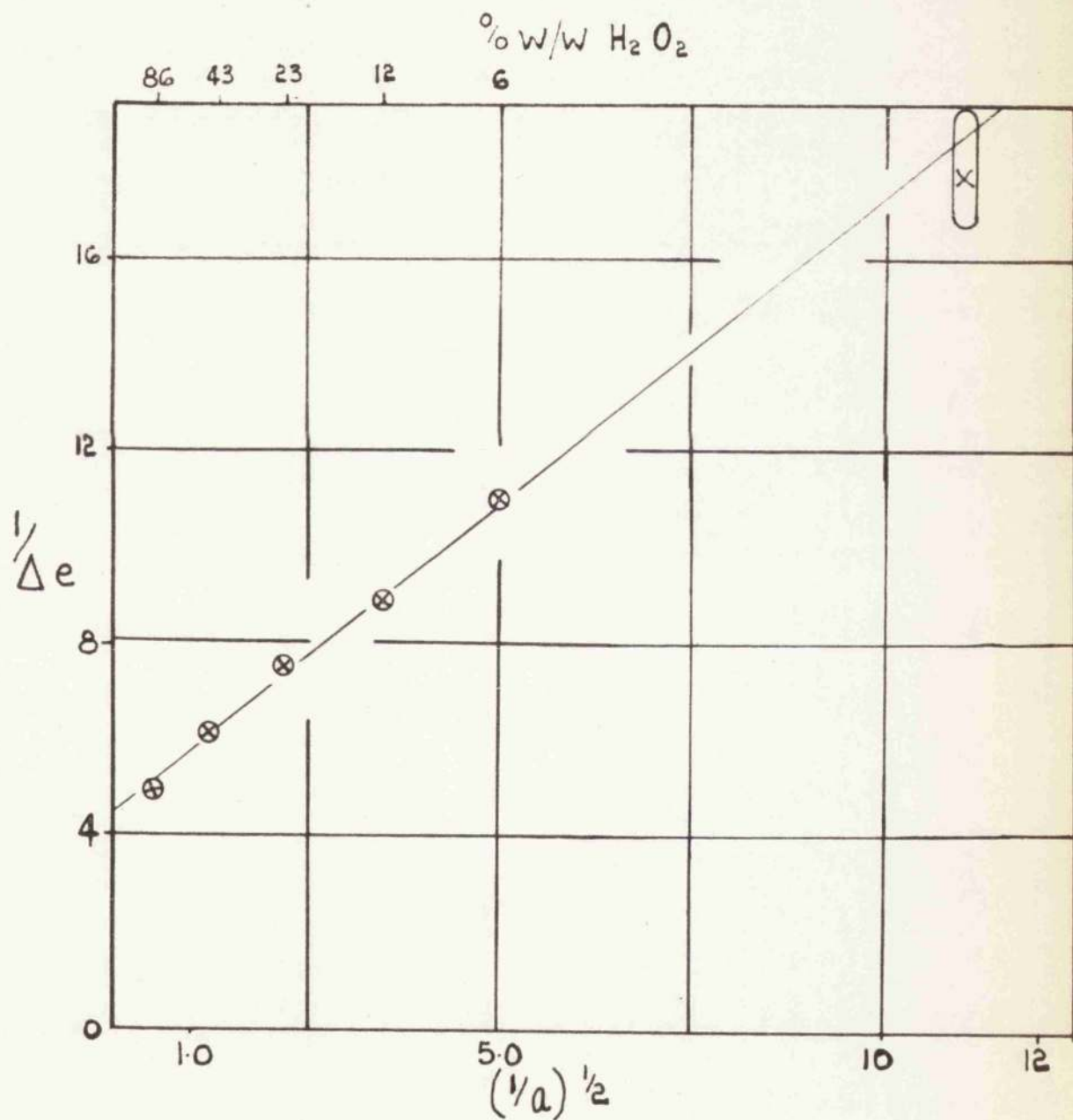


FIG 24 STANDARD POTENTIAL OF A₉ ELECTRODES
IN H₂O₂ SOLUTIONS AT pH = 6

$$\frac{(\frac{1}{a} \text{H}_2\text{O}_2)^{1/2}}{1/\Delta e}$$

$$(\Delta e = E_{\text{MEAS}} - E[\text{H}_2\text{O}_2] \rightarrow 0)$$

Fig. 25 indicates the failure of a simple equation of the type

$$E = \text{const.} + 0.059 \log_{10} \alpha \text{H}_2\text{O}_2 \dots\dots\dots(110)$$

to explain the results. This equation would arise from some process in which the H₂O₂ participated as an oxidising reagent.

It may be mentioned that Markovic⁷⁰ noted anodic - cathodic area separation with lead in H₂O₂ solutions.

An important requirement of the above scheme is the occurrence of [H₂O₂] in the equation to the square root. This implies the 2-electron, non radical type of decomposition step.

2. Rate of Catalysis at Electrodes.

The second order kinetics in all dilute solutions suggests, if the complicating effect of pH and [Ag⁺] are ignored, that oxygen evolution requires a four point adsorption at the metal surface, probably involving 4-electrons. However the catalysis is extremely sensitive to the above and other influences. The pH effect is shown in fig.12. It is similar but more exaggerated than found by Gerischer and Gerischer⁵⁵ for platinum. Between pH4 and 8 the rate declines monotonously with increasing pH. This is the region in which the potential of the electrode is virtually independent of the pH but, in which, as pH increases, the fraction of surface covered with Ag₂O increases.

This could explain the reduction in oxygen evolution if the Ag₂O layer is regarded as being less conducting than an etched surface. Equally it may be due to the effect on

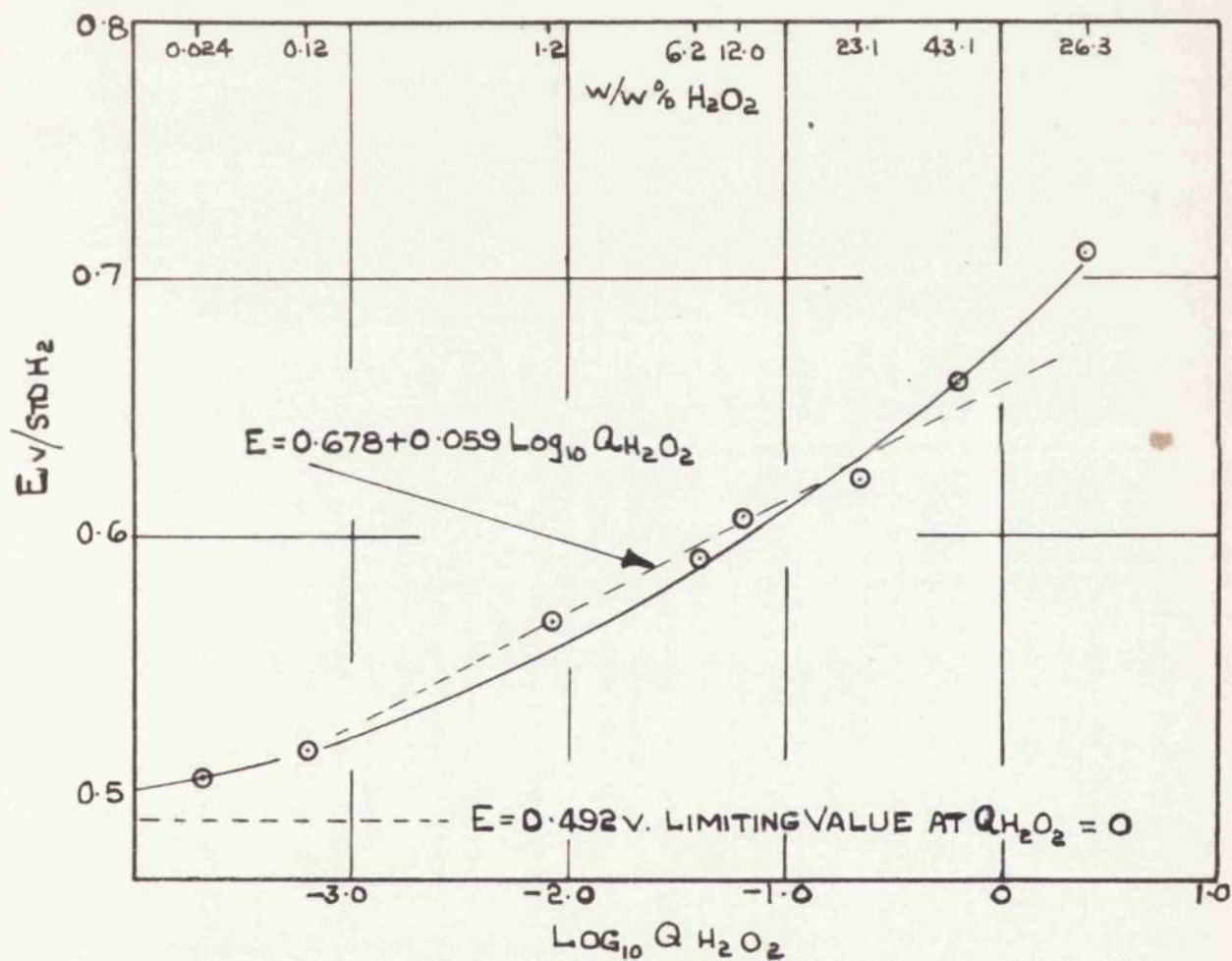


FIG 25. SHOWING THE VARIATION IN POTENTIAL WITH THE ACTIVITY OF H_2O_2 AT $pH = 6.0$.

75

[Ag⁺]. The direct effect on catalysis of adding Ag⁺ as AgNO₃ is shown in fig.14. Generally the effect is to reduce catalysis sharply for small additions of Ag⁺ - of the order of the amount required to satisfy the equation.

$$E = 0.799 + 0.059 \log_{10} [\text{Ag}^+] \dots \dots \dots (102)$$

in which the potential of the electrode is inserted for E. The [Ag⁺] found here is the value which would be expected to exist at the electrode surface. When the bulk solution contains a lower [Ag⁺] than this there will be a tendency for the metal to dissolve by a normal Nernst diffusion process in which

$$\text{Rate of Ag dissolution} = k(c_s - c_b) \dots \dots \dots (111)$$

in which c_s is the surface concentration of silver, found as above, and c_b that in the bulk solution. This equation has been confirmed by Maggs and Sutton³⁸. Thus the point of minimum (but not zero, it may be noted) catalysis is the point at which silver no longer dissolves. At pH4-6 the reduction in solution of silver is very small but the reduction in oxygen evolution is quite dramatic. At the maximum inhibition the silver still catalyses but not more rapidly than does smooth platinum in a similar solution. From this is concluded that the behaviour of silver as a specially effective catalyst is directly due to the passing into solution of Ag⁺ ions. Each Ag⁺ passing from the metal into solution seems on this picture to release a burst of catalysis of many H₂O₂ molecules.

3. The Effect of Small Currents.

The effect of small currents on catalysis is quite marked. Fig. 15 illustrated the increase with a 0.9M H₂O₂ solution at pH6 with anodic currents and the smaller effect of cathodic currents. At first there is in fact a slight suppression of O₂ evolution with cathodic currents and this is even more marked with those experiments made with Ag⁺ present (fig. 21).

To explain these and the other results with currents we accept the concept of a considerable "exchange current" flowing through the metal and through the solution between the two different anodic and cathodic areas during catalysis when there is no external current, i.e. under the conditions of the observed equilibrium potential.

If the electrode processes are given by equations (96) and (97) the anodic at any time is given by (rate)₁ in equation (98) and the cathodic by (rate)₂, and equation (99). When there is a net overall current in one direction or the other it will be given by ±[(rate)₁ - (rate)₂], the positive sign referring to an anodic current.

If we now introduce now the term of overpotential, where

$\eta = E_{\text{observed}} - E_{\text{equilibrium}}$, and i_a for a net anodic and i_c for a net cathodic current. Then, for these equations

$$\left[\frac{d\eta}{d \ln i_a} \right]_{T, pH, H_2O_2} = \frac{RT}{2\theta, F} \dots\dots\dots(112)$$

and

$$\left[\frac{d\eta}{d \ln i_c} \right]_{T, pH, [H_2O_2]} = \frac{RT}{2(1 - \beta_2)F} \dots\dots\dots(113)$$

With $\beta_1 = \beta_2 = 0.5$, we should find the slope of $\eta / \ln i_c$ line to be RT/F . In practice i_a or i_c can only be observed independently of the exchange current when the applied current is very much greater than the exchange current.

The effect of this procedure, commonly used in overpotential studies is shown in fig.18. Perfectly linear $\log_{10} i / \eta$ graphs are found. The cathodic slope is precisely 0.120 for pH's in the range 2-7. This value is twice that predicted from equation (113) with $\beta_2 = 0.5$. It could be obtained if $\beta_2 = 0.75$ or more plausibly with $\beta_2 = 0.5$ and with a 1-electron process e.g. equation (94) rather than equation (90) as the basic cathodic mechanism. The anodic process has a slightly lower slope, viz., 0.080 which could be obtained from equation (112) if β_1 were 0.375. This is a not unreasonable value but again it would be more plausible to choose $\beta_1 = 0.5$ and use a 1-electron step; equation (92) rather than (97).

Fig. 19 strikingly demonstrates that over a substantial range of $[H_2O_2]$ there is no change in the value of $d\eta / d \log_{10} i$. This shows that β_1 and β_2 are not affected by $[H_2O_2]$ nor by the conditions created by the H_2O_2 catalysts. From this graph we may evaluate $(d \ln i / d \ln [H_2O_2])_{\eta \rightarrow 0}$ and find it to be close to 0.4 in the range (up to 2.7M H_2O_2) in which the relation is linear. We may perhaps take this to indicate a value of $\frac{1}{2}$ and for the number of H_2O_2 molecules associated

with one activated complex in the rate process.

The same result is found by plotting i_0 , the exchange current, against $[\text{H}_2\text{O}_2]^{1/2}$ as in fig. 26. A linear relation is obtained which confirms that there are two transition complexes formed in the rate determining step for every H_2O_2 appearing in the stoichiometric equation.

To return now to the derivation of equations (109) and (110) and use this information we obtain for the right hand side of equations (112) and (113) the values, for a 2-electron process, $\frac{2RT}{2\beta_1 F}$ and $\frac{2RT}{2(1-\beta_2) F}$ which lead to the value of $\frac{2RT}{F}$ or 0.120 for the cathodic process with $\beta_2 = 0.5$, and 0.08 for the anodic with $\beta_1 = 0.75$. A 1-electron process would not be so easy to fit to all texts.

We may summarise the most reasonable requirements of these electrode kinetic results, then, as (i) a 2-electron forward and backward process and (ii) a rate determining step which occurs twice per each H_2O_2 molecule decomposing.

Hoar⁷¹ in a recent paper on the kinetics of the oxygen electrode obtains similar values for $d\eta/d \ln i$ to the above i.e. about 2 in moderately alkaline solution. Hoar puts forward a most interesting mechanism to account for this. Since it involves the formation and subsequent decomposition of adsorbed H_2O_2 it is of great interest to the investigation. The process is as follows:

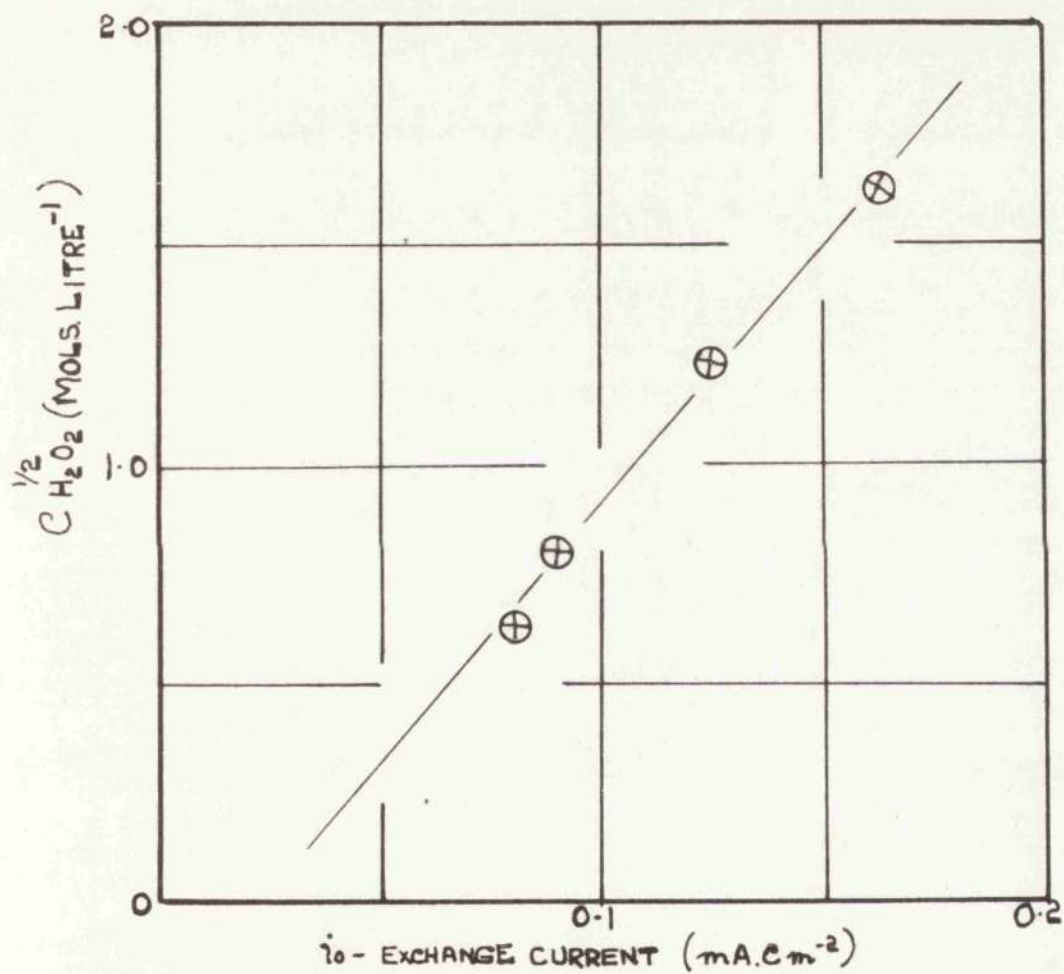
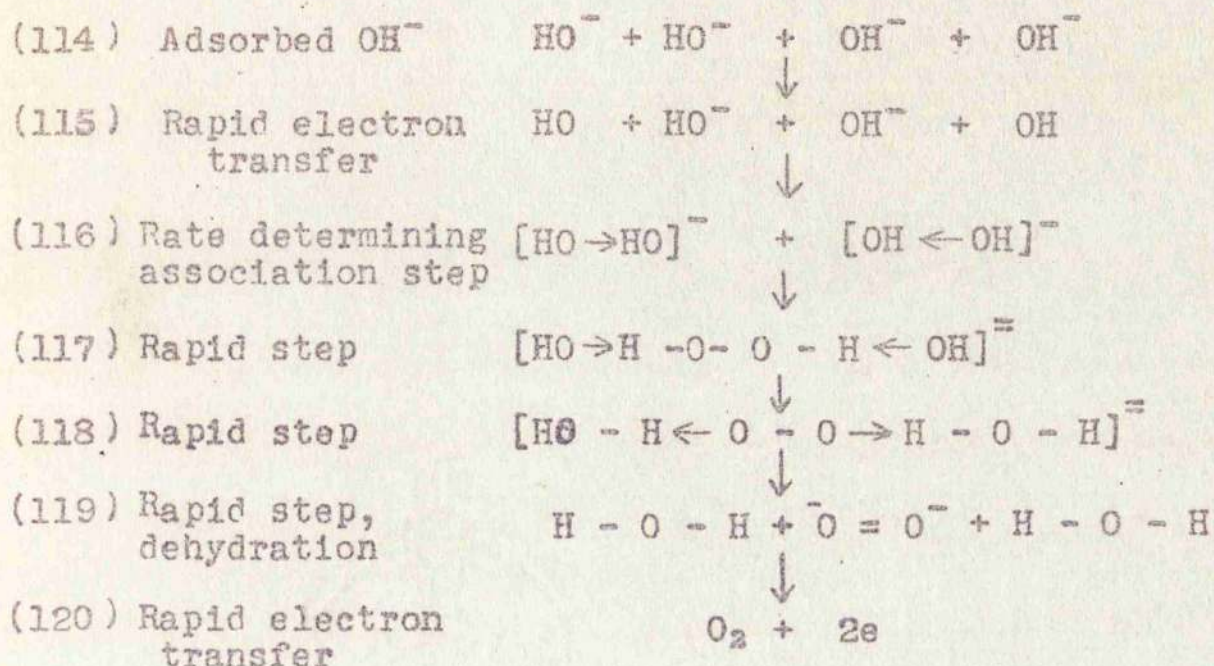
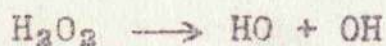


FIG 2.6 SHOWING THE LINEAR DEPENDENCE
OF THE EXCHANGE CURRENT ON THE
SQUAREROOT OF THE (H_2O_2).

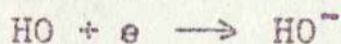


The catalysis of H₂O₂ can be explained by a similar scheme if the rapid 2-electron adsorption precedes the rate determining step. The stages (115) to (120) can then follow as above. It appears however in the case outlined the rate determining step occurs only once per H₂O₂. For the purpose of the present investigation it would be necessary to place the slow step somewhat earlier, e.g. dividing step (114) then

(114)a dissociative adsorption - rapid



(114)b electron transfer, rate determining



with the final return of an electron to the metal as in (119) or (120) above.

One aspect of this general picture which further commends

it, is that it fits in with the second order dependence of catalysis on $[H_2O_2]$ and fits in also with the absence of any first order kinetics. When the surface is fully covered with H_2O_2 zero order kinetics would, of course, supervene, as found in practice (cf. fig.10).

The rate of solution of Ag^+ which is in fact, the factor which influences the rate of catalysis rather than $[Ag^+]$, would have a direct influence on the electron concentration of the metal surface itself. pH will affect the process simply by virtue of the need for OH^- to be adsorbed to give the overall effect.

In discussing the Hoar mechanism it has been assumed that the adsorbing surface is the bare metal. It is of course quite possible that the scheme should be separated into the two parts of the earlier picture, viz., an anodic area in which the surface of the solid would be an oxide layer, and the cathodic layer which might quite possibly be bare metal.

REFERENCESPART I.

1. Thénard, Ann. chim. et phys., 1818, 8, 306.
2. Wynne-Jones, Tobe and Jones, Trans. Far. Soc., 1959, 55, 91.
3. Thénard, Ann. chim. et phys., 1832, 50, 80.
4. Brodie, Phil. Trans., 1850, 2, 759.
5. Bredig and von Berneck, Z. phys. Chem., 1899, 31, 258.
6. Wiegel, ibid., A, 1929, 143, 831.
7. Maggs, R.A.E., R.P.D. Report, 1954
8. McLane, J. Chem. Phys., 1949, 17, 379.
9. Satterfield and Stein, J. Phys. Chem., 1957, 61, 537.
10. Giguère and Liu, Can. J. Chem., 1957, 35, 283.
11. Hoare, Protheroe and Walsh, Trans. Far. Soc., 1959, 55, 548.
12. Spitalsky, Z. phys. Chem., 1926, 122, 257.
13. Abel, Z. Electrochem., 1908, 14, 598.
idem., Z. phys. Chem., 1920, 96, 1.
14. Bray and Livingston, J. Amer. Chem. Soc., 1928, 45,
1251 and 2043.
15. Haber and Willstätter, Ber., 1931, 64, 2844.
16. Haber and Weiss, Proc. Roy. Soc., A, 1934, 147, 332.
17. Baxendale, Evans and Park, Trans. Far. Soc., 1946, 42,
155.

18. Dainton and Rowbottom, ibid., 1953, 49, 1160.

19. Weiss, Disc. Far. Soc., 1947, 2, 212.

20. Barb, Baxendale, George and Hargrave, Nature, 1949, 163, 692.

21. Weiss and Humphrey, ibid., 1949, 163, 691.

22. Wynne-Jones, Tobe, Kitching and Jones, Trans. Far. Soc., 1959, 55, 79.

23. Kremer and Stein, ibid., 1959, 55, 959.

24. Chance, Arch. Biochem., 1949, 21, 416.

25. Wang, J. Amer. Chem. Soc., 1955, 77, 822 and 4715.

26. Baker and Oullet, Can. J. Res., B, 1945, 23, 167.

27. Mackenzie and Ritchie, Proc. Roy. Soc., A, 1946, 185, 207.

28. Giguère, Can. J. Res., B, 1947, 25, 135.

29. Hart and McFadyen, In course of publication, Glasgow.

30. Hart and Ross, ibid.

31. Hart and Taylor, ibid.

32. Brodie, Proc. Roy. Soc., 1860, 11, 442.

33. Berthelot, Ann. chim. et phys., 1891, 11, 217.
 idem., ibid., 1897, 11, 223.
 idem., Compt. rend., 1901, 132, 897.

34. Bredig and Ykeda, Z. phys. Chem., 1901, 37, 1.
 Bredig and Reinders, ibid., 1901, 37, 323.
 Bredig and Weinmayer, ibid., 1903, 42, 601.
 Bredig and Fortner, Ber., 1904, 37, 798.

35. Teletof, Khim. Referat. Zhur., 1941, 4, 8.
36. Wentworth, M. I. T. Report No32, 1951.
37. Maggs, and Sutton, Trans. Far. Soc., 1958, 54, 1861.
38. Idem., ibid., 1959, 55, 974.
39. Weiss, ibid., 1935, 31, 1547.
40. Dowden and Reynolds, Disc. Far. Soc., 1950, 8, 184.
41. Pauling, Phys. Rev., 1933, 54, 399.
42. Broughton and Wentworth, J. Amer. Chem. Soc., 1947, 69,
741.
43. Broughton, Wentworth and Farnsworth, ibid., 1949, 71, 2346.
44. Voltz and Weller, ibid., 1954, 76, 1586.
45. Garner, Grey and Stone, Proc. Roy. Soc., A, 1949, 197, 294.
46. Weir, Ph.D. Thesis, Glasgow University, 1958.
47. Parsons, Trans. Far. Soc., 1951, 47, 1332.
48. Thénard, Ann. chim. et Phys., 1830, 44, 72.
49. Schöne, Liebig's Ann., 1903, 197, 137.
50. Tanatar, Ber., 1903, 36, 199.
51. Bornemann, Z. anorg. Chem., 1903, 34, 1.
52. Wolff, Compt. rend., 1933, 196, 1131.
53. Berl, Trans. Electrochem. Soc., 1943, 83, 253.
54. Hickling and Wilson, J. Electrochem. Soc., 1951, 98, 425.
Bockris and Oldfield, Trans. Far. Soc., 1955, 51, 249.
55. Gerischer and Gerischer, Z. phys. Chem., 1956, 6, 178.

56. Schumb, Satterfield and Wentworth, Hydrogen Peroxide, Rheinhold, New York, 1955.
57. Hart, A.M.L. Report 1949.
58. Hart and Aitken, Unpublished, Glasgow, 1956.
59. Graham, Diploma Thesis, R.C.S.T., Glasgow, 1959.
60. Menzel, Z.anorg.Chem., 1927, 167, 193.
61. Partington and Fathallah, J. Chem. Soc., 1949, 4, 3420.
62. Hart and von Döhren, A.M.L. Report, 1949.
63. Wynne-Jones and Mitchell, Trans-Far.Soc., 1955, 51, 1690.
64. Wynne-Jones, Private Communication.
65. Hoar and Mowat, Nature, 1950, 165, 64.
66. Davey, Phys. Rev. 19, 243, 22.
67. C.I.T.C.E., Sixth Report, 1954, p.30.
68. Latimer, Oxidation States, Prentice-Hall, New York, 1952.
69. Kavanagh, Scathard and Ticknor, J. Amer. Chem. Soc., 1936, 74, 319.
70. Markovic, Werkstoff u Korr, 1955, 3, 136.
71. Hoar, C.I.T.C.E., Eighth Report, 1956, p.439.

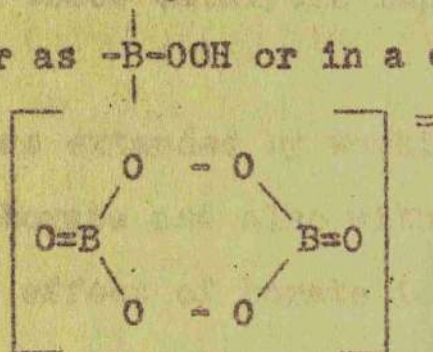
P A R T II
=====

The loss of oxygen from sodium peborate tetrahydrate.

The evolution of oxygen from sodium
perborate tetrahydrate.

Introduction

It was suggested that the problem of the mechanism of decomposition of sodium perborate tetrahydrate was of special interest because oxygen loss occurred from the substance in the solid state. Although, as will be seen later, the nature of the active oxygen in the crystalline compound has not been fully elucidated it seemed likely that it would occur as $-B-OOH$ or in a dimeric perborate ion



rather than as " H_2O_2 of crystallisation".

The arrangement of the O-O bond might be similar to that in an H_2O_2 molecule adsorbed at a catalytic surface.

It seemed thus, to be instructive and a suitable balance to our work with the highly catalytic silver surfaces and to the other work with highly catalytic oxides such as Cu_2O , NiO , CoO , etc., in this department to examine the loss of oxygen from the $-O-O-$ group when in proximity to a boron atom in the perborate ion.

As the work progressed, however, we learned that the decomposition of the perborate tetrahydrate was not a crystalline process at all but one preceded by fusion of the crystal. It was in fact concluded that the ion in the crystal lattice was very stable indeed and showed no loss of oxygen after many hours at 100 °C.

The observed loss of oxygen at or just above room temperature from the apparently quite dry solid was attributed to small amounts of liquid formation and seemed to be catalysed by trace catalytic impurities such as iron and copper.

The study was extended by working with wholly fused samples of the perborate and also with dilute solutions to demonstrate the effect of borate ion on the decomposition of the peroxide. The investigation concluded with a brief study of the action of iron and copper catalysts in borate-containing alkaline solution and was able to provide a clear picture and a reasonable explanation of the action of added Mg and Zn salts as stabilisers.

The description of this work takes the form first of an account of experiments which demonstrate the importance of liquid formation in oxygen loss from the crystalline tetraborate, then a description of the decomposition in the fused material and the role of iron and copper catalysts and magnesium stabilisers. Finally some experiments in the dilute solution with the aim of elucidating the action of the stabiliser.

Experimental

A. Materials

(i) Hydrogen Peroxide.

The hydrogen peroxide used in the subsequent investigation was the same unstabilised 86% w.w., supplied by Laporte Chemicals Ltd., as described under Materials in Part I.

(ii) Sodium metaborate tetrahydrate ($\text{NaBO}_2 \cdot 4\text{H}_2\text{O}$).

40 gm. Analar NaOH were dissolved in 156 ml. of distilled water in a 600 ml. beaker and 191 gm. Analar sodium tetraborate ($\text{Na}_2\text{B}_2\text{O}_7 \cdot 10\text{H}_2\text{O}$) were added. The beaker and contents were heated to 70°C then allowed to cool. After several hours pure crystals of $\text{NaBO}_2 \cdot 4\text{H}_2\text{O}$ were obtained, washed in pure ethanol, dried in a current of cold air, filtered to remove dust and stored in an air tight container to prevent efflorescence.

(iii) Sodium perborate tetrahydrate ($\text{NaBO}_3 \cdot 4\text{H}_2\text{O}$).

200 mls. of distilled water were placed in a 2-litre beaker contained in a larger vessel through which cooling water was circulating. To the beaker were added slowly and simultaneously a saturated solution of $\text{NaBO}_2 \cdot 4\text{H}_2\text{O}$ and a 30% w.w. solution of H_2O_2 (approx. 9m H_2O_2), the temperature being maintained below 30°C . During these additions the metaborate was kept in excess. This was

checked by continually withdrawing samples of the mother liquor and adding a few drops of thymol violet indicator. This gave a deep blue colour if metaborate was in excess. Finally the H_2O_2 was adjusted to stoichiometric equality by titrating to the end point (greenish-yellow) of the thymol violet indicator.

The temperature of the liquid was then held at $15^\circ C$ until crystallisation was completed. The crystals were filtered from the mother liquor, washed with ethanol, and dried in a current of warm air with continual stirring. Water contents of the perborate were determined periodically to ensure that overdrying of the compound did not take place.

(iv) Zinc, magnesium, copper and iron metaborates.

Stoichiometric quantities of solutions of the analar Zn, Mg, Fe^{+++} , and Cu^{++} sulphates and sodium metaborate were added slowly with stirring to a large volume of hot distilled water from which the precipitate was subsequently filtered, washed and dried.

Any other reagents employed were of Analar analytical grade material.

B.

Analysis of $NaBO_3 \cdot 4H_2O$.

By the method of Partington and Fathallah¹, sodium perborate tetrahydrate was analysed as $Na_2O \cdot B_2O_3 \cdot O_2 \cdot 3H_2O$. Thus for the pure compound the theoretical percentages of

alkali, acid, available oxygen, and removable H_2O , would be 20.13, 22.73, 10.39 and 46.75 respectively. The individual methods of analysis are as follows.

1. Estimation of total alkali and acid.

About 2 gm. of perborate were accurately weighed into a 400 ml. beaker. 45 ml. of 0.5N HCl were added from a burette and about 25 ml. of water were added, the beaker covered by a clock glass and the contents brought to boiling and allowed to simmer gently for 10 mins. Care was taken not to boil the solution vigorously as boric acid is steam volatile. On cooling, 2 drops of methyl orange were added and the solution titrated against 0.5N NaOH. 60 ml. of glycerol were added, the solution shaken well, two drops of phenolphthalein added and a further titration was conducted against 0.5N NaOH.

2. Estimation of available oxygen.

150 mls. of $2NH_2SO_4$ were measured into a 600 ml. beaker and $N/10$ $KMnO_4$ was added drop by drop until the solution was coloured a faint pink. About 3 gm. of $NaBO_3$ $NaBO_3 \cdot 4H_2O$ were weighed out accurately and added to the dilute H_2SO_4 . After dissolving, the solution was transferred to a 500 ml. graduated flask and made up to the mark with distilled water.

100 mls. of dilute H_2SO_4 , previously coloured faint

pink with $N/10$ $KMnO_4$, were measured into a 600 ml. beaker and 50 ml. of the perborate solution added. This solution was titrated against $N/10$ $KMnO_4$ to the same faint pink colouration as had persisted prior to the perborate addition. The result was calculated as % available oxygen or as atoms of available oxygen per atom of boron.

3. Estimation of water content.

(The term "H₂O content" includes that from any H₂O₂ present i.e. it is the H₂O when the perborate is written $NaBO_3 \cdot x H_2O$).

About 2 gm. were weighed accurately into a 100 ml. pyrex beaker and covered with a watch glass. The beaker and contents were heated on a water bath for 2 hr. then transferred to an oven at 140 °C for 12 hr.

The beaker etc. were then removed to a muffle furnace at approximately 100 °C and the temperature raised to 550 °C, retained this temperature for 1 hr., allowed to cool and then reweighed. The solid was tested for residual available oxygen. It was never found.

4. Estimation of iron.

This was done colorimetrically using thiocyanate with the aid of a Spekker. To cultivate the method 5 mls. dilute HCl were pipetted into two 100 ml. graduate flasks containing 2 g. $NaBO_3 \cdot 4H_2O$ and diluted to 75ml. with

7

distilled water 20 mls. of ammonium thiocyanate solution were pipetted into both blasks. 1.5 mls. of a standard iron solution were pipetted into one of the flasks. Both flasks were diluted to volume and shaken well. The absorption of the pink iron solutions was measured against the blank on a "Spekker" absorptiometer. This was repeated for several iron solutions and a calibration graph drawn. The colour began to fade after several minutes and it was necessary to obtain the absorption readings as soon as possible after colour development. For the actual determination about 5 gm. of $\text{NaBO}_3 \cdot 4\text{H}_2\text{O}$ were weighed accurately into a 250 ml. beaker. 50 ml. of distilled water were added and the perborate solution was partially decomposed by boiling. The solution was cooled slightly and 5 ml. conc. HCl were added followed by 1 ml. bromine water, and the solution boiled until all excess bromine was driven off, while the volume was maintained at approximately 25 ml.

The solution was then transferred to a 100 ml. graduated flask, 20 ml. of 40% ammonium thiocyanate solution added, made up to volume and shaken well.

The blank solution was prepared by pipetting 5 mls. conc. HCl into a 250 ml. beaker containing 5 g. $\text{NaBO}_3 \cdot 4\text{H}_2\text{O}$, adding 30 ml. distilled water and 1 ml. bromine water, boiling until all excess bromine had boiled off, cooled and

transferred to a 100 ml. graduated flask. 20 ml. NH_4CNS were added, made up to volume and shaken well.

The absorption of the sample against the blank was measured on the "Spekker" and the iron content determined from the calibration graph. The result was recorded as grams of Fe per million $\text{NaBO}_3 \cdot 4\text{H}_2\text{O}$ (i.e. p.p.m.)

5. Estimation of copper.

The "Spekker" was calibrated by means of standard copper solutions and sodium diethyldithiocarbamate. About 10 gm. of $\text{NaBO}_3 \cdot 4\text{H}_2\text{O}$ were weighed into a 250 ml. beaker. 75 ml. dilute H_2SO_4 were added, the solution was evaporated to decompose the peroxide then cooled. 50 ml. of distilled water, 10 ml. citric acid, 2 ml. E.D.T.A., 20 ml. 0.380 ammonia and 10 ml. sodium diethyldithiocarbamate solution were added. The solution was then transferred to a 250 ml. separating funnel. 10 ml. redistilled CCl_4 were added and the solution shaken for 2 mins. On separation of the two layers, the lower CCl_4 layer was run off into a 50 ml. separating funnel. This procedure was repeated with 3 further 10 ml. portions of CCl_4 .

The accumulated CCl_4 solution was then filtered through a Whatman No. 1 filter paper into a dry 50 ml. graduated flask. The separating funnel was washed clean with a further 5 ml. CCl_4 and the flask was diluted to volume with CCl_4 .

The absorption of this solution was measured on the "Spekker" against a blank.

The blank solution was prepared by weighing about 5 gm. $\text{NaBO}_3 \cdot 4\text{H}_2\text{O}$ into a 250 ml. beaker then adding 75 ml. dilute H_2SO_4 , 10 ml. citric acid, 2 ml. E.D.T.A., 20 ml. 0.33 ammonia, 10 ml. sodium diethyldithiocaramate solution and 10 ml. redistilled CCl_4 . The extraction and filtration were as above. This drum reading was subtracted from that of the sample and from this corrected drum reading the copper was determined from the calibration graph.

C. Decomposition Studies.

1. Solid $\text{NaBO}_3 \cdot 4\text{H}_2\text{O}$.

The $\text{NaBO}_3 \cdot 4\text{H}_2\text{O}$ used in the decomposition measurements was from one large batch which had the following analysis:- Na_2O , 20.43%; B_2O_3 , 23.00%; O_2 , 10.00%; H_2O , 46.52%. This corresponds with the formula $\text{NaBO}_2 \cdot 0.97^a \cdot 3.98\text{H}_2\text{O}$. Special reference will be made should the composition of the perborate differ from these figures.

(1) At atmospheric pressure.

A 0.3 g. weighed sample of the finely powdered solid dry solid was spread in a thin layer on the base of a 100 ml. conical flask. The ground stopper, sealed in with wax, lead via fine polythene tubing to a capillary flow meter held horizontally against a mirror scale. 1 mm. displacement of the soap film in the capillary tube

indicated 0.003 ml. of gas evolved. The conical flasks were completely immersed in thermostat baths at 40 °C, 50 °C, and 60 °C. The rate of oxygen evolution was measured at intervals until decomposition was almost complete. In these "closed" experiments the perborate softened and fused during the experiment.

(ii) Under vacuum.

For vacuum work, thin layers of the perborate were spread on the bottom of a flask connected to a rotary oil pump. Samples of the solid, which remained dry and powdery in the vacuum experiments, were taken at measured intervals of time and analysed in duplicate for Na_2O , B_2O_3 and available oxygen by the methods indicated above.

(iii) Sealed and open tests.

The decomposition measurements mentioned in (i) above left some doubt as to whether (a) the aqueous soap films had raised the partial pressure of the water vapour over the solid and so promoted liquefaction (the long length of narrow connecting tubing was designed to prevent this) or, (b) a loss of hydrate water might have occurred by entrainment with the oxygen evolved so that liquefaction might have been slower than otherwise.

Hence the atmospheric type measurements were followed by a sealed test-tube sample method. In this method 0.3 gm.

11

samples of $\text{NaBO}_3 \cdot 4\text{H}_2\text{O}$ were accurately weighed into dry test-tubes, previously cleaned in a HNO_3 -alcohol mixture washed with distilled water and baked out at 200°C . The tubes were then drawn out near the open end over a small flame and sealed. The lower part of the tube containing the perborate was wrapped in wet filter paper to avoid any heat reaching the perborate sample during the sealing-off.

These test tubes were placed in aluminium racks and completely immersed in the thermostats. At 15 min. intervals a test tube was removed, the pressure released by snipping off the drawn end under 100 ml. dil H_2SO_4 in a beaker and the tube cut up into sections using a glass knife. These sections were immersed in the acid and the remaining available oxygen was determined by titration against $\text{N}/100 \text{ KMnO}_4$. In the tubes the perborate assumed a viscous state and did not readily leave the glass.

Some similar sample tube experiments were also conducted using "open" tubes plugged with cotton wool. They were almost completely immersed in thermostats at the required temperature and removed from time to time for analysis.

(iv) Tensimetric measurements.

Neither method (i) or (iii) was sensitive enough for a detailed study of say the first 1% of decomposition. This

was an important range to study because during this part of the process there was no sign of liquid formation and it was clearly here if anywhere that the solid perborate decomposition would be found.

A differential tensimetric method was therefore adopted to study initial decomposition. Fig. 1 shows a diagram of the apparatus. One of the 10 ml. bulbs contained 1 gm. accurately weighed of $\text{NaBO}_3 \cdot 4\text{H}_2\text{O}$ and the other 1 gm. of $\text{NaBO}_2 \cdot 4\text{H}_2\text{O}$. The bulbs were attached one on each side of the butyl phthalate manometer by waxed B7 joints, then immersed in the thermostat. After 15 mins. the side arms were quickly sealed with soft wax. From a knowledge of the total free volumes of the bulbs and connecting tubes (2 mm. bore) a calibration curve (Fig. 2) was constructed relating pressure differences to oxygen evolved (the volume of the solid was calculated from density data). 1 mm. of oil pressure indicated $2.38 \times 10^{-2} \%$ loss of oxygen per gm. $\text{NaBO}_3 \cdot 4\text{H}_2\text{O}$. The calculations were as follows:

Let original pressures on both sides, when $h = 0$, be p_0 atmospheres. At a height of h cm. (i.e. difference in levels), the pressure on R.H.S. was

$$\frac{R}{p_1} = \frac{p_0 V_0}{V_1 R}$$

Originally on L.H.S. $R.T.n_0 = p_0 V_0$, where n_0 = number of moles of oxygen originally present. At height "h" cm. due to evolution of " Δn " mols of oxygen:-

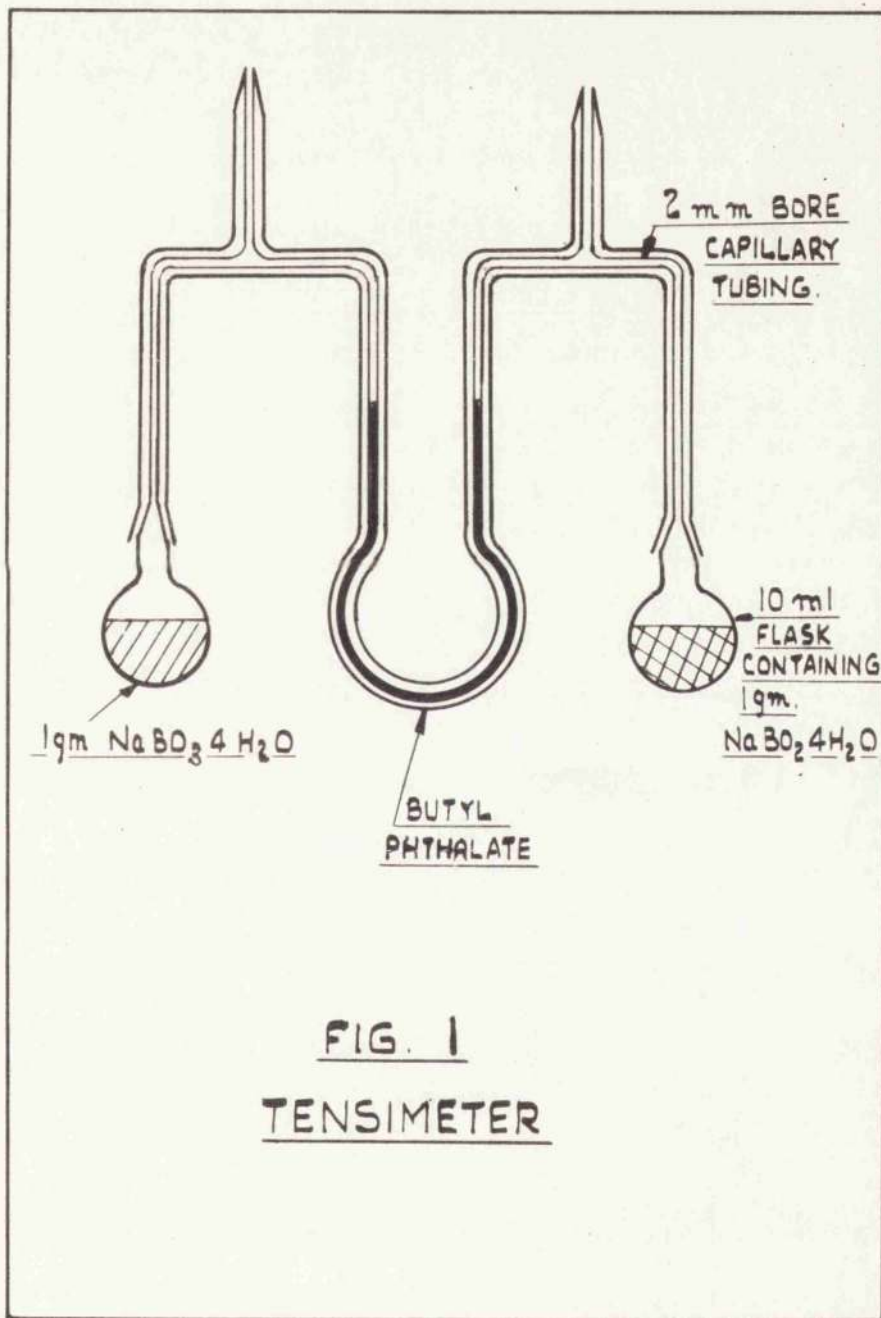


FIG. 1
TENSIMETER

L.H.S. $RTn_0 + RT\Delta n = P_1^L V_1^L$
 $= (P_1^R + \Delta P) V_1^L$ where $\Delta P =$
 difference in pressure due to h cm.

$$= P_1^R V_1^L + \Delta P V_1^L$$

$$\therefore RT\Delta n = P_0 V_0 \left[\frac{V_1^L}{V_1^R} - 1 \right] + \Delta P V_1^L$$

$$= P_0 V_0 \left[\frac{V_0 + \alpha - \Delta V}{V_0 - \alpha} - 1 \right] + \Delta P (V_0 + \alpha - \Delta V)$$

where $\alpha =$ difference in capillary volume for any difference in levels (for $h = 1$ cm., $\alpha = 1 \times 10^{-5}$ ml. for a 2 mm. bore capillary) and $\Delta V =$ correction for volume of solid.

$$= P_0 V_0 \left[\frac{V_0 + \alpha - \Delta V - V_0 + \alpha}{V_0 - \alpha} \right] + \Delta P (V_0 + \alpha - \Delta V)$$

$$= P_0 V_0 \left[\frac{2\alpha - \Delta V}{V_0 - \alpha} \right] + \Delta P (V_0 + \alpha - \Delta V).$$

for 1 gm. $\text{NaBO}_3 \cdot 4\text{H}_2\text{O}$, $\Delta V \approx 0.4$ ml., $\therefore V_1^L = (0.0096 + \alpha)$
 $V_0 = 0.01$ l., $P_0 = 1$ atm., $\alpha = 1 \times 10^{-5} h$, $\Delta P = \frac{h}{76 \times 13.6}$

$w = 1$.

From these figures the results shown in Table I were obtained.

TABLE I

h(cm.)	Δn (% oxygen evolved)
1	2.33×10^{-2}
5	11.90×10^{-2}
10	24.0×10^{-2}
20	47.8×10^{-2}

There was no difficulty in following the decomposition reproducibly to within 0.5%

Measurements were also carried out on samples of $\text{NaBO}_3 \cdot x\text{H}_2\text{O}$ where x ranged from 1.5 to 4.49 at 35°C . Some tensimetric experiments were also conducted at $20.5^\circ\text{C} \pm 0.1^\circ$.

The partly dehydrated perborate samples used in the tensimetric experiments were obtained by partial dehydration of $\text{NaBO}_3 \cdot 4\text{H}_2\text{O}$ samples in thin layers in an open vessel at 60°C .

The perborate samples with excess water present were obtained by incomplete drying during the preparation of certain batches of $\text{NaBO}_3 \cdot 4\text{H}_2\text{O}$.

2. Melting of borate-perborate mixtures.

It was observed in the decomposition experiments that softening of the $\text{NaBO}_3 \cdot 4\text{H}_2\text{O}$ crystal mass occurred as soon as a 2-5% of decomposition had taken place. At 40°C liquefaction was complete at about 40% decomposition. It was inferred that softening of the crystals and conversion of the dry mobile powder into a clinging mass was due to superficial fusion and furthermore it seemed apparent that the occurrence of this well below the melting point (63.5°C) of the solid was due to melting point lowering by intimate intermixing of the hydrated perborate with metaborate produced by decomposition. A simple test by rubbing together in a test tube an

equimolar mixture of the dry powders at 40 °C confirmed this - rapid melting occurred.

A study of the first fusion temperature of perborate metaborate mixture was undertaken to demonstrate the formation of liquid at relatively low temperatures.

The dry solids were mixed at room temperature (18 °C) by gently grinding and shaking together and the first melting point taken as the temperature at which a small column of the mixture began to shrink. Three methods were used (i) with the solid in a melting point tube and the temperature raised by 3 °C per minute, (ii) with a column of the solid in a $\frac{5}{8}$ " test tube held compressed by a powerful coil spring. The tube was immersed in a thermostat and the movement of the spring was observed with a microscope. The temperature was raised from room temperature by 2 °C increments and held at each temperature for 15 min. (iii) 2-3 mm. thick pellets of mixtures were held between 1 cm. diameter spring loaded stainless steel electrodes in a sealed tube in a thermostat. The pellets had been formed in a stainless steel cylindrical die with a 2 ton compression force supplied by a hydraulic press. The resistance of the pellets was measured on an A.C. bridge. Temperatures, starting at room temperature, were raised in 2 °C steps, and held at each value for periods of 4-18 hours,

depending on how long the resistance took to reach a steady value.

3. Single crystal Observations.

A small batch of $\frac{1}{8}$ " $\text{NaBO}_3 \cdot 4\text{H}_2\text{O}$ crystals, obtained after five recrystallisations, was supplied by Laporte.

One crystal was placed on the slide of a heating stage microscope and encircled by a $\frac{1}{8}$ " wide layer of ground, laboratory prepared, $\text{NaBO}_3 \cdot 4\text{H}_2\text{O}$ powder, on top of which was placed a cover slip. In this way the single crystal could be heated at its equilibrium vapour pressure.

The crystal was heated through the temperature range 50-70°C while being observed through the microscope.

4. Decomposition in the melt.

From the preceding observations on pure $\text{NaBO}_3 \cdot 4\text{H}_2\text{O}$ crystals at different temperatures, it appeared that there was no inherent decomposition of an absolutely pure dry $\text{NaBO}_3 \cdot 4\text{H}_2\text{O}$ crystal and that the decomposition must take place in the fused material. Consequently a series of experiments in the completely fused material was planned. The following method provided both a simple and satisfactory method of conducting such experiments.

Method of conducting fused perborate experiments.

0.3 gm. samples of perborate were weighed into clean dry test tubes which were subsequently drawn and sealed. The solid was melted by immersing the test tube

in boiling water for a standard length of time, (45 secs.) and then the tubes were immediately transferred and immersed in a thermostat at the reaction temperature. Tubes were removed at appropriate time intervals, carefully opened, and the contents analysed for available oxygen by titration. Additives, in the form of $\text{Cu}(\text{BO}_2)_2$, $\text{CuSO}_4 \cdot 5\text{H}_2\text{O}$, FeCl_3 , $\text{FeSO}_4 \cdot 7\text{H}_2\text{O}$, $\text{Mg}(\text{SO}_4) \cdot 7\text{H}_2\text{O}$, $\text{Mg}(\text{BO}_2)_2$, $\text{ZnSO}_4 \cdot 7\text{H}_2\text{O}$, $\text{Zn}(\text{BO}_2)_2$, H_3BO_3 and powdered glass were introduced with the solid after intimate mixing in an agate mortar to test the effect of catalysts and stabilisers.

Some experiments were also conducted with vessels painted black in order to test for photochemical effects. They showed that light had no accelerating effect.

Effect of added water.

In order to establish whether water molecules participated in the decomposition process it was deemed necessary to conduct several experiments on the effects of added water to perborate tetrahydrate prior to fusion and subsequent decomposition.

To 0.3 gm. samples of perborate in test tubes 0.1, 0.2, 0.4 and 1.0 gm. H_2O were added via a microburette. The subsequent experimental procedure was as above.

Experiments with dilute solutions of perborate.

Solutions were made up either by dissolving the requisite amount of $\text{NaBO}_3 \cdot 4\text{H}_2\text{O}$ in distilled water, or by adding the stoichiometric quantities of H_2O_2 and $\text{NaBO}_2 \cdot 4\text{H}_2\text{O}$.

In fact the latter solutions always decomposed at a measurable slower rate than the former although the form of the process was identical in the two cases. This was ascribed to the presence of impurities introduced during laboratory handling and drying of $\text{NaBO}_3 \cdot 4\text{H}_2\text{O}$.

The apparatus consisted of a 400 ml. vessel with three necks, the first incorporating a condenser to prevent changes in concentration due to evaporation of the solution. The second held a micropipette through which additions could be made to the solution of either stabiliser or catalysts in the form of a preheated solution. The third neck was for sampling purposes. It was not essential to stir the solutions.

200 ml. of the perborate solution, preheated to the reaction temperature, was placed in the reaction vessel contained in the thermostat. At five minute intervals the solution in the reaction vessel was swirled vigorously to free oxygen bubbles and then a 5 ml. sample withdrawn by pipette. In this way no oxygen bubbles were removed in the sample. These samples were added to 100 ml. of 2N H_2SO_4 and titrated against $\text{N}/100 \text{ KMnO}_4$.

pH measurement.

Whenever pH measurements are quoted they are direct measurements made with a "Pye" glass electrode assembly

calibrated in standard borate at 25°C, corrected where appropriate for temperature but not for ionic strength or liquid junction, or affect on an asymmetry potential of the peroxide solution.

It should be explained that the potential measured in the standard borate solution is not affected by the presence of hydrogen peroxide in the solution.

(1) *Electrode response to hydrogen peroxide*

Figure 3 shows the potential response of the electrode to a series of standard hydrogen peroxide solutions. The potential increases linearly with the logarithm of the peroxide concentration. The slope of the line is 59.2 mV per decade, which is the theoretical value for a one-electron reaction. The intercept on the y-axis is 1.10 V, which is the standard potential of the electrode.

The following table shows the potential response of the electrode to a series of standard hydrogen peroxide solutions.

- (a) A delay period of 10-15 minutes is required before the potential stabilizes.
- (b) A rapid rise in potential is observed when the peroxide concentration is increased.
- (c) A further increase in potential is observed when the peroxide concentration is increased further.
- (d) A rapid fall in potential is observed when the peroxide concentration is decreased.

Results

1. Decomposition of solid $\text{NaBO}_3 \cdot 4\text{H}_2\text{O}$.

In what follows the rate of loss of oxygen is quoted as % of available oxygen lost in a given time. It should be explained that the figure refers to the diminution in the "% available oxygen" value.

(1) At atmospheric pressure.

Figs. 2 and 3 show the results obtained at atmospheric pressure in the form of a plot of rate of decomposition (i.e. oxygen evolved) against time. Complete decomposition was effected in 12 days, 6 days and 14 hr. at 40° , 50° and 60°C respectively. Fig. 4 relates the rate of oxygen evolution to the amount of perborate decomposed.

The main features of the rate changes were as follows:-

- (a) A delay period during which there was no measurable gas evolution. This lasted for $\frac{1}{2}$ - 1 hr. at 60°C .
- (b) A rapid rise to a rate level which remained steady for 5%-10% decomposition (except at 60°).
- (c) A further period of accelerating growth of rate which lasted from 5 to 20% decomposition and then steadied up until, at about 50% decomposition, a maximum was reached.
- (d) A rapid fall in rate which set in as soon as the maximum was attained and was at first linear with the amount decomposed. * These changes occurred at the same fraction

DECOMPOSITION OF $\text{Na}_2\text{BO}_3 \cdot 4\text{H}_2\text{O}$

Plot of Rate v. Time.

NO PUMPING.

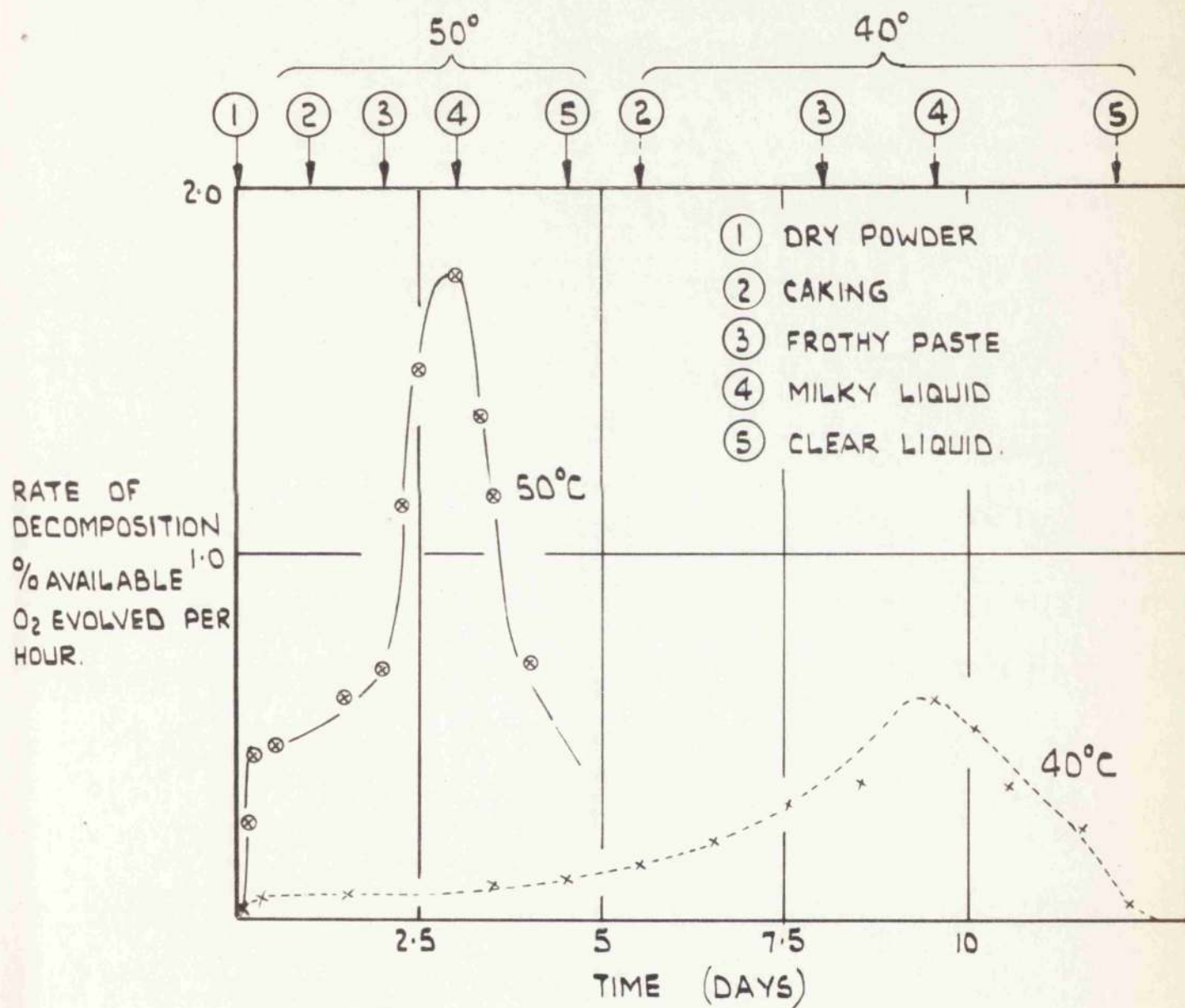


FIG. 2

DECOMPOSITION OF $\text{Na}_2\text{B}_4\text{O}_7 \cdot 10\text{H}_2\text{O}$

PLOT OF RATE v TIME

NO PUMPING

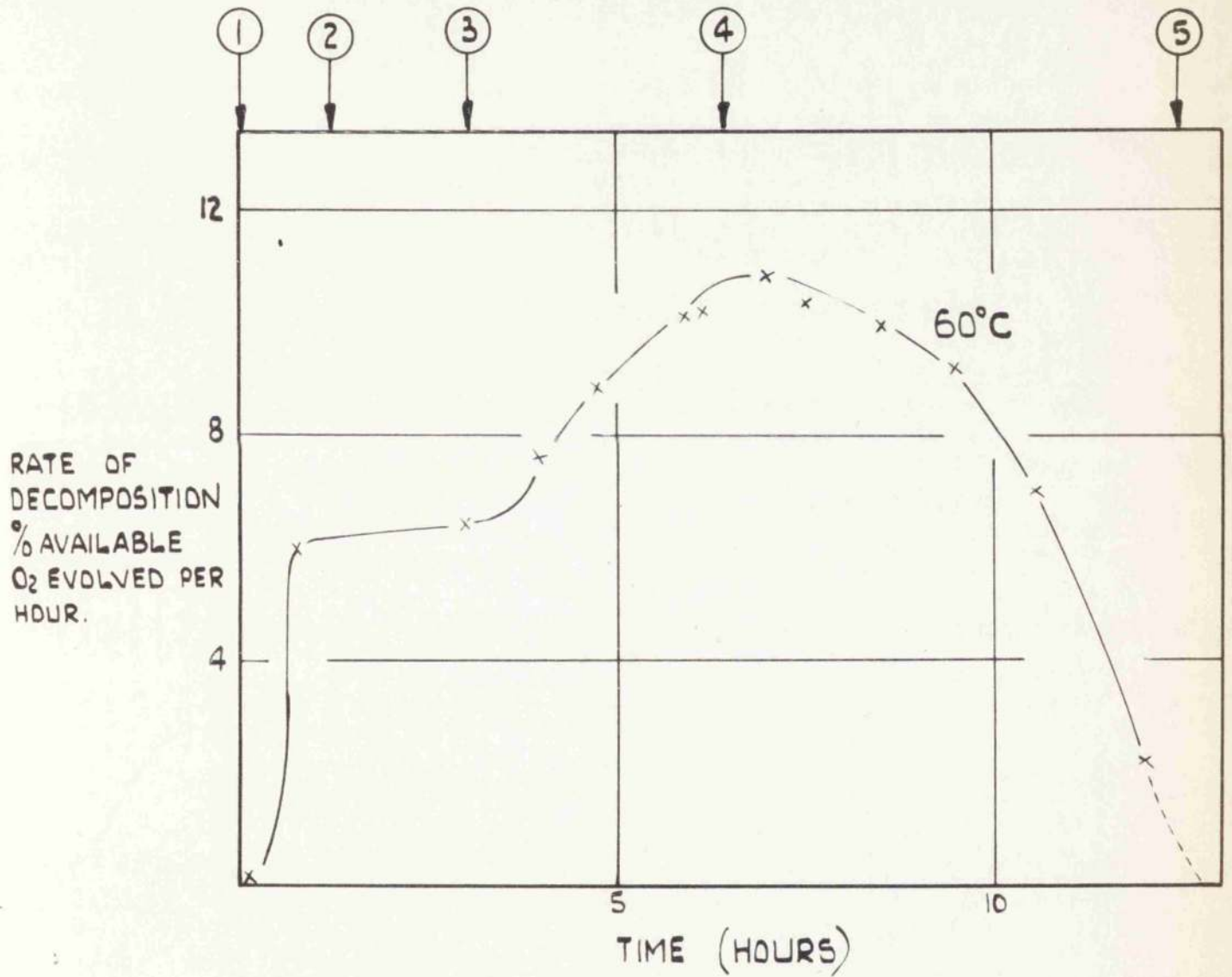


FIG. 3

of decomposition whatever the time, as shown in Fig. 4.

On Figs. 2, 3 and 4 is also indicated the state of the $\text{NaBO}_3 \cdot 4\text{H}_2\text{O}$ at various stages of decomposition. Thus when stage (c), the accelerating decomposition, was evident, the powder was 'clinging'. At the maximum rate it had the form of a frothy paste and at or just after this it became a viscous milky liquid. Microscopic examination showed that the whiteness was due to a multitude of minute oxygen bubbles. The eventual residue was a clear viscous liquid, which contained no measurable oxygen and which set on cooling, after many days, to a crystalline slab of the metaborate tetrahydrate.

(ii) Under vacuum.

For the evacuated runs at 60°C the results are shown in Table I which indicates the average composition of the hydrate at various times as shown by the analyses.

The molecular formula is written $\text{NaBO}_2\text{O}_x \cdot y\text{H}_2\text{O}$ where 'x' is the number of g.atoms of available oxygen and 'y' the number of moles of water in one mole of the compound.

Table I.

Time (Hours)	x	y
0	0.96	3.95
1/2	0.97	2.25
1	0.97	1.71
2	0.97	1.16
3	0.97	1.05
4	0.97	1.03

DECOMPOSITION OF $\text{Na}_2\text{B}_4\text{O}_7 \cdot 10\text{H}_2\text{O}$

PLOT OF RATE ν CONCENTRATION

NO PUMPING.

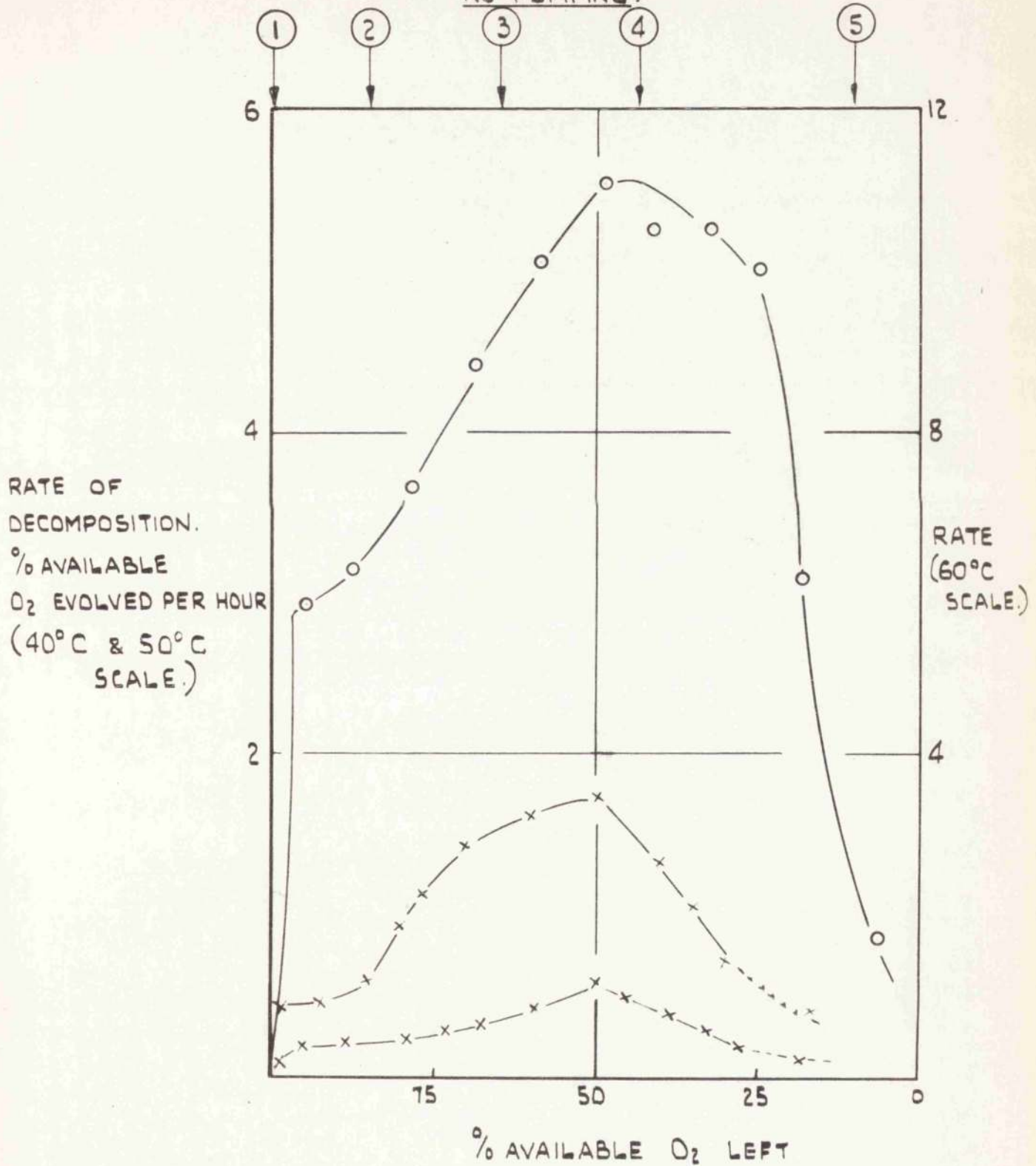


FIG. 4

In four hours, which was sufficient to change the solid almost wholly to the monohydrate, no detectable loss of oxygen occurred. The compound remained in the form of a dry powder throughout. In the closed vessel experiments 30% of the available oxygen would have been lost in the same period.

(iii) Sealed and open tests.

Fig. 5 illustrates the results obtained at 50°C. following the decomposition by analysis of samples after various times. Apart from the failure to observe the initial build up of rate mentioned in (i) above, the results for the $\text{NaBO}_3 \cdot 4\text{H}_2\text{O}$ material in the closed tube was the same as before -fusion, and rapid liquid phase decomposition. The same was true for partly dehydrated material ($1.5 \text{H}_2\text{O}$) but a commercially prepared, Mg-stabilised, sample showed only a slight change in five days. In open tests fusion was avoided with the $\text{NaBO}_3 \cdot 4\text{H}_2\text{O}$ samples used.

(iv) Tensimetric studies.

(a) At 35°C

At 35°C with the carefully dried $\text{NaBO}_3 \cdot 4\text{H}_2\text{O}$ an immediate initial decomposition of 0.024% per day of available oxygen was observed. After $2\frac{1}{2}$ days the rate rose fairly sharply to 0.55% per day.

From one batch to another large differences were obtained both in the value of the initial rate and in the

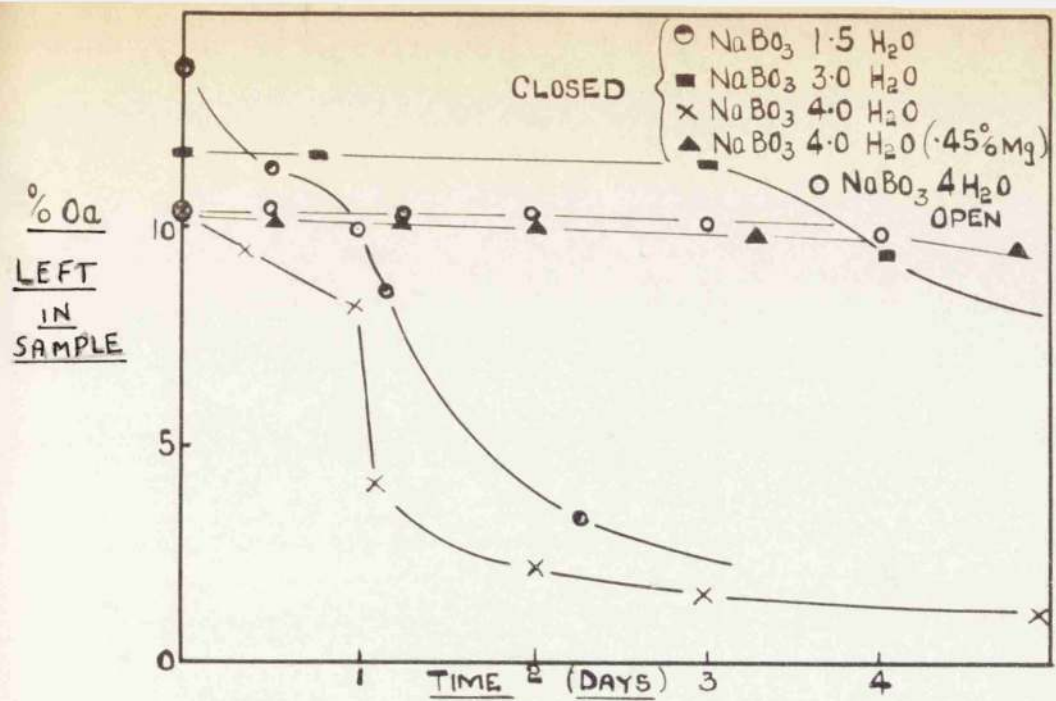


FIG. 5
 SHOWING DECOMPOSITION AT 50°C AS FOLLOWED
 BY ANALYTICAL METHOD

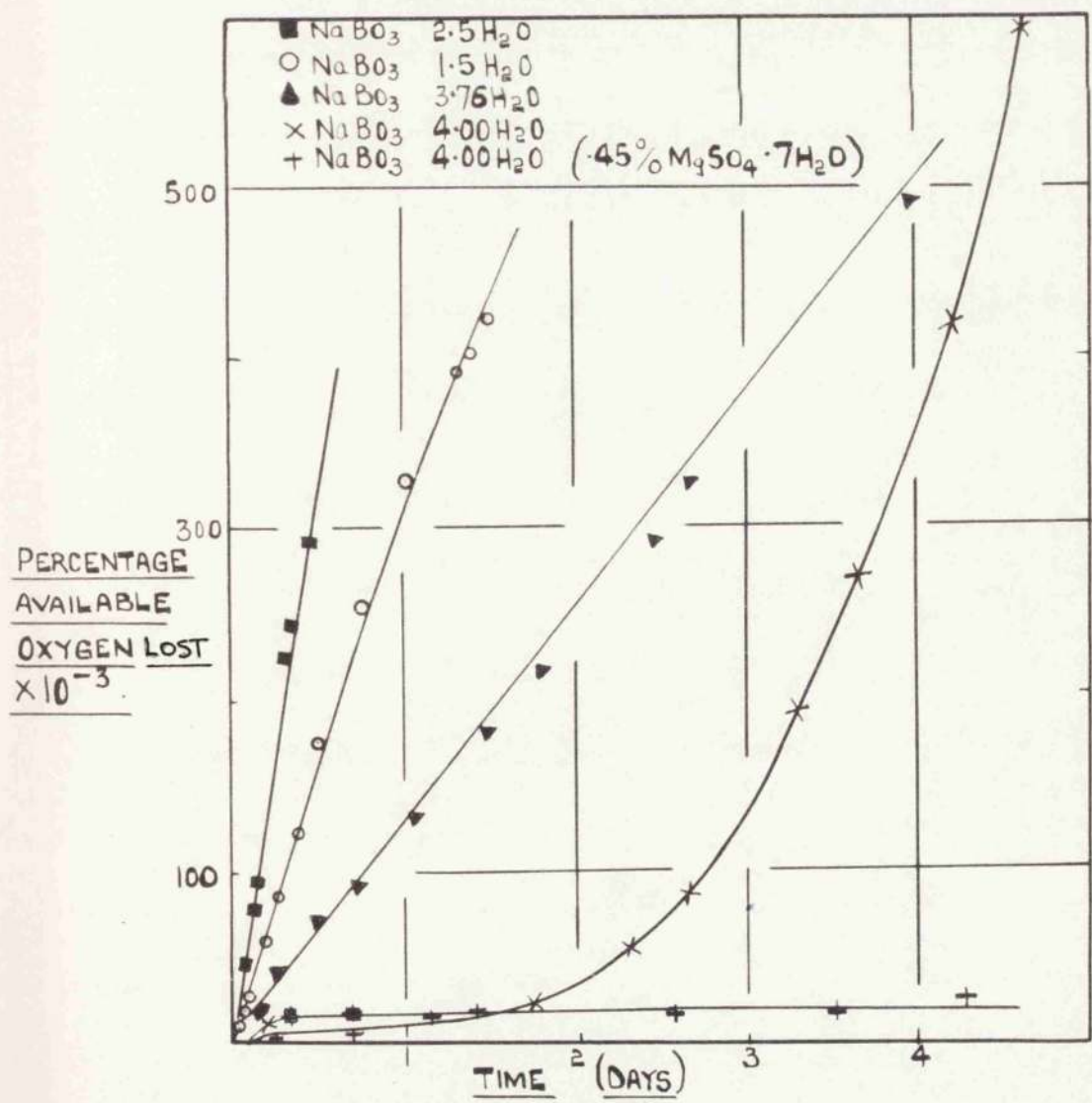


FIG. 6
 TENSIMETRIC STUDIES AT 35°C SHOWING INITIAL
 RATES OF DECOMPOSITION.

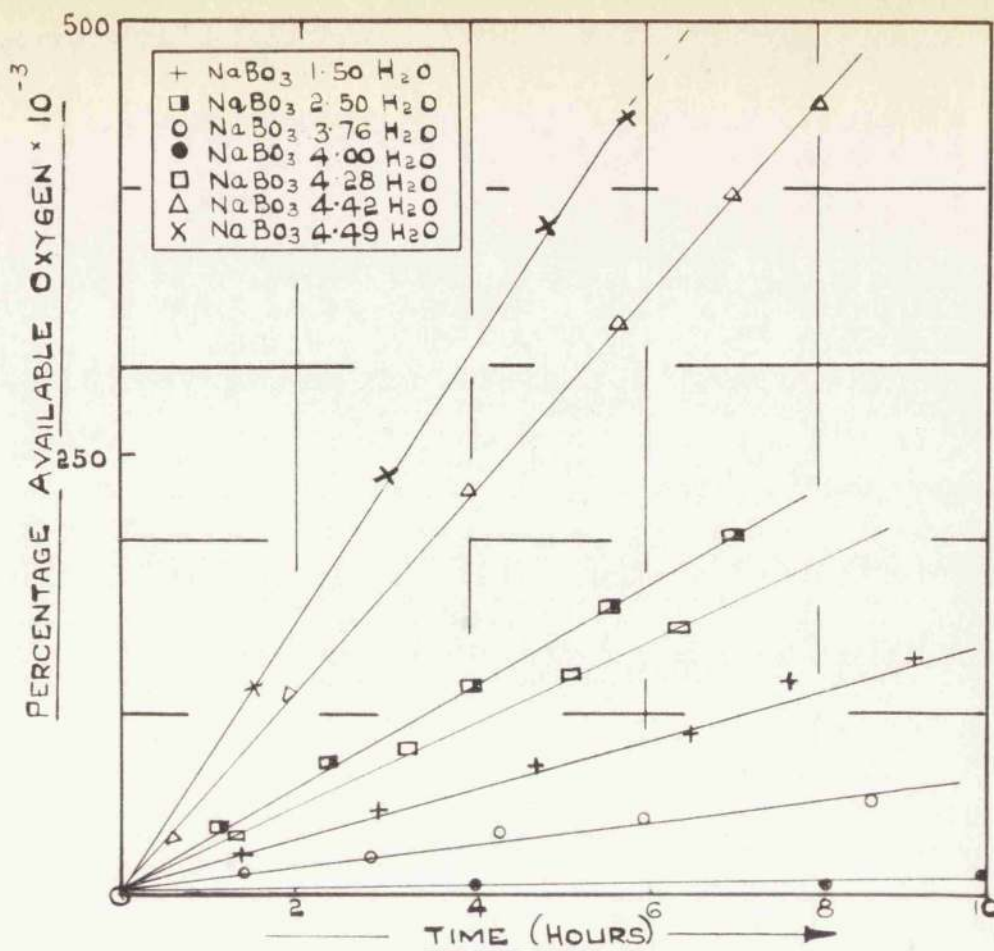


FIG: 6a SHOWING THE INITIAL DECOMPOSITION RATES OF DIFFERENT HYDRATES AT 35°C.

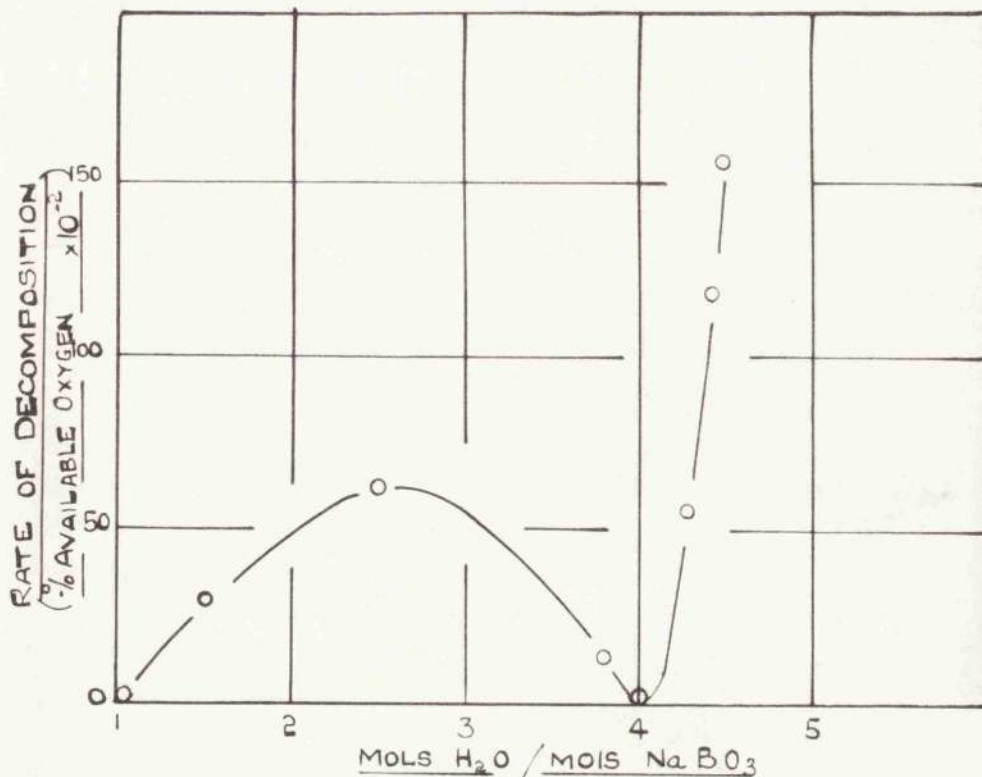


FIG: 6b SHOWING THE DIFFERENCE IN RATES OF DECOMPOSITION OF PERBORATE SAMPLES OF OVERALL COMPOSITION $\text{NaBO}_3 \times \text{H}_2\text{O}$ ($x=1-5$) AT 35°C BY A TENSIMETRIC METHOD

time at which the faster and accelerating rates set in. It was found in an overdried sample that the initial slow rate was almost eliminated. To investigate this further a range of samples partially dehydrated in vacuo were prepared. Results are given in Fig. 6 and 6a for samples of average composition $3.76 \text{ H}_2\text{O}$, $2.5 \text{ H}_2\text{O}$, $1.5 \text{ H}_2\text{O}$ as well as $4\text{H}_2\text{O}$. Also included is a sample of a commercial product with a reputed commercial addition of $0.45\% \text{ MgSO}_4 \cdot 7\text{H}_2\text{O}$ as stabiliser. Its effect is to fix the slow initial decomposition for a considerably longer period than in the unstabilised material (No change to a higher rate had occurred within 10 days by which time a total decomposition of 0.25% had occurred).

Also indicated in Fig 6(a) are the rates of samples containing small amounts of excess water indicated by the average composition $4.49 \text{ H}_2\text{O}$, $4.42 \text{ H}_2\text{O}$, and $4.23 \text{ H}_2\text{O}$. These were prepared by exposing the normal product to water vapour.

Fig 6 (b) indicates graphically the dependence of rate on moles H_2O per mole NaBO_3 . Clearly small increments are more active than small decrements. In both cases the effect is less sharp close up to $4.00 \text{ H}_2\text{O}$ than a little removed from this value. This is fortunate. It means that the precise nature of the $\text{NaBO}_3 \cdot 4\text{H}_2\text{O}$ crystal is not so critical as may have been the case.

(b) At 20.5°C.

The results obtained from a tensimetric study of a $\text{NaBO}_3 \cdot 3.76 \text{H}_2\text{O}$ sample at $20.5^\circ\text{C} \pm 0.1^\circ$ are shown in Fig. 7. $\text{NaBO}_3 \cdot 4\text{H}_2\text{O}$ did not yield measurable rates of decomposition at this temperature over a period of several days. More fully dehydrated samples or incompletely dried samples, did show a measurable decomposition but did not show at all clearly the slow initial rates of decomposition. From Fig. 7 however the two rates of decomposition (for two samples of $\text{NaBO}_3 \cdot 3.76\text{H}_2\text{O}$ tested) are clearly distinguished. Initially there was a slow rate of $2.38 \times 10^{-3}\%$ of available O_2 per day lasting for 30 hr. followed by a 10 times faster rate of $2.38 \times 10^{-2}\%$ per day. This latter rate corresponds with the rate given by the $3.76 \text{H}_2\text{O}$ material at 35°C , which gave a decomposition rate value more than three times as great. This gives an activation energy of 18.6 Kcal mol. - a value that agrees well with that obtained from results from the prefused state (cf. Section 4(a))

The slow initial rate, which was not distinguished at 35°C for $\text{NaBO}_3 \cdot 3.76\text{H}_2\text{O}$ corresponds to the slow rate of decomposition of the $\text{NaBO}_3 \cdot 4\text{H}_2\text{O}$ sample at 35°C but since this process is very sensitive to dehydration it was not profitable to compare the two.

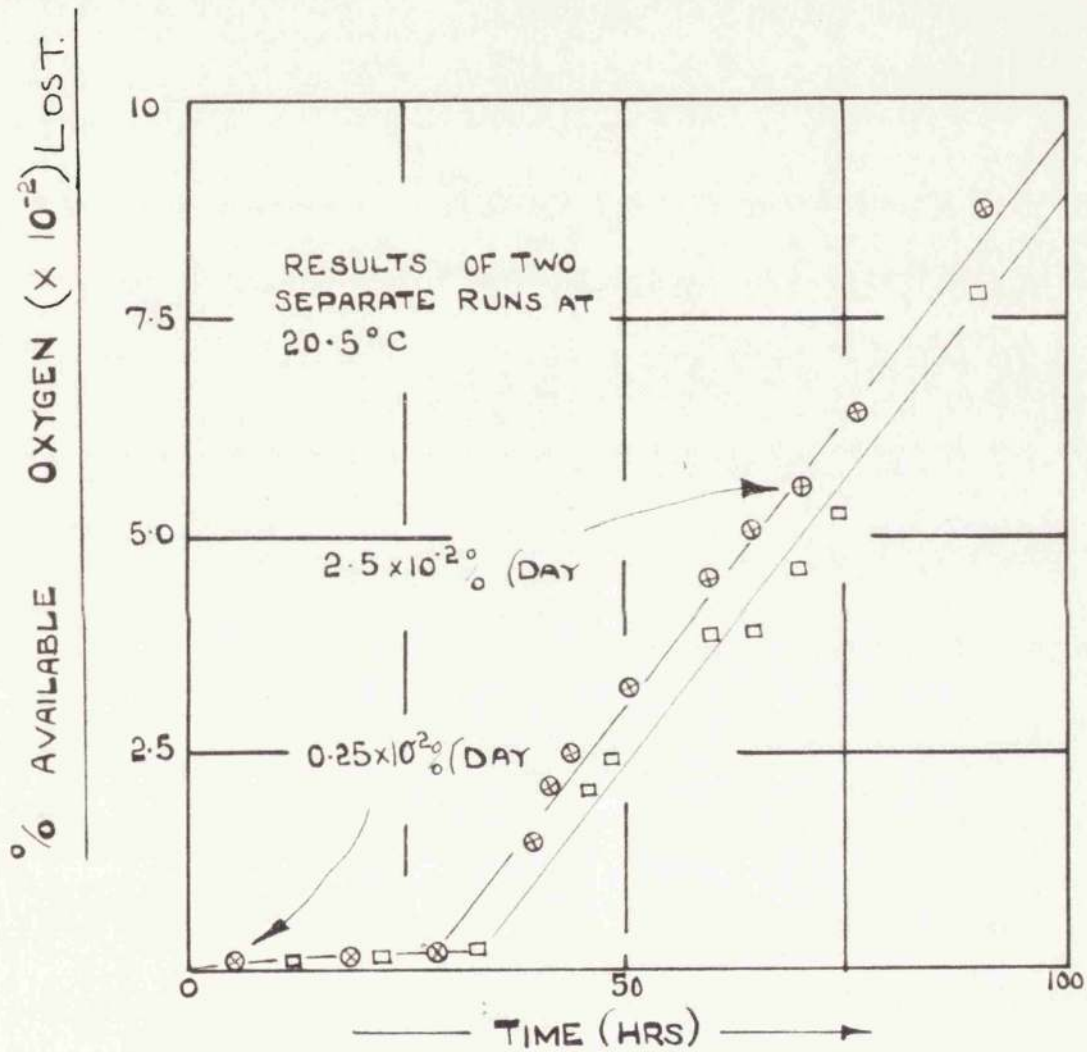


FIG: 7 TENSIMETRIC STUDY OF $\text{NaBO}_3 \cdot 3.76\text{H}_2\text{O}$

AT $20.5^\circ\text{C} \pm 0.1^\circ$

2. Softening of perborate tetrahydrate during decomposition.

It was clear that softening of the decomposing perborate was due to melting of the $\text{NaBO}_3 \cdot 4\text{H}_2\text{O} / \text{NaBO}_2 \cdot 4\text{H}_2\text{O}$ mixture and perhaps to the fact that during decomposition some $\text{NaBO}_3 \cdot 3\text{H}_2\text{O}$ could slowly form from the tetrahydrate. The following table gives the temperatures at which melting of the solids consisting of an intimate mixture of the $\text{NaBO}_2 \cdot 4\text{H}_2\text{O}$ and $\text{NaBO}_3 \cdot 4\text{H}_2\text{O}$ was first observed on raising the temperature from 20°C at about 2° per minute. Onset of melting was taken as the point when the compressed powder showed signs of shrinking.

Table II.

% NaBO_3 in mixture	Temp. at which shrinkage occurred.
100	63.6° (melting)
90	50.05
80	42.10
70	38.00
60	40.05
50	41.00
20	46.05
10	49.60

The results show that shrinkage was not observable in 2-3 minutes when held at temperatures below 33°C when the onset of shrinkage was observed more sensitively by microscopic movement of a spring compressed against a 1 cm. deep pellet in a $\frac{5}{8}$ " test tube, a somewhat lower temperature of 32°C was observed. In this case, largely owing to the requirements of the experiment, the use of a $\frac{5}{8}$ " diameter sample tube requires more time (5-10 min.) at each temperature. The sample was held in a small thermostat.

Finally the method of detecting liquid formation by observing the conductivity of a compressed pellet of an equimolar mixture of the two components again gave lower temperatures for liquid formation. At 30-30.5°C the resistance (Table IV) fell by a factor of 10 in 2-3 hours. At temperatures below 29°C no fall in conductivity was observed in 2 days.

Table III

Temp. °C	Electrical Resistance in Ohms ³
24.8	1.40 x 10 ⁵
26.7	1.25 x 10 ⁵
28.8	1.12 x 10 ⁵
29.9	1.07 x 10 ⁵
30.8	0.14 x 10 ⁵
32.5	0.10 x 10 ⁵

These results indicate that liquefaction does occur when $\text{NaBO}_3 \cdot 4\text{H}_2\text{O}$ and $\text{NaBO}_2 \cdot 4\text{H}_2\text{O}$ are brought into contact at temperatures of 30°C and above. They do not exclude restricted liquefaction at lower temperatures, but give no evidence of its occurrence. It should be mentioned that there could be an important difference in the behaviour of mechanically mixed crystals of the two hydrates and an intimate mixture of the two which would result from the loss of oxygen from the surface of a $\text{NaBO}_3 \cdot 4\text{H}_2\text{O}$ crystal. This might lead easily to a very thin layer of fused material spreading over the surface of the crystals.

3. Single crystal observations.

Observations through a microscope showed that even after 60 minutes at $50\text{-}53^\circ\text{C}$ no changes were observed in or on the surface of a pure crystal. The surface remained polished and apparently dry.

On raising the temperature to $55\text{-}58^\circ\text{C}$, after 15-20 min., a series of what appeared to be small fissures appeared at the crystal surface. By 30 mins. the crystal had become almost completely opaque but there was no sign of gas bubbles or other indication of liquefaction. The opacity was due to a network of cracks appearing over the surface of the crystal. Owing to the method used to maintain the partial pressure of H_2O at or slightly above the equilibrium value for the crystal it was not possible to rule out completely the possibility that this superficial cracking

could have been due to dehydration.

On inserting a fresh crystal and quickly raising the temperature to 63-70 °C, liquid patches almost immediately appeared on the surface but again no evolution of gas was observed over the crystal surface, although the surrounding powdered perborate sample was frothing and decomposing freely by this time.

This would possibly indicate that there is no inherent decomposition of a pure $\text{NaBO}_3 \cdot 4\text{H}_2\text{O}$ crystal. Some large crystals were inserted in a small test tube which was sealed, then immersed for 60 secs. at 100 °C (the crystals did not melt completely although their surfaces were wet), and submerged in a thermostat at 60 °C i.e. just below their melting point. After 14 hr. no change appeared to have taken place i.e. the crystals were still wet but no further melting or decomposition had taken place. This seemed to confirm the single crystal observation.

4. Decomposition in the melt.

(a) Kinetics.

Decomposition was approximately zero order for the first part of the process, i.e. a given weight of a sample gave a steady rate of evolution of oxygen. This is shown by plotting the percentage of available oxygen against time.

Since we may assume the volume of liquid was constant in the samples this parameter is a measure of the concentration of active oxygen, peroxide, or perborate, remaining in the sample. Fig. 8 demonstrates this for 40°, 50°, 60° and 70°C. There was usually a small discrepancy at the beginning due to a small accelerated loss of oxygen during initial melting. The temperature coefficient leads to an activation energy of 19.0 K cal. mol. as shown in Fig. 9 in which $\log_{10} (-dO^a/dt)$ is plotted against $1/T^\circ K$.

(b) Effect of surface or light.

The addition of 0.5 gm. of ground glass to a sample more than doubled the rate of decomposition, but when glass beads were added in quantity sufficient to double the wall area of glass exposed to the liquid, the decomposition was affected negligibly. It was concluded that decomposition at the wall of the vessel did not contribute a significant amount to the rate of decomposition. It is however clear that glass surfaces accelerate rather than inhibit the oxygen loss.

Experiments with blacked out vessels showed that photochemical decomposition by normal subdued daylight was of negligible importance and that special precautions to exclude light were not required.

(c) Effect of iron and copper catalysts.

Iron and copper were chosen for study for two reasons. First, they are catalysts much studied in the

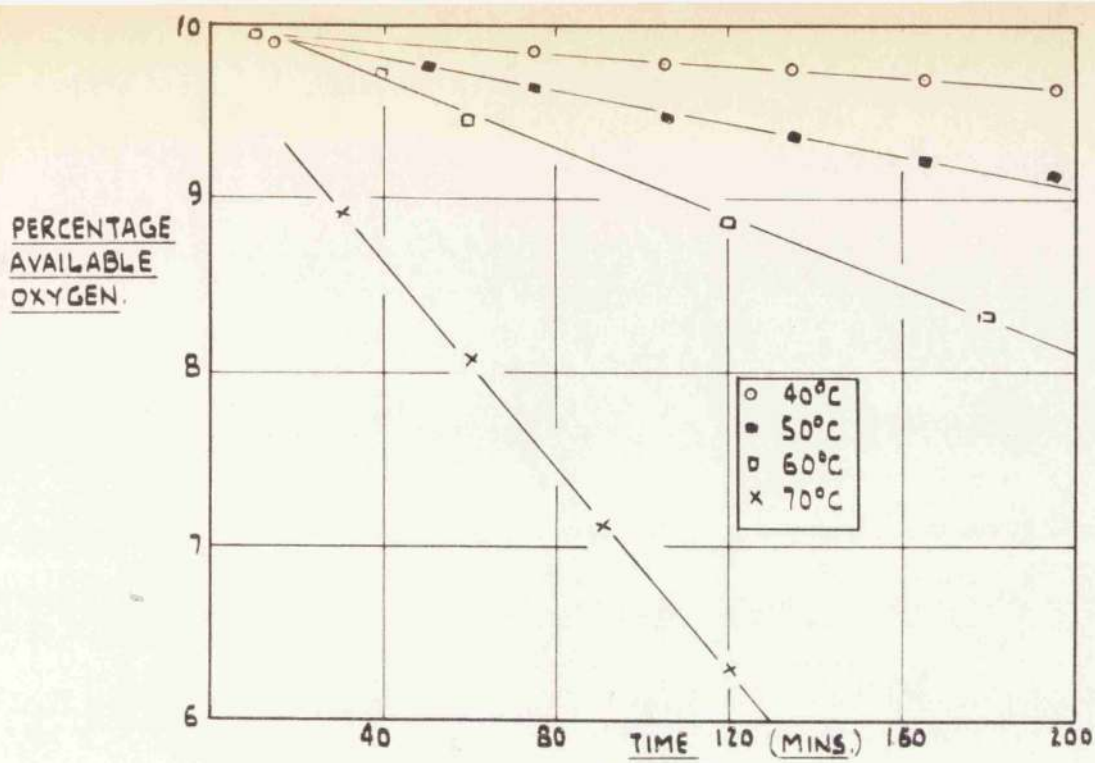


FIG. 8
 SHOWING ZERO ORDER DECOMPOSITION OF
 $\text{NaBO}_3 \cdot 4\text{H}_2\text{O}$ IN THE FUSED STATE.

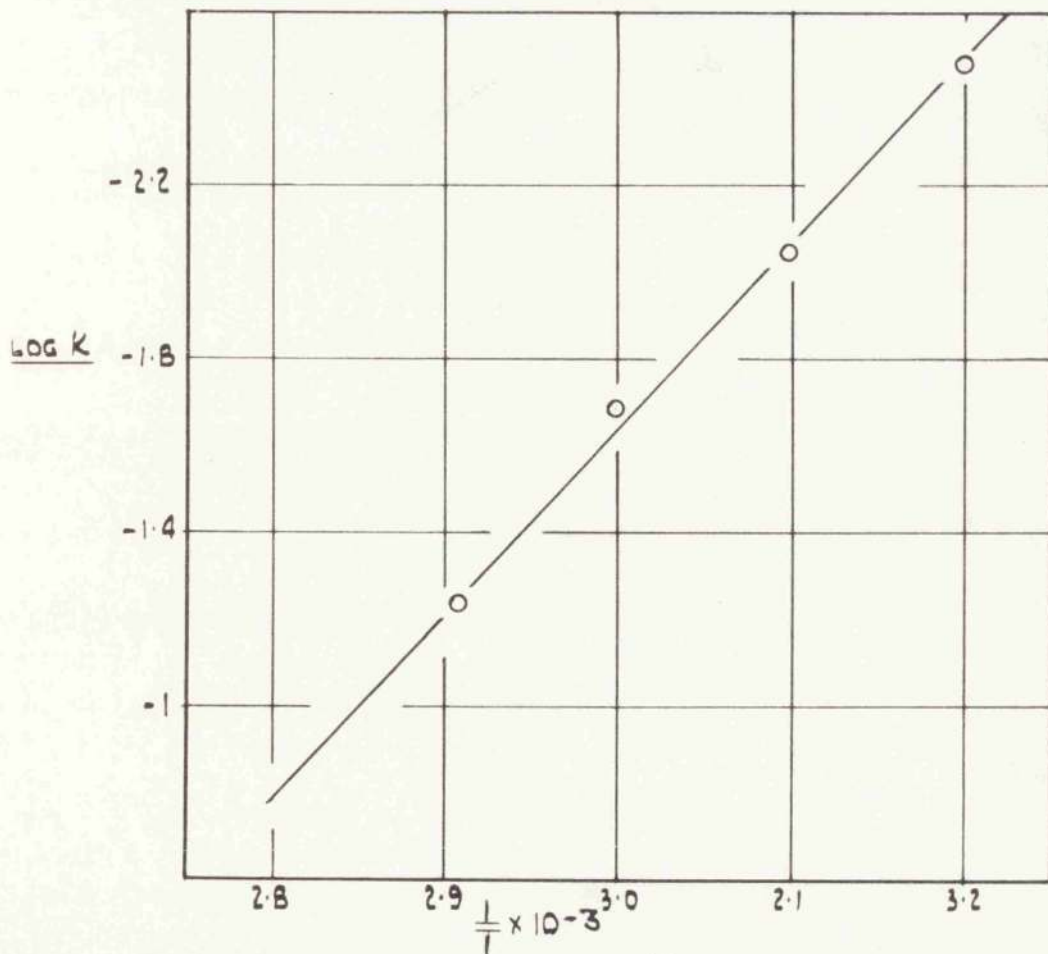


FIG. 9
 ARRHENIUS PLOT FOR ACTIVATION ENERGIES.

homogeneous decomposition of H_2O_2 (though it must be admitted not at the pH's of our experiments), and secondly because they represent the type of catalytic impurity likely to be present in trace amounts in a normal commercial perborate product.

(i) Catalysis by copper.

Fig.10 shows the effect of added $CuCl_2$ at $60^\circ C$. Additions of 10.7, 22.2, and 41.2 p.p.m. (by analysis) were made. The original perborate was found to contain 3.2 p.p.m.

From the graph it is seen that the initial high rate of decomposition values yielded, after about 1 hr., steady zero order rates which were proportional to the concentration of copper in the solution (Fig.13).

It was discovered on adding equal quantities of other copper salts, viz. $CuSO_4 \cdot 5H_2O$ or $Cu(BO_2)_2$, that irrespective of the anion, the same decomposition rates were recorded, i.e. the effect of the anion was negligible.

(ii) Catalysis by iron.

The results to the iron additions (as $FeCl_3$) are shown in Fig.11. The quantities of iron added to the perborate were 3.3, 4.4, 6.6 and 8.8 p.p.m. (by analysis) respectively. On testing the original perborate material it was found that iron present was less than 1 p.p.m.

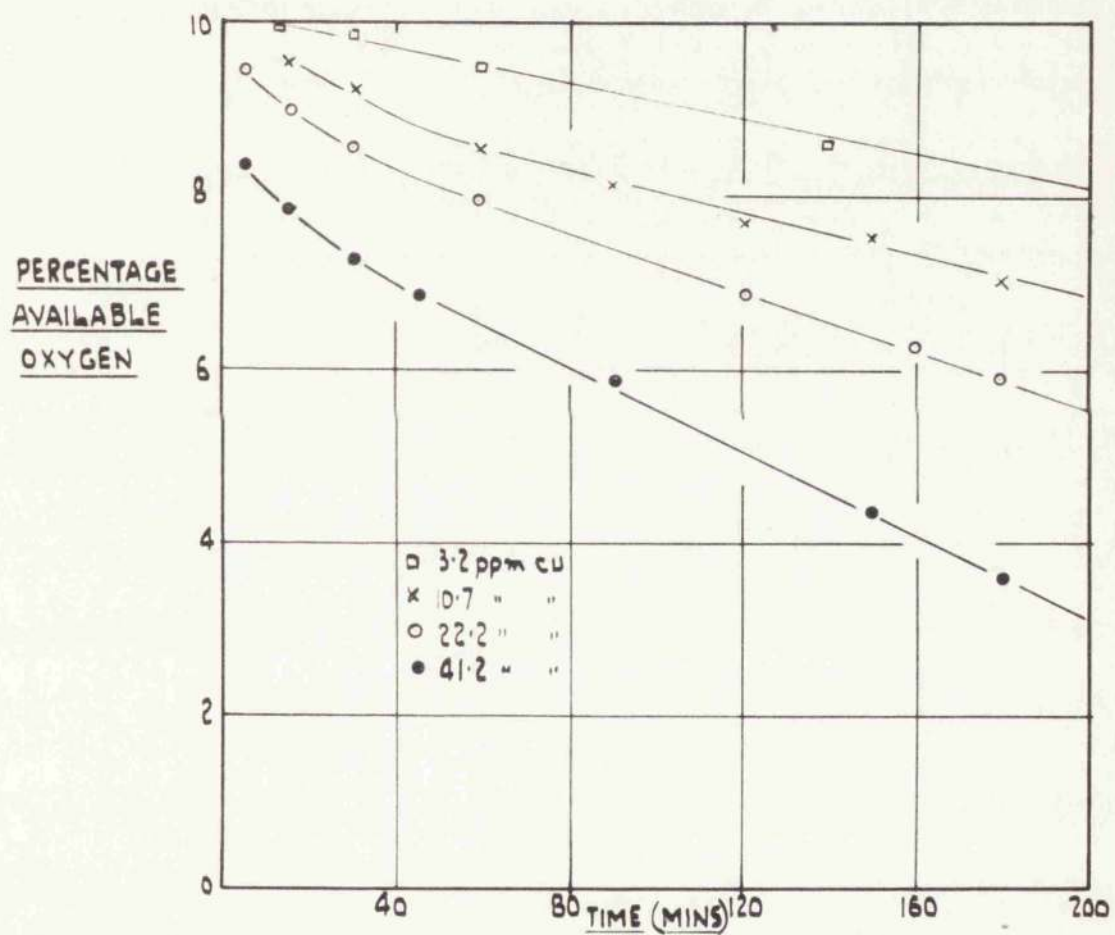


FIG. 10

SHOWING CATALYTIC EFFECT
OF ADDED CU AT 60°C.

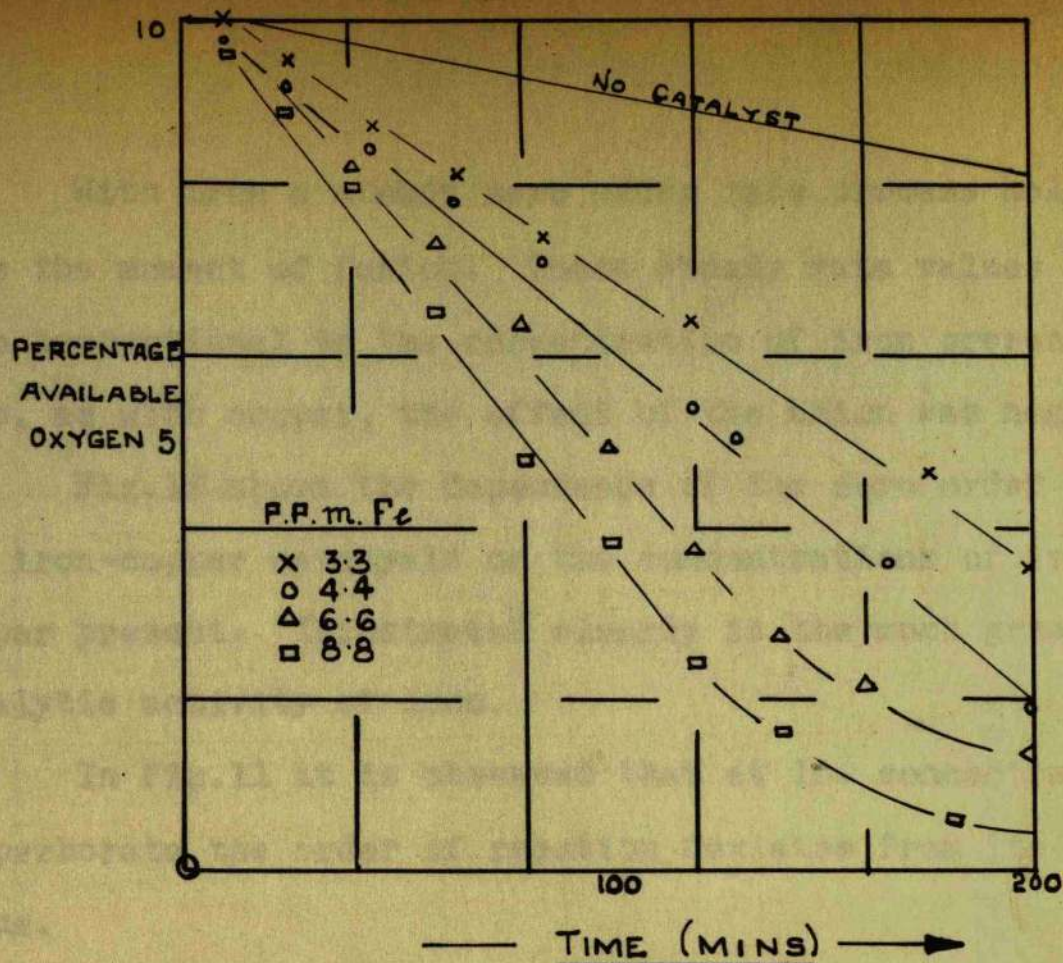


FIG: 11 CATALYTIC EFFECT OF IRON ON DECOMPOSITION OF FUSED PERBORATE AT 60°C .

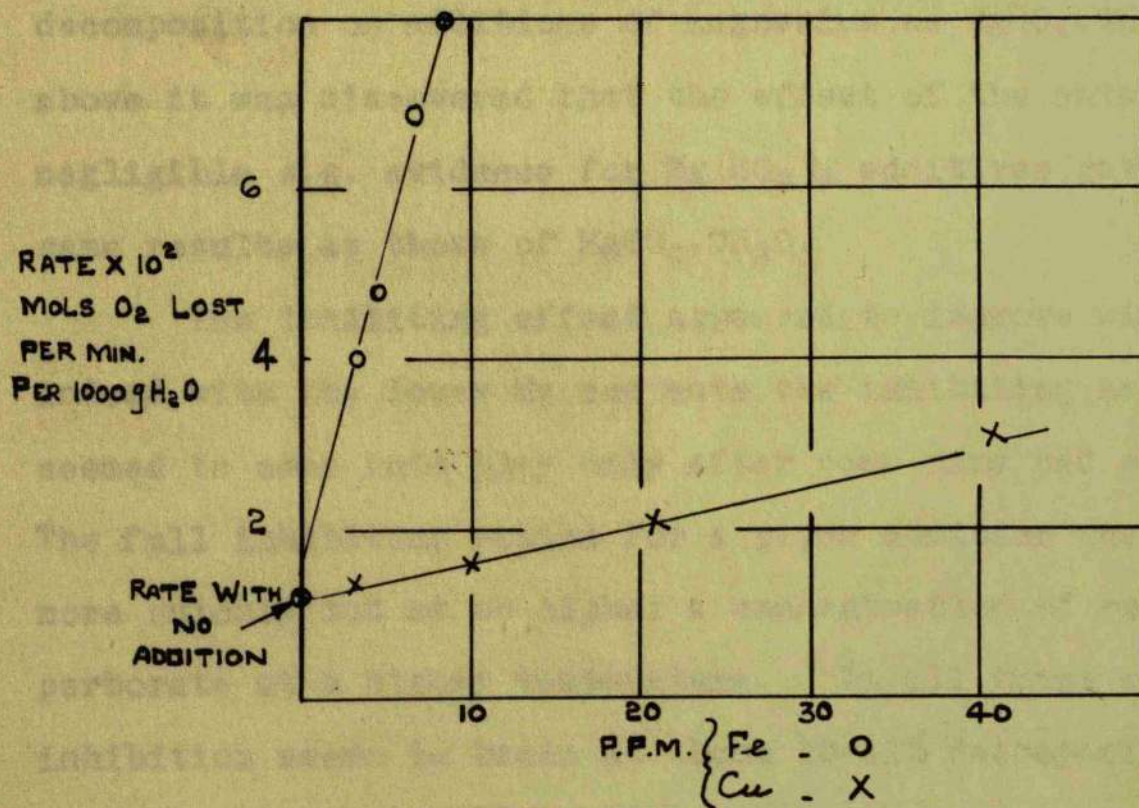


FIG: 12 ZERO ORDER RATE DEPENDENCE ON AMOUNT OF ADDED CATALYST .

With iron a steady zero order rate process holds from the moment of fusion. These steady rate values are also proportional to the concentration of iron present. Also, as with copper, the effect of the anion was negligible.

Fig.12 shows the dependence of the zero order rates for iron-copper catalysis on the concentrations of iron and copper present. Illustrated clearly is the much greater catalytic activity of iron.

In Fig.11 it is observed that at low concentrations of perborate the order of reaction deviates from its zero value.

(d) Addition of magnesium.

Figs. 13 and 13a illustrate the effect on decomposition on additions of magnesium as $\text{MgSO}_4 \cdot 7\text{H}_2\text{O}$. As above it was discovered that the effect of the anion was negligible e.g. evidence for $\text{Mg}(\text{BO}_2)_2$ additives gave the same results as those of $\text{MgSO}_4 \cdot 7\text{H}_2\text{O}$.

The inhibiting effect appeared to improve with time, indeed with the lower Mg contents the inhibiting action seemed to come into play only after some time had elapsed. The full inhibiting action for a given addition was observed more quickly but at no higher a concentration of residual perborate at a higher temperature. In all three cases inhibition seems to begin at about 10-11% decomposition but at different times, viz. at 24, 10 and 4 hr. for the runs at 35, 50 and 60°C. There was no evidence that the

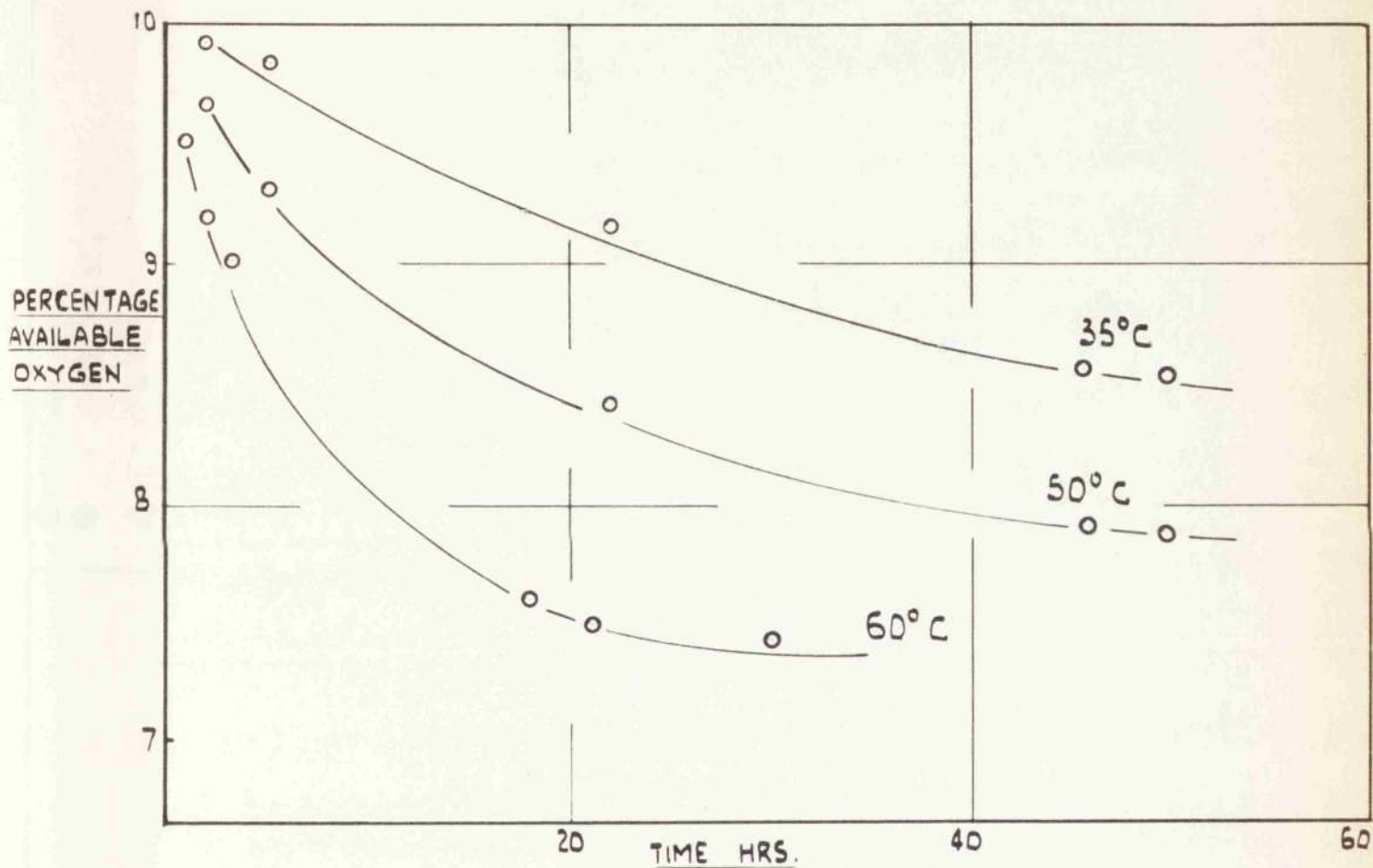


FIG. 13

SHOWING EFFECT OF ADDED $Mg\ SO_4\ 7H_2O$ (2%)
AT DIFFERENT TEMPERATURES.

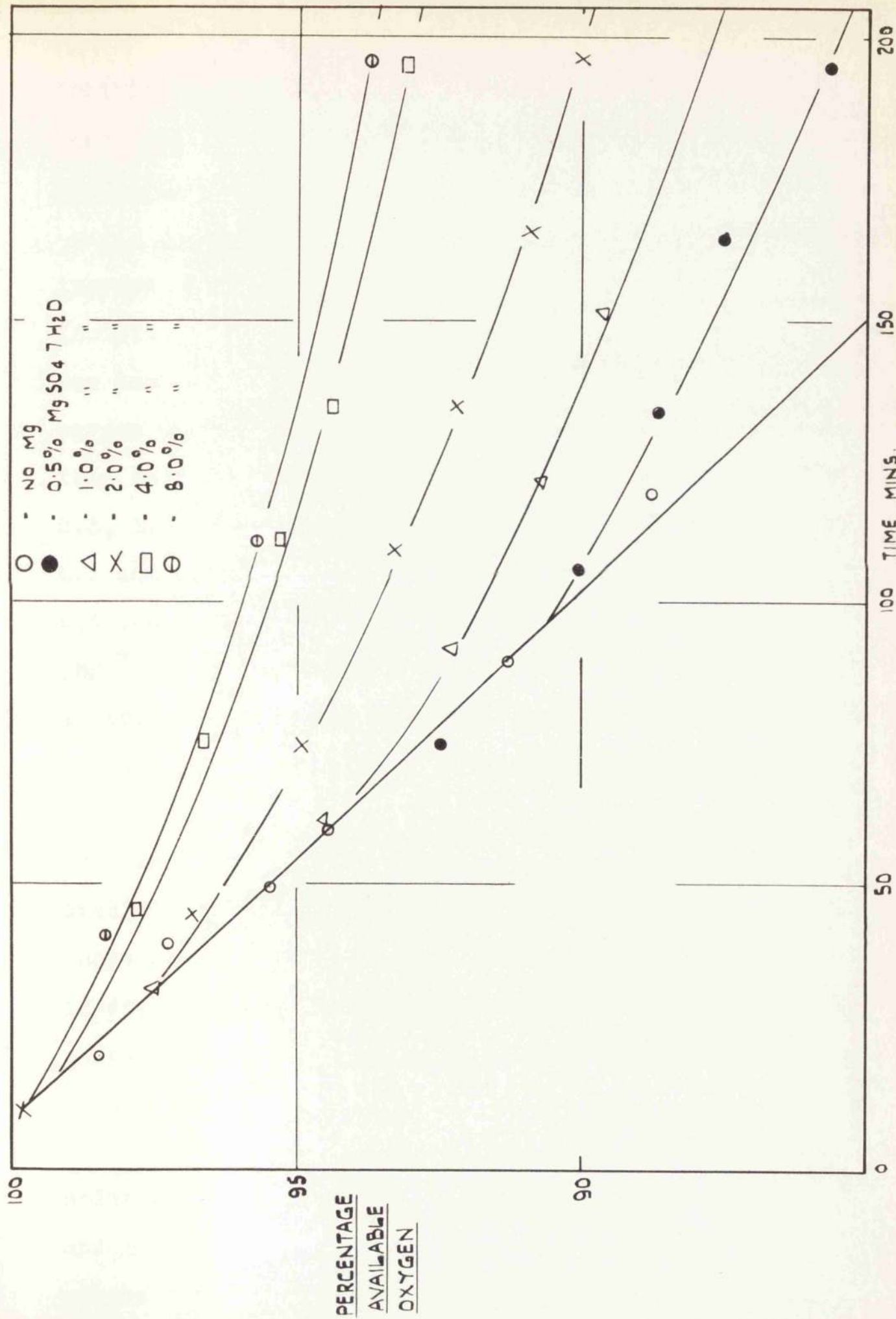


FIG. 13a

SHOWING THE EFFECT OF Mg AS A STABILISER DURING SHORT RUNS AT 60°C

inhibiting effect did not continue to improve and the long run at 60°C suggests that a zero (or very small) rate of decomposition was eventually achieved.

Increase in the amount of Mg ion continued to improve stability even up to 8%. The point at which inhibition just began to be noticeable was a function of the amount of added [Mg] and of the amount of available oxygen decomposed (or of the amount of BO_2^- ion formed). This is only clearly demonstrable for the Mg additions of 0.5, 1.0 and 2.0% where inhibition first occurs at 0.25, 0.5 and 1.0% of available O_2 loss. In these cases we could put the $[\text{BO}_2^-]$ as in the ratio of 1:2:4 and the product $[\text{Mg}^{++} \text{ added}][\text{BO}_2^-]$ is constant at the point of onset of inhibition. The addition of 4 and 8% also conform roughly to this interpretation. Work on dilute solution to be described later suggested that the inhibition by Mg was associated with the formation of a precipitate. The precipitate must thus be represented as $\text{Mg}(\text{BO}_2)(\text{BO}_2)$ to explain these results, the $[\text{BO}_2^-]$ being roughly constant in the above cases. The process might be, however, controlled by pH which does of course alter during the decomposition.

(e) Effect of H_2BO_3 .

Fused perborate may be regarded as a fairly dilute solution of H_2O_2 in a strong salt solution (Na^+ , BO_3^- , BO_2^- and more complex ions) at a pH determined by the hydrolysis of the borate and perborate ions.

The apparent pH of the fused material supercooled to 30°C when measured with a glass electrode (immersed the glass electrode and the saturated calomel reference electrode directly into the fused material) was 9.76. This could be adjusted by the addition of either H_3BO_3 or NaOH. Fig.14 shows the effect of addition of small amounts of H_3BO_3 (1-4%) on the decomposition of perborate at 60°C.

The initial loss of oxygen was greatly enhanced by the H_3BO_3 , which was added as a fine powder to the perborate before fusion. Thus with 4% H_3BO_3 (more than this could not be dissolved in the standard fusion time) one quarter of the available oxygen was found to be gone at the end of 10 mins. By the end of 1 hour the usual zero order rate process was established and the rate was then found to be increased only slightly (ca.15%) for a pH drop of 0.6, as measured by the glass electrode. This result indicates a strong heterogeneous catalytic effect of H_3BO_3 and a small accelerating effect in the fused state. If the effect is produced through the medium of the pH we would conclude that the decomposition is one slightly accelerated by increase in $[H^+]$. It is impossible to draw a quantitative conclusion but one important result stands out: traces of H_3BO_3 enhance decomposition in the initial stages of fusion.

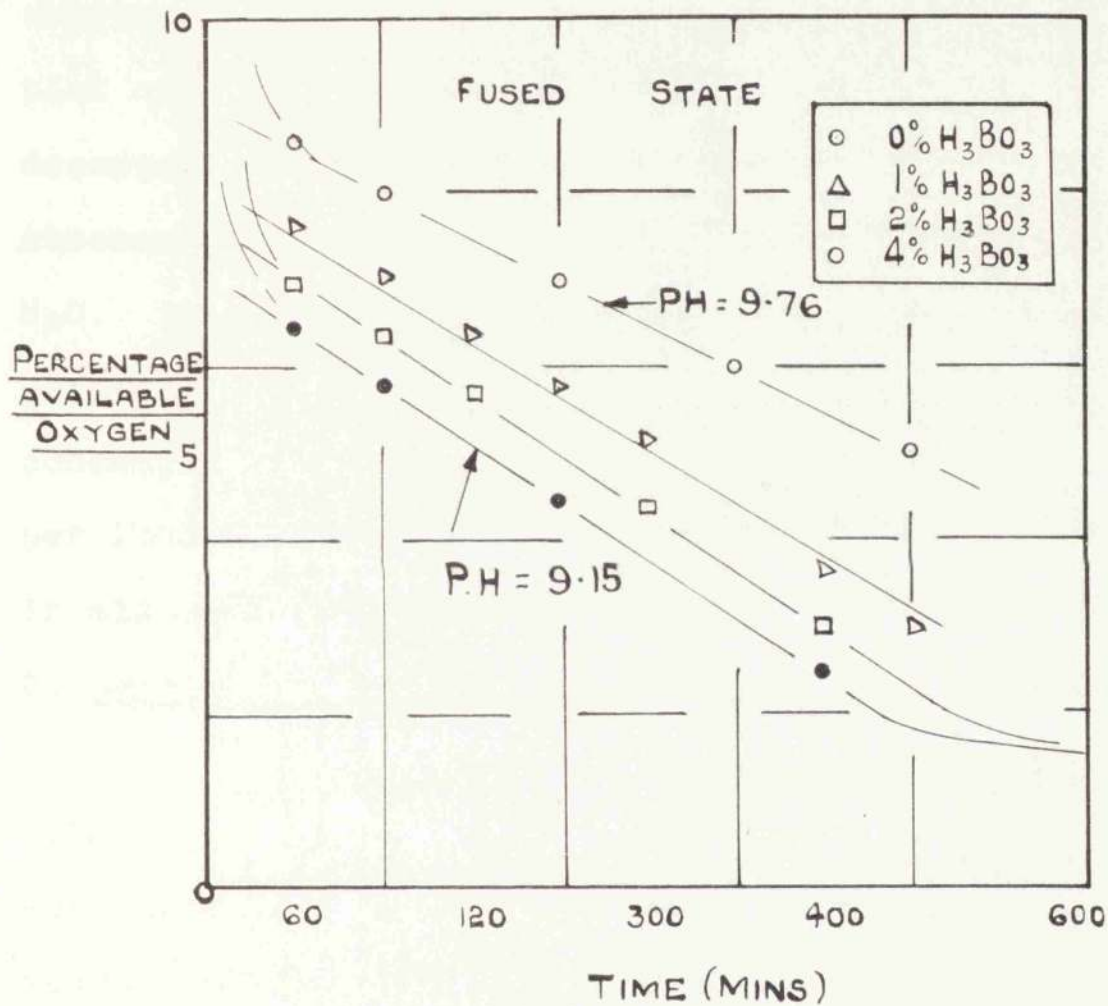


**FIG: 14 EFFECT OF ADDED H₃B₃O₃
AT 60°C .**

(f) The results of adding water to perborate (0.3 gm.) samples prior to fusion etc. are shown in fig.15 in a plot of titre against time. Thus the time for half decomposition at 60°C was 480 min. for the fused state in the absence of H₂O, 150 min. with 0.1 gm. H₂O, 100 min with 0.2 gm. H₂O. This graph also shows that the zero order process persists until roughly $\frac{1}{2}$ decomposition. However if the concentration units are expressed as moles NaBO₃ changed per 1000 gm. H₂O, then, the same zero order rate is observed in all cases.

5. Decomposition of dilute solutions.

Fig.16 illustrates the decomposition of 0.7M and 0.3M solutions of NaBO₃.4H₂O at 60°C. Also shown on the same graph are the corresponding decomposition of perborate solutions made up from adding the requisite amounts of NaBO₃.4H₂O and H₂O. Kinetic treatment of this range of concentrations show that following a zero order process which holds down to 0.25 molar a first order region is observed. This is shown in Fig.17.

At low concentrations, i.e. \leq 0.1M, the reaction becomes slower and eventually obeys second order kinetics. This is illustrated in Fig.18.

Action of added copper.

The effect of adding Cu, in the form of CuSO₄.5H₂O

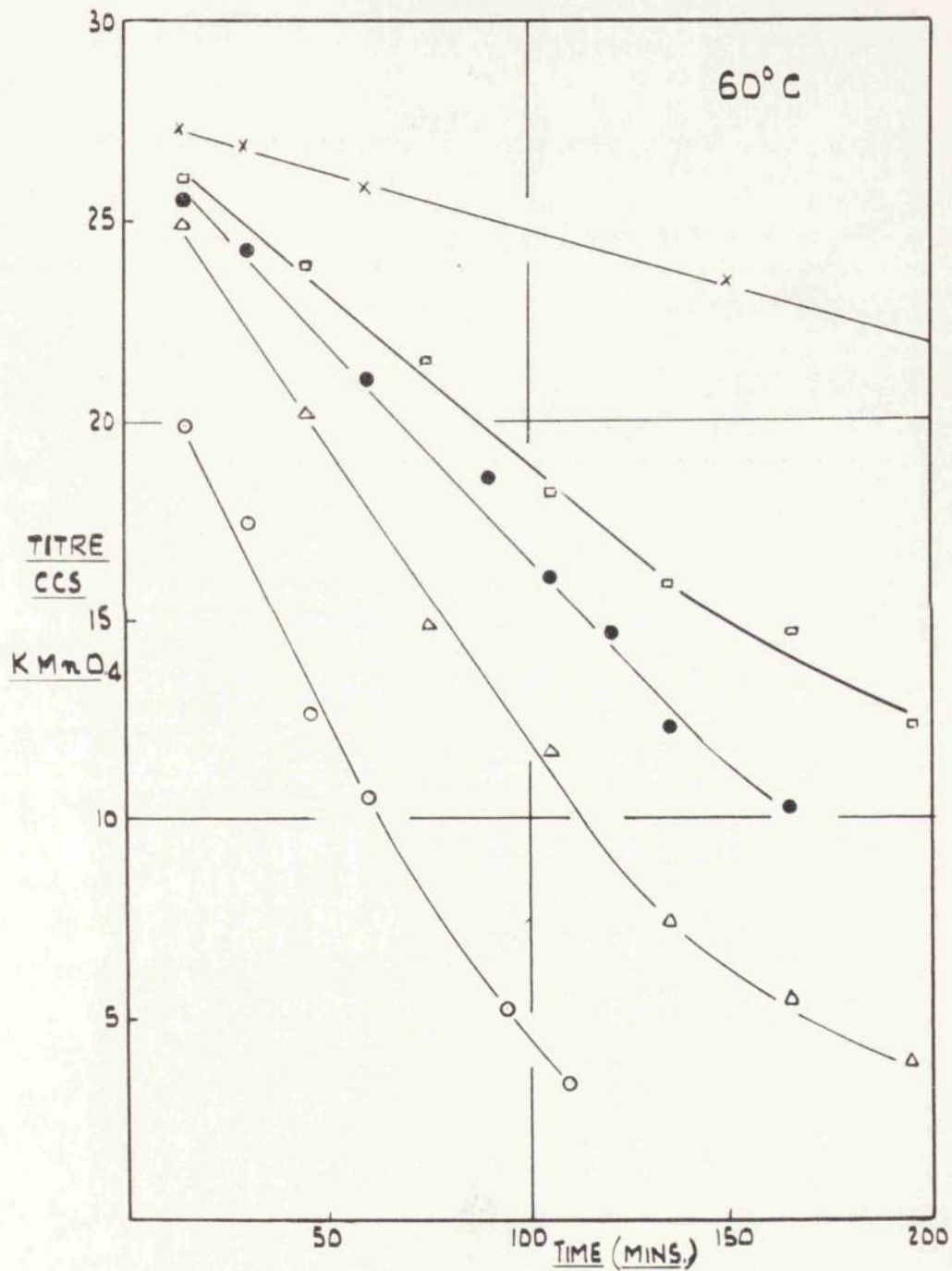


FIG. 15

SHOWING LOSS OF AVAILABLE OXYGEN FROM 0.3g
 SAMPLES OF $\text{NaBO}_3 \cdot 4\text{H}_2\text{O}$ WITH ADDED WATER IN
 AMOUNTS SHOWN BELOW.

x - 0g; □ - 0.1g; ● - 0.2g; △ - 0.4g; ○ - 1.0g.

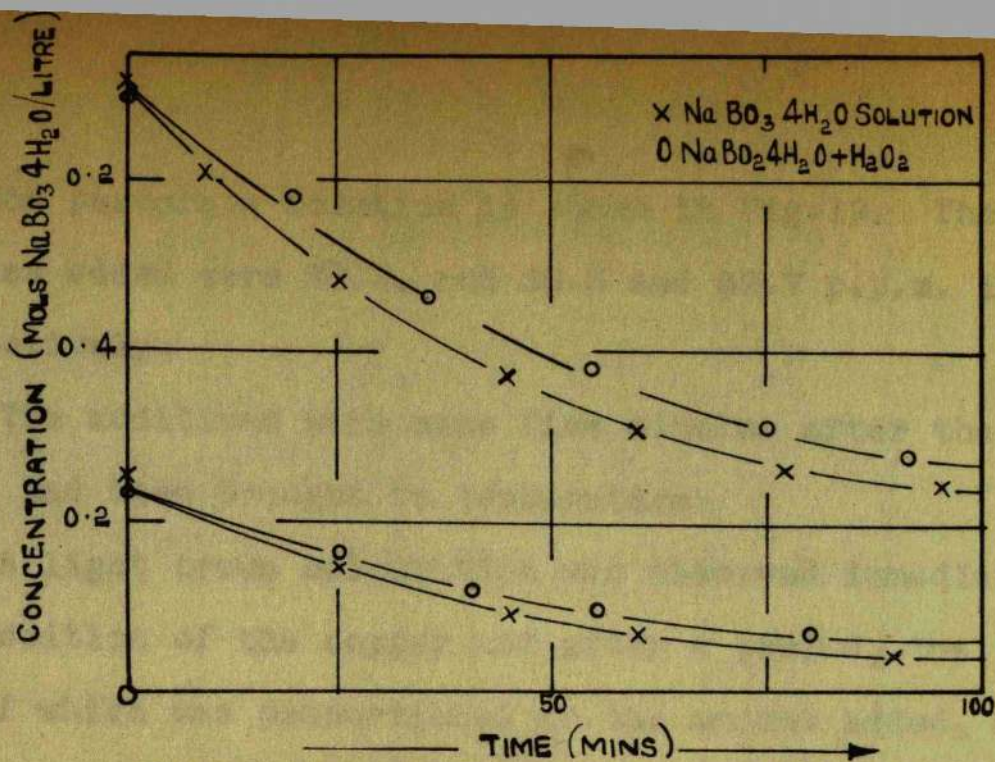


FIG. 16 DECOMPOSITION OF DILUTE PERBORATE SOLUTIONS AT 60°C.

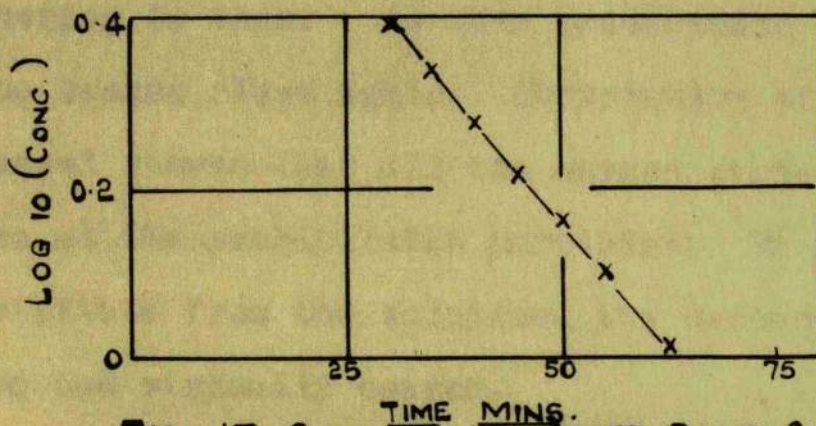


FIG: 17 SHOWING 1ST ORDER RATE OVER A LIMITED CONCENTRATION RANGE FOR A DILUTE PERBORATE SOLUTION AT 60°C.

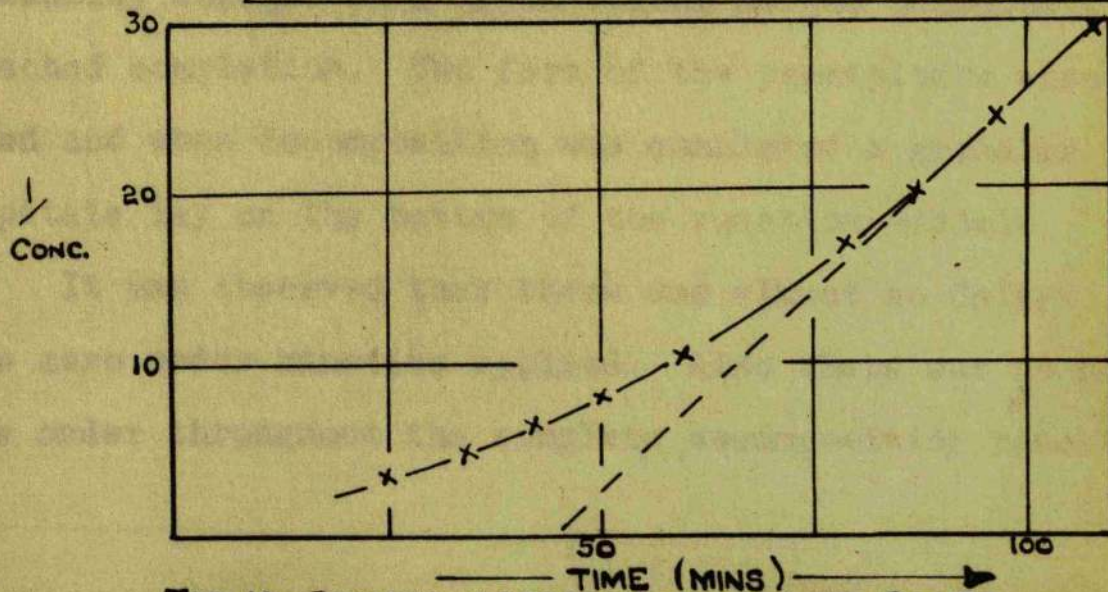


FIG: 18 SHOWING APPROACH TO SECOND ORDER KINETICS AT LOW CONCENTRATIONS OF $\text{Na}_2\text{B}_2\text{O}_7 \cdot 4\text{H}_2\text{O}$ (< 0.1M) AT 60°C.

to a 0.25M perborate solution is shown in Fig.19. The quantities added were 27.2, and 36.3 and 52.7 p.p.m. in Cu respectively.

The additions were made five minutes after the solution had been brought to temperature.

A light brown colouration was observed immediately on the addition of the copper and after a period, the length of which was proportional to the amount added, a light brown turbidity appeared in the solution and began to flocculate, the particles being supported by the oxygen bubbles adhering to them. As this precipitate appeared, the solution became clear again. Observation of the reaction vessel showed that all the oxygen evolution was taking place at the precipitated particles. On removal of the precipitate from the solution, the decomposition of the solution had virtually ceased.

However, if the precipitate was left in the solution it gradually changed to a green colour as the decomposition approached completion. The form of the precipitate also changed and when decomposition was completed a granular precipitate lay on the bottom of the reaction vessel.

It was observed that there was almost no delay before zero order kinetics applied. Also there was no change in the order throughout the complete decomposition reaction.

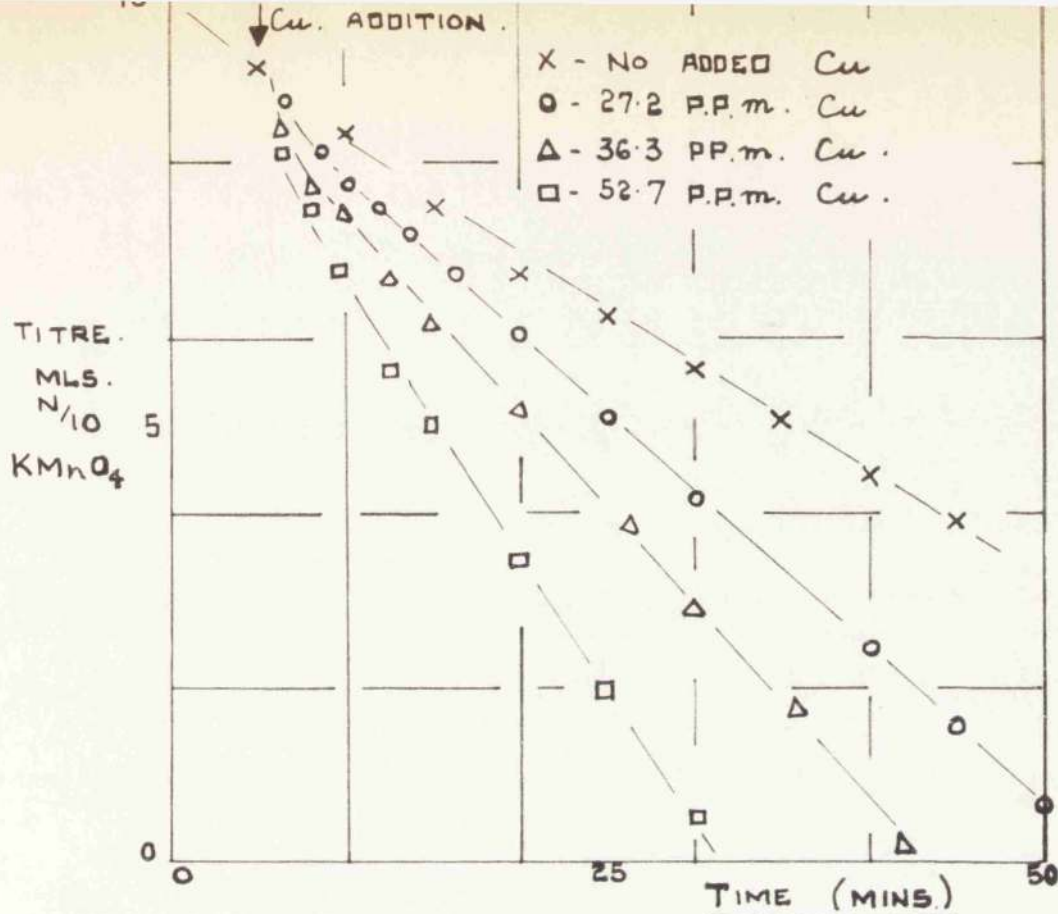


FIG. 19 THE EFFECT OF ADDED COPPER IN
 A 0.25M PERBORATE SOLUTION AT 60°C.

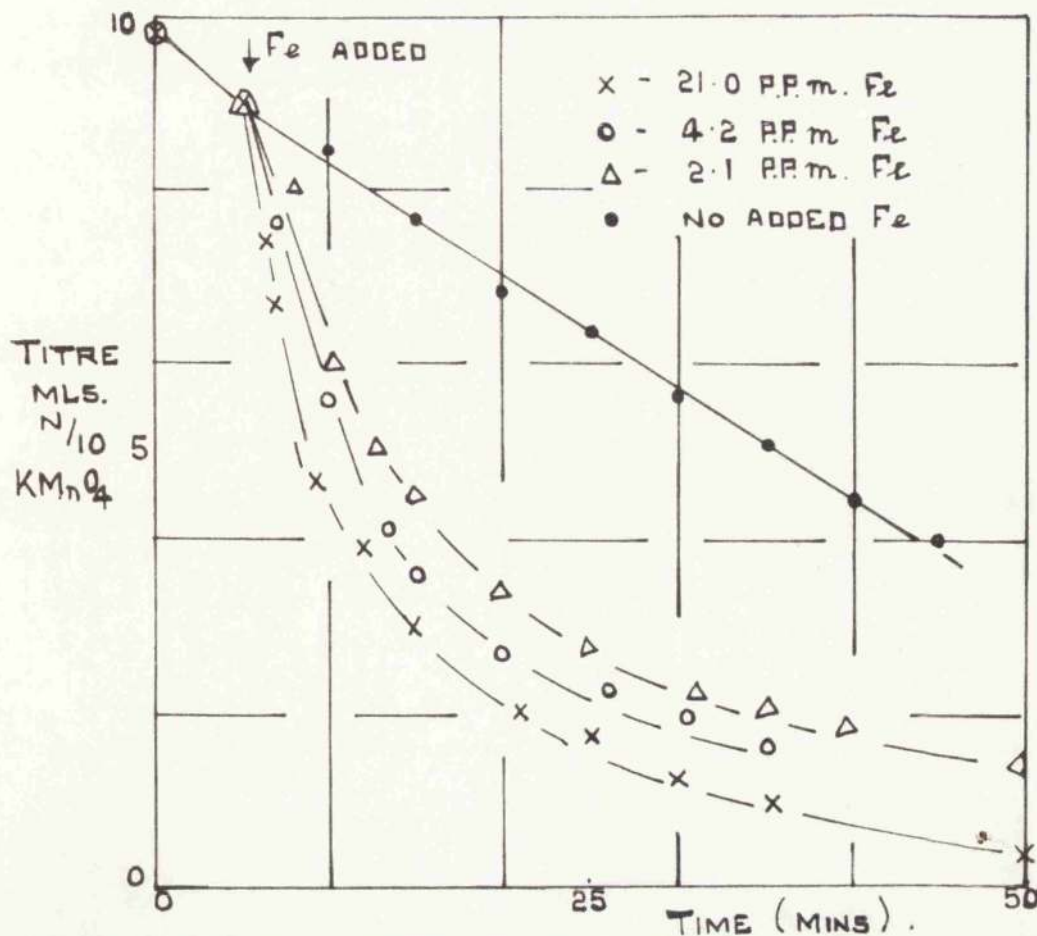


FIG. 20 THE EFFECT OF ADDED IRON IN A DILUTE PERBORATE
 SOLUTION (0.25M) AT 60°C.

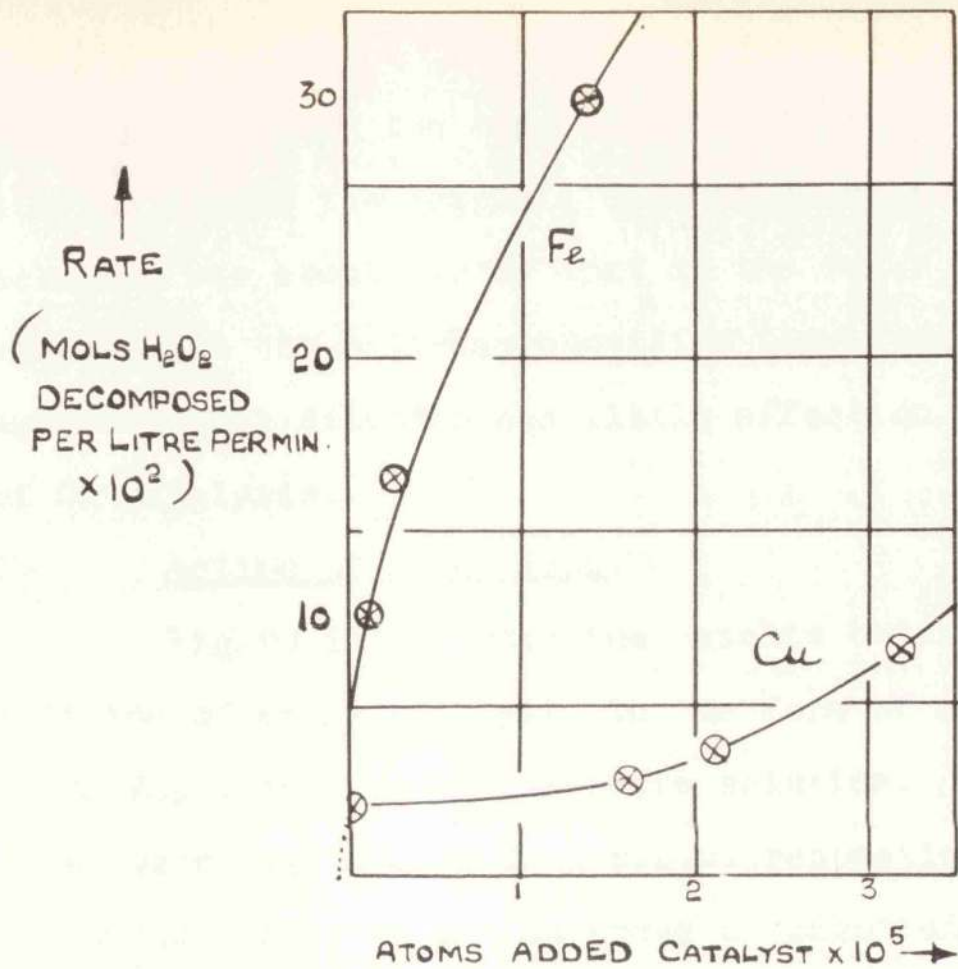


FIG: 22 THE RATE OF DECOMPOSITION AS A FUNCTION OF ADDED Fe OR Cu. IN 0.25 M SOLUTIONS AT $60^\circ C$

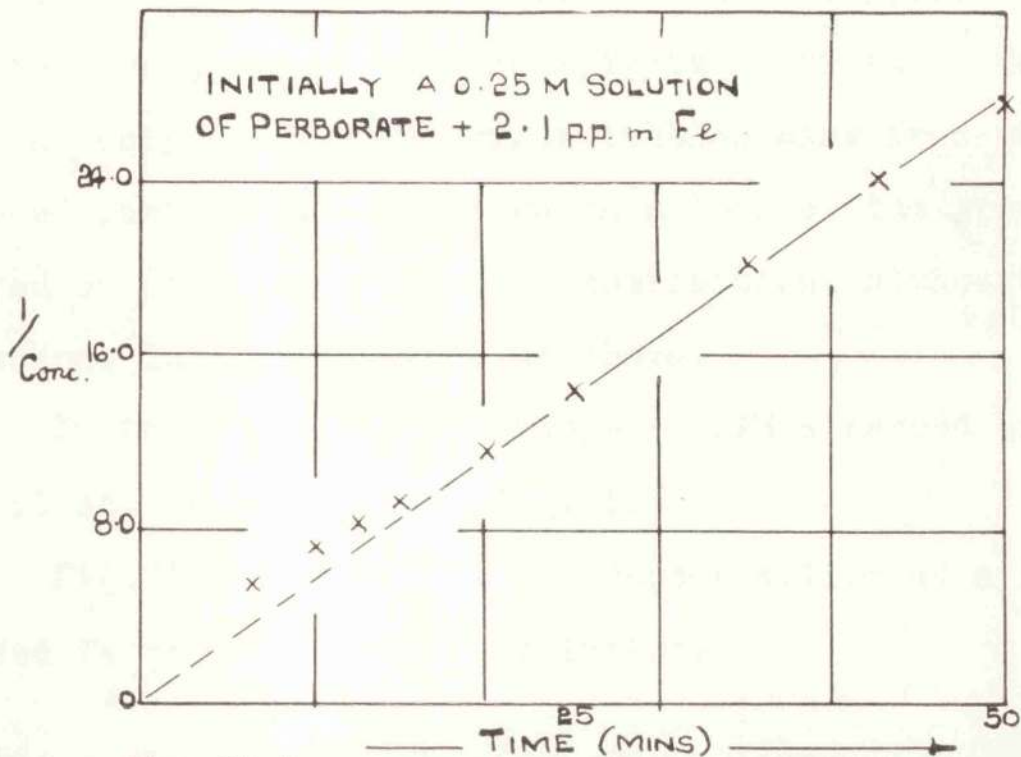


FIG: 21 ILLUSTRATING SECOND ORDER KINETICS AT LOW ($< 0.1M$) CONCENTRATIONS OF PERBORATE IN A SOLUTION CATALYSED BY IRON

For approximately the same concentration of catalyst the time to effect the complete decomposition of the dilute solution was about $\frac{1}{8}$ th of that in the fused state. This agrees with the half-decomposition time quoted above and suggests that dilution has little effect on the mechanism of Cu catalysis.

Action of added iron.

Fig. 20 illustrates the results obtained on the addition of an Fe catalyst, in the form of a solution of $\text{FeSO}_4 \cdot 7\text{H}_2\text{O}$, to a 0.25M perborate solution. The quantities added were 2.1, 4.2, and 21 p.p.m. respectively. These additions were of the same order of magnitude as those added to the fused state.

As was observed with copper, a brown colouration of the solution appeared which subsequently disappeared when a reddish-brown flocculent precipitate appeared. Once again the only observable oxygen bubbles came from the suspended particles. No change in colour of the precipitate appeared on completion of the decomposition, although the same change in form occurred as above.

In the concentration range $< 0.1\text{M}$ a second order rate law applied, as is shown in Fig. 21.

Fig. 22 shows the rate of decomposition as a function of added Fe or Cu in a 0.25M solution.

6. Stabilisation of dilute solutions.

Fig.23 shows the results obtained when sufficient stabiliser, in the form of $\text{MgSO}_4 \cdot 7\text{H}_2\text{O}$ or $\text{ZnSO}_4 \cdot 7\text{H}_2\text{O}$, was added to 100 mls. of dilute perborate solution, (0.25M) at 60°C , after 15 minutes. Total inhibition was soon effected. The actual quantity of stabiliser added was 2 mls. of a 0.15M solution.

On the addition of the Mg solution an immediate cloudiness appeared, but it was approximately 35 minutes later before this cloudiness became a flocculent precipitate with a resultant clearing of the rest of the solution. When the Zn solution was added an immediate bulky flocculent precipitate appeared.

If the stabilising precipitate was left in contact with the solution it was observed, after about 5-7 hours, that a further very slow decomposition of the perborate commenced. This subsequent decomposition also appeared to be of zero order. Fig.24 illustrates this effect. Similar experiments were carried out with solutions to which Fe and Cu catalyst were added. Fig.25 shows the results for Cu. The solution is 0.25M perborate solution at 60°C , containing 27.2 p.p.m. Cu and three different concentrations of a $\text{MgSO}_4 \cdot 7\text{H}_2\text{O}$ solution were added after 20 mins. With each increase of [Mg] there was a definite reduction in the zero order rate.

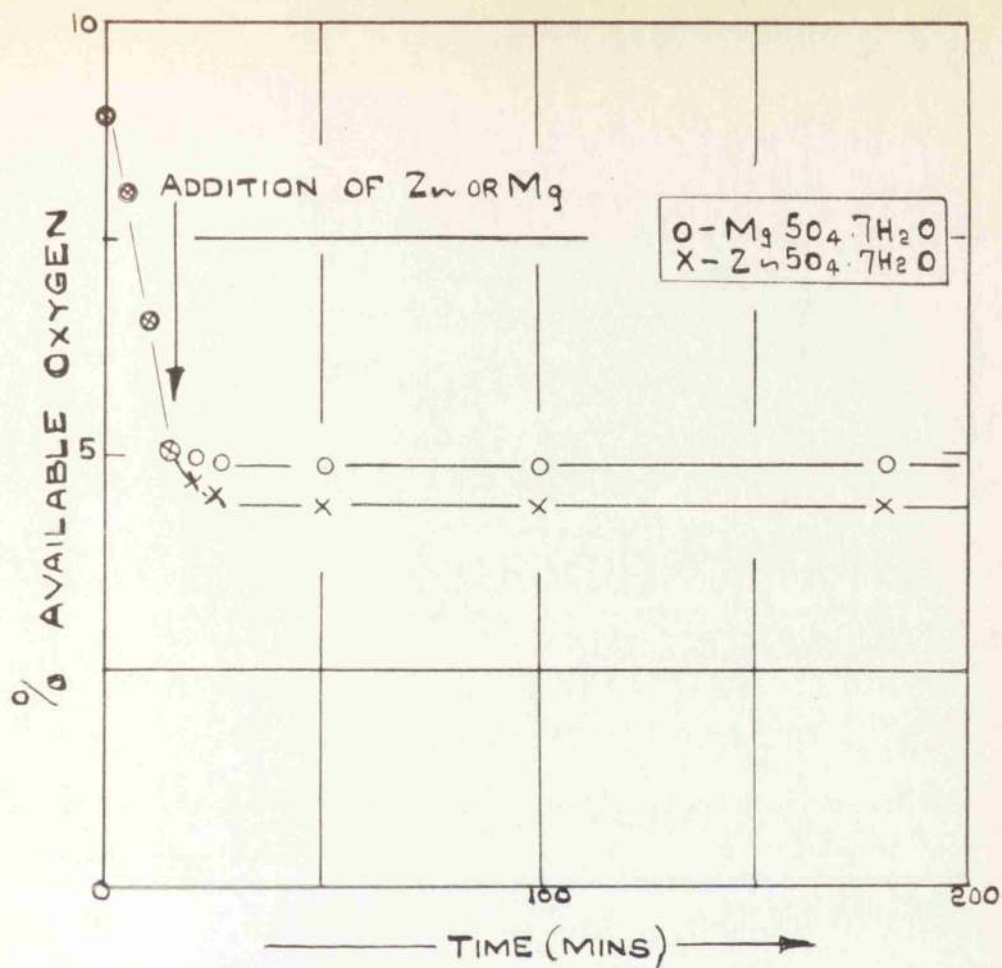


FIG: 23 SHOWING TOTAL INHIBITION OF CATALYSIS ON THE ADDITION OF SUFFICIENT STABILISER TO A 0.25 M. PERBORATE SOLUTION AT 60°C

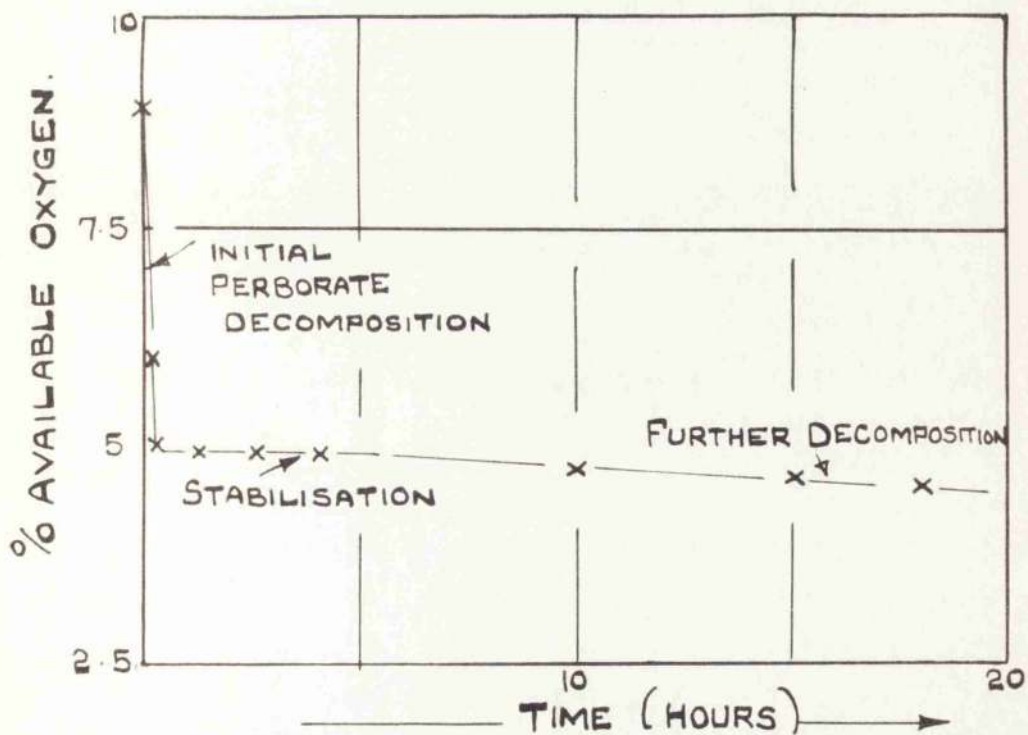


FIG: 24 SHOWING THE SUBSEQUENT DECOMPOSITION AFTER SEVERAL HOURS IF A STABILISING PRECIPITATE IS LEFT IN CONTACT WITH A DILUTE PERBORATE SOLUTION AT 60°C.

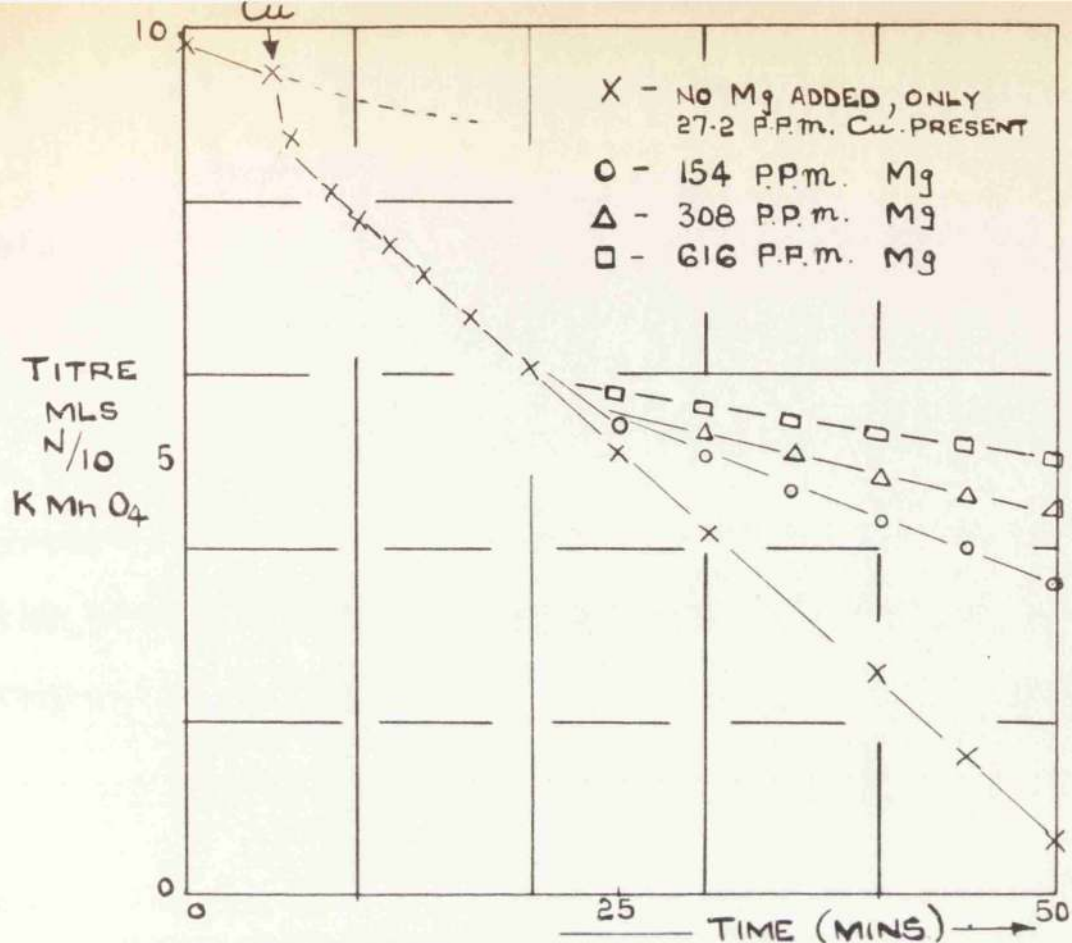


FIG. 25 THE STABILISING EFFECT OF Mg ADDITIONS TO A Cu. CATALYSED DECOMPOSITION OF A 0.25 M PERBORATE SOLUTION AT 60°C.

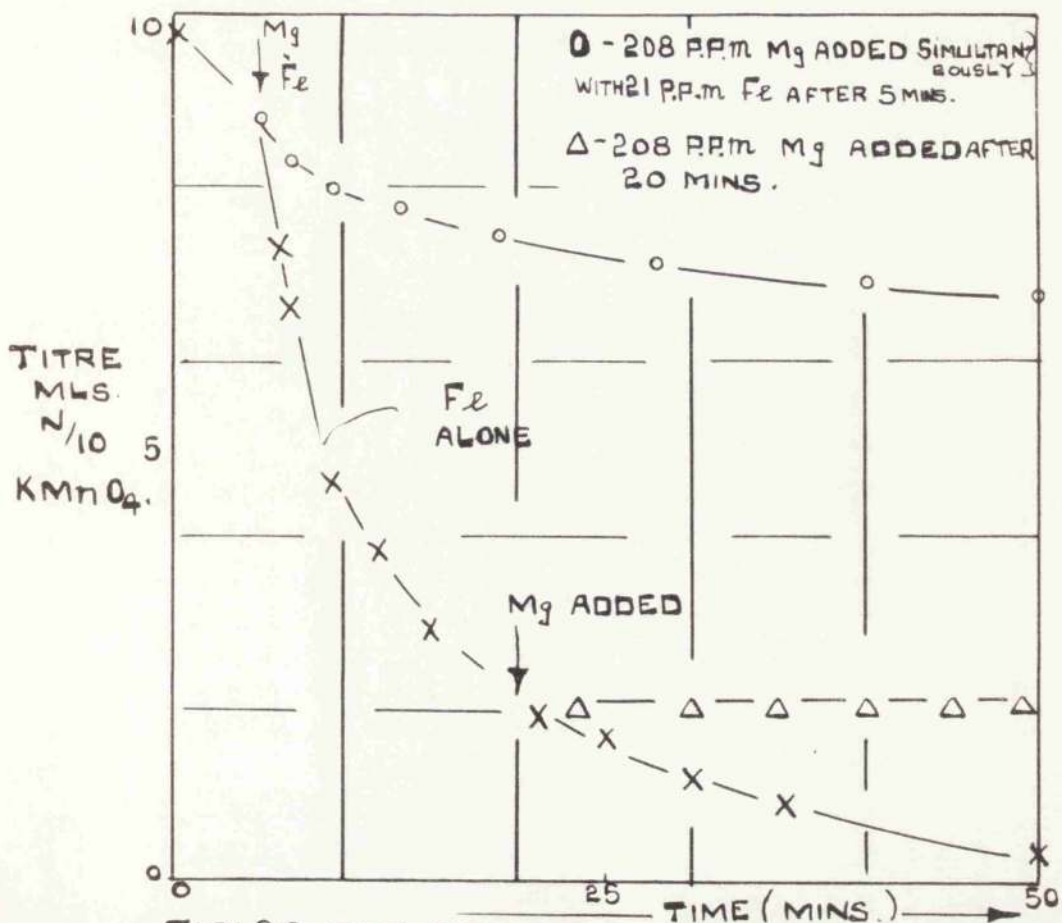
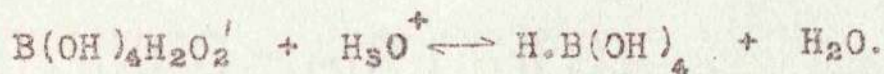


FIG. 26 THE EFFECT OF ADDING A CONSTANT [Mg] AT DIFFERENT STAGES OF AN IRON CATALYSED REACTION AT 60°C.

Fig. 26 shows the effect of adding the same quantity of stabiliser at two widely differing stages of a decomposition of a 0.25M perborate catalysed by 21 p.p.m of Fe at 60°C. There was a definite inhibition which was improving with time. When the Mg was added after 20 mins. complete inhibition was observed at once where as when it was added at the same time as the Fe its inhibition effect began slowly and continued to increase.

The pH of perborate metaborate solutions.

The pH of mixtures of perborate and metaborate solutions is indicated graphically for a range of concentrations of metaborate solution with H₂O₂ or vice-versa. From Menzel's^a data for the BO₂' / H₂O₂ / BO₃' equilibrium we may calculate that a decrease in pH is expected when passing from BO₂' to BO₃' and this amounted to about 1.5 units in the more concentrated solutions. In the more dilute solutions our results confirmed Menzel's and may be represented as a determination of the equilibrium.



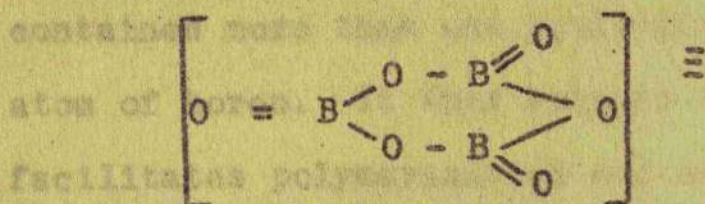
where B(OH)₄.H₂O₂' represents the perborate ion in the form chosen non-committally by Kemp.³ In the more concentrated solutions our results go outside the range previously reported. The above equilibrium constant is no longer constant and we may conclude, with Menzel, that association (dimerisation and trimerisation and mixed complexes) complicates the solution to an extent which defies simple representation. However,

the results show that a sensitive pH measurement could well be used as a method of following the decomposition of perborate. Hood,⁴ in this laboratory, has carried out a study using this method. The bearing of the pH changes on interpretation of the decomposition process will be discussed later.

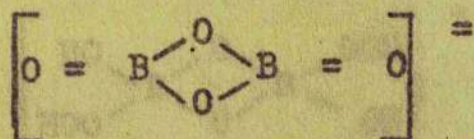
DISCUSSION

1. The nature of sodium perborate tetrahydrate and its solution.

As Kemp's recent (1956) review shows, the nature of the metaborate ion in solution is fairly well agreed upon, at least in not too concentrated solutions, but there is much less known, or agreed, about the perborate ion. The metaborate ion, as shown by cryoscopic and Raman data, is monomeric with the accepted structure $B(OH)_4^-$. Activity determinations (calculated from the activity of the solvent) suggest that sodium metaborate behaves like a typical 1:1 electrolyte up to at least 1M. There is no direct evidence for polymerisation of the ion though, of course, the crystalline anion is recognised as trimeric, thus:



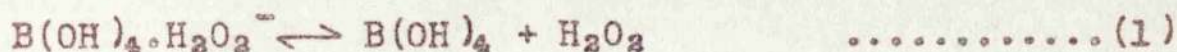
Kemp considers this evidence following Wells⁵ and others. The dimeric grouping does not occur, possibly because it involves a very considerable distortion of the bond angle in



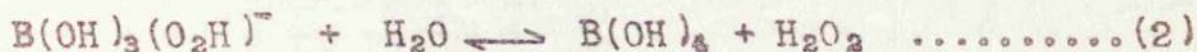
The nature of the boron containing ion in a metaborate solution containing H_2O_2 is less clearly or definitely

understood, although Menzel², from cryoscopic, conductimetric, solubility and partition (of H₂O₂, using amyl alcohol) measurements, was able to conclude that a monomeric ion containing peroxide oxygen and represented as [B(OH)₄.H₂O₂]⁻ occurred in very dilute solution (< 0.05 M).

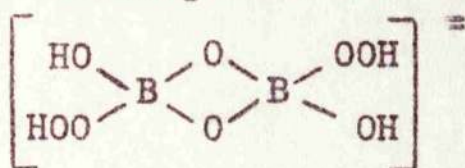
He was able to measure the constant for the exchange.



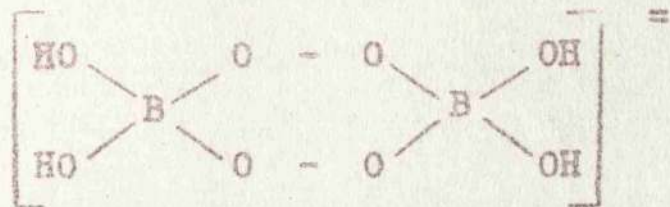
as 2×10^{-2} . Menzel claims no evidence for exchange but for the sake of simplicity we shall write the ion as B(OH)₃.(O₂H)⁻ and the equilibrium as



At concentrations in the range 0.1 - 0.2M complex ions appeared, and in the presence of extra H₂O₂ the anions contained more than one equivalent of peroxide oxygen per atom of boron. It thus appears that the presence of H₂O₂ facilitates polymerisation and complex ion formation and there is little doubt that in solutions of 1M and above the monomer ion is no longer found. Most authors favour the dimeric structure for the ion under these conditions in the crystal. Partington and Fathallah¹ and Menzel² favour

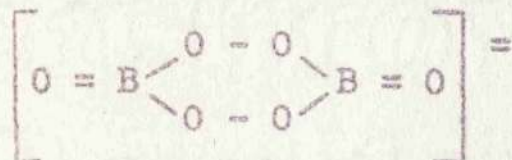


but this quite ignores the fact that the oxygen bridge does not appear in the metaborate case. Thus on oxygen strain grounds we would prefer the structure of Carpéni⁶:



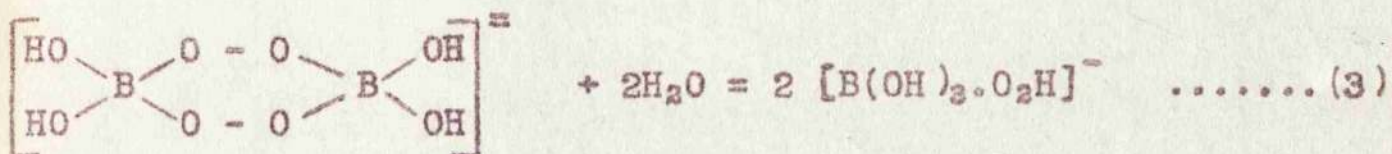
and would point to the sterically favourable double oxygen bridge as the reason for early onset of complex ion formation in the presence of H₂O₂ - a dinuclear form would always be expected to form sooner, if permissible, than a trinuclear one.

Recent N.M.R. work by Connor and Richards⁷ suggests that in the crystalline state the ion contains only one type of proton interaction - that associated with H₂O₂. Thus there can be no free H₂O₂ and furthermore we should write the ion for the crystal as

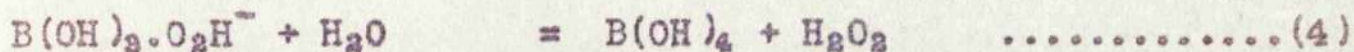


It is not impossible, however, to speculate with much confidence in the absence of an X-ray study, which is still awaited in the case of the perborate.

In solution the situation is, of course, even less precise, but we may expect, in most of the cases dealt with by us, a preponderance of dimeric ions, probably hydrated, with all the peroxy oxygen in bridged double oxygen positions. Two hydrolytic processes will occur, viz:



and



The first will yield an appreciable proportion of the "peroxygen" in "unprotected" positions.

We can take it that oxygen loss during catalytic decomposition comes from HO_2^- , H_2O_2 or the unprotected HO_2 group in the monomeric perborate ion.

These experiments indicate the importance from a kinetic point of view of the more detailed study of the decomposition during the first phase of decomposition.

2. Loss of oxygen from the solid tetrahydrate.

The results of heating the perborate tetrahydrate at 60 °C in vacuo show that during dehydration from the dry solid no loss of oxygen occurred. They are substantiated by the open tube experiments. In all other experiments the nature of the crystal mass indicates that at least local fusion occurs, as shown by "clinging" of the crystals, or loss of fluidity of the powder, and eventual fusion.

Experiments (Figs. 2, 3 and 4) show that the rate of oxygen evolution increases rapidly until about 40% decomposition and that liquefaction is determined solely by

the amount of decomposition.

The 60°C in vacuo experiment shows quite negligible decomposition, even at this elevated temperature from a truly dry crystal. The single crystal observations support this and show no evidence of oxygen loss from a clean crystal surface even in the presence of water vapour at temperatures in the range 50-70°C.

A review of the results of the study of the initial 1% of the decomposition process at 35°C and 20.5°C gives no certain evidence of loss of oxygen from the solid but in both cases there seems to be an indication of a very slow initial rate which is difficult to regard as other than a solid phase, pre-fusion, probably surface, process. At 35°C this initial process varied greatly in rate from one sample to another and this leads to the suggestion that the specific surface area of the solid has a bearing on the initial rate of oxygen loss and in fact that this process represents loss of oxygen from the crystal surface.

At 35°C the striking feature is the sharp change from the slow initial process to a 10 times faster process which does not seem to be associated with the obvious onset of melting phenomena in the powder (loss of mobility, clinging etc). This secondary rate may perhaps be associated with formation

of a liquid film in the surface fissures. At first the rate of this liquid film process is sensitive to surface state and possibly therefore to surface area. But later, perhaps when the crystallites and their cracks and fissures become swamped with liquid the rate of oxygen loss shows no relation to the original form of the crystal.

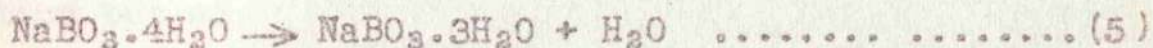
With this picture in mind the results with the partly dehydrated powders can be explained in terms of their surface areas. The small crystals of the normal $\text{NaBO}_2 \cdot 4\text{H}_2\text{O}$ are converted into an apparently amorphous form by dehydration and it is quite clear that the remaining tetrahydrate, after some water has been removed, will have a very greatly increased surface area which will be covered with multitudinous deep cracks and fissures. Conditions in these fissures may favour liquid formation and accumulation once the crystals are restored to an atmosphere with the equilibrium water vapour pressure. This may explain the lack of the initial "solid" decomposition with the partly dehydrated samples. On the other hand it could be that the "solid" decomposition, being a surface process, is now so fast that it passes over without observable break to the "liquid film" process. A difficulty is the fact that $\text{NaBO}_3 \cdot \text{H}_2\text{O}$ does not seem to act as a dehydrant, preventing the formation of a saturated

solution near the remaining tetrahydrate as it might have been expected to do so.

The enhanced rates of decomposition with samples containing more than 4.00 moles H₂O per NaBO₃, i.e. less than perfectly dried, are easier to explain. Here the slight excess of water available will ensure that the crystals are sufficiently wet from the start of the experiment. At this point we may conclude that the most stable form of the hydrated perborate should be well formed, clear crystals, kept at the equilibrium vapour pressure.

3. (1) Fusion of the tetrahydrate.

To answer the question "how does fusion occur in the sodium perborate tetrahydrate" at temperatures as low as 29°C and even as low as 20.5°C one must turn to the work of van Gelder,⁸ who has made studies of the system NaBO₃, NaBO₂, H₂O. Van Gelder found that the behaviour of the system is complicated by the fact that below 35°C the trihydrate is the stable form of the perborate and that the reaction



occurs with loss of water. This is an extremely slow process, however, and does not occur noticeably in crystals of the tetrahydrate but could well be faster at disrupted interfaces of crystals. The importance of this change is

the loss of water which, if it is not removed to the vapour phase, would remain to form a saturated solution.

A more complete account of the system containing metaborate reveals that very low eutectics occur and that a solid compound $\text{NaBO}_3 \cdot \text{NaBO}_2 \cdot 4\text{H}_2\text{O}$ is formed. Thus at 22°C and above a dry mixture of $\text{NaBO}_2 \cdot 4\text{H}_2\text{O}$ and $\text{NaBO}_3 \cdot 4\text{H}_2\text{O}$ could slowly form $\text{NaBO}_3 \cdot \text{NaBO}_2 \cdot 4\text{H}_2\text{O}$ and saturated solution if kept in an enclosed space, i.e. if no water vapour is allowed to escape. While the transformation in a mechanical mixture may be expected to be negligible it could be quite rapid when BO_3^- ions lose oxygen in a surface layer of the crystal and then give $\text{BO}_3^- \cdot \text{BO}_2^-$ ions in close proximity.

The explanation of signs of melting at 20.5°C - below van Gelders lowest eutectic must lie in the presence of extra water and in the closeness of the vapour pressure of the saturated solution and the equilibrium pressure above the hydrate mixtures.

Plainly there is ample justification for assuming that fusion occurs in a perborate mixture partly as a result of decomposition but also it is possible at an extremely slow rate even without decomposition due to the tetrahydrate - trihydrate transition. It would not of course occur if the water vapour pressure is kept just below that of the saturated solution.

A later section may be anticipated to mention that the stabilising action of Mg ions at the perborate crystal surface can be seen to be limited with the formation of an insoluble precipitate probably $Mg(BO_2 \cdot BO_3)$ which could remove any BO_2^- found and prevent its participation in eutectic liquefaction.

3. (ii) Decomposition of fused tetrahydrate.

The object of the study of the decomposition of fused perborate was to establish its main kinetic features and to obtain evidence on which to base a suggested mechanism both for the decomposition and for its inhibition, particularly by Mg.

It seemed reasonable in view of the conclusion of the first part of the work to conclude that these results would then apply to the observed decomposition of the 'solid' perborate.

The graph in fig.8 demonstrates quite clearly that the process is zero order in available oxygen during the majority of the decomposition.

Unfortunately available oxygen is not the only changing entity, for during this change from BO_3^- to BO_2^- ion in concentrated solutions the pH increase of 1.5 units has not to be overlooked. We shall discuss this below in connection

with more dilute solutions.

We may show here one consequence of the zero order decomposition. Addition of water Fig. 15, to a given sample of NaBO_3 increases the rate of loss of oxygen since it increases the volume in which the constant zero order process is operating. This observation gives rise to some difficulty if the decomposition is regarded as heterogeneously catalysed, since dilution would not be expected to increase, in proportion to the volume, the efficiency of the catalyst. This point will be returned to later.

The temperature coefficient of the zero order rate agrees with the temperature coefficient of the apparent solid process.. From $\log_{10} (\text{rate}) / \frac{1}{T}$ the Arrhenius calculation of energy of activation gives 19.0 Kg.cals. in the range 40, 50, 60, 70°C (See Fig 9). This supports the proposition that it is a fused perborate decomposition which is observed in the "solid" state process and that the solid takes no part in the decomposition either directly or by catalysing the liquid decomposition.

3. (iii) Catalysis in the fused state.

Neither Fe nor Cu catalysts additions substantially modifies the form of the decomposition process although both substantially increase its rate, Fe much more so than Cu. However, both show for the bulk of the decomposition a zero order process. Cu has the rather curious effect of appearing

to maintain the zero order process to a lower concentration of available oxygen than is found in the absence of added Cu or with Fe.

Fig. 12 gives some ground for the contentions that the decomposition of the perborate as proposed is wholly due to catalysis and not to an inherent decomposition of the pure NaBO_2 . Thus extrapolation of the linear rate of decomposition / [catalyst] graph to the "natural rate would predict a reasonable amount of both Fe and Cu. In fact traces of other impurities, e.g. Mn, Cr, may be sufficiently high to act as catalysts and to enhance the action of the traces of Fe and Cu actually present.

3. (iv) Stabilisation in the fused state.

Stabilisers are quite well known in peroxide technology. Organic substances which sequester potentially catalytic ions like Fe^{+++} have been used for many years as additives to less pure technical H_2O_2 solutions. Inorganic salts, particularly phosphates, have also been used for the same purpose. Their precise mode of action has not been the subject of a definite investigation until very recently by Wynne-Jones et al.⁹ who have shown that complex ion formation with the potential catalyst is effective here also. These peroxide stabilisers seem to act as catalyst poisons rather than as chain terminators in a peroxide chain. The inhibitory

action of metal ions other than the transition element ions has not been remarked upon to any great extent though it is known that Zn^{++} and Cd^{++} do partially inhibit the decomposition of pure H_2O_2 solutions in neutral or slightly alkaline solutions. No work is known which explains the action of these ions.

In the case of commercial preparations of crystalline perborate, Zn and Mg salt additives during manufacture are both known to effect stabilisation. As shown in Fig. 6, $MgSO_4 \cdot 7H_2O$, added during crystallisation of the tetrahydrate to the extent of 4% of the resulting crystal mass, produces a dramatic suppression of the "liquid phase" decomposition, though it does not eliminate the slower "prefusion" decomposition. The latter is, of course, extremely small.

Figs. 13 and 13a illustrate a surprising feature of the action of Mg^{++} in fused perborate. Thus the decomposition is slowed down only after an appreciable time - or after an appreciable amount of metaborate is formed (the effect could also be related to pH). After about 25% decomposition the decomposition with 2% $MgSO_4 \cdot 7H_2O$ present has been reduced to a negligible amount. With less Mg the fraction of decomposition required to reach a low or zero rate is greater. Of interest too is the result that onset of inhibition, (fig. 13a) with a given Mg addition, occurs at a fraction of decomposition

which can be related linearly to the $[\text{BO}_2^-]$ formed. Thus at the onset of inhibition the product $[\text{Mg}^{++}][\text{BO}_2^-]$ is a constant. In this expression the term $[\text{Mg}^{++}]$ is written for the concentration of added $\text{MgSO}_4 \cdot 7\text{H}_2\text{O}$.

The possibility that it is the pH which decides the onset of inhibition in the presence of added Mg^{++} cannot be completely rejected since there is in fact an increase in pH with decomposition, but the change is very small. Thus at onset of inhibition with 0.5% MgSO_4 the $[\text{OH}^-] = 4.2 \times 10^{-8}$ and for 2% it is 3.7×10^{-5} . We shall therefore set aside the pH as the decisive influence in controlling Mg inhibition.

4. Decomposition in dilute solutions.

Work in the dilute solutions was undertaken with the main purpose of investigating the mechanism of catalysis and inhibition. The overall kinetics are clearly similar in the whole range of concentrations from fused perborate to dilute solutions.

This is illustrated in the experiments to show the effect of water addition to fused perborate. In each case the decomposition is zero order in peroxide or available oxygen from high concentrations down to a value of about 0.15 M after which the rate falls off, passes through a range during which it is approximately first order and then below 0.04M becomes second order. The metaborate acts as an inert electrolyte. Furthermore since there is no evidence

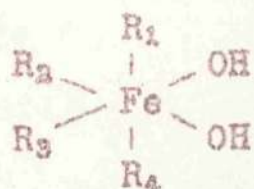
of any kinetic effect of the inert salt we may assume that there is no charge change involved in the formation of the transition state in the rate determining step in the kinetic scheme.

Added catalysts affect the form and rate of decomposition in dilute solution in the same way as in the fused liquid though the effects are more striking. Iron tends to bring to higher concentrations the onset of the non-zero order process, while copper addition maintains the zero order rate down to the lowest concentrations. We can use the result to support the hypothesis that decomposition in the "pure" perborate is in fact catalytic and due mainly to iron. Fig. 22 suggests this.

5. Mechanism of decomposition.

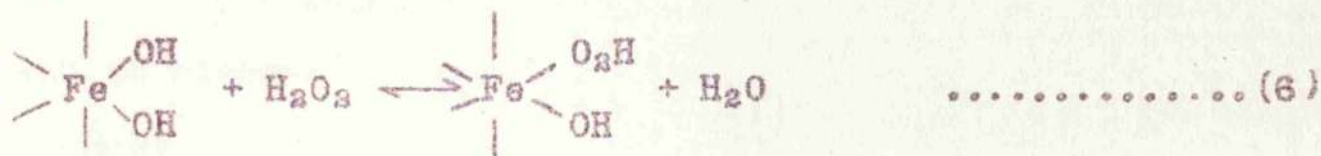
The kinetic form of the decomposition suggests a catalytic process involving a fixed concentration of a catalyst and the formation of addition compounds between the catalyst and the peroxide in which there are one or two equivalents of peroxide. Such a process is encountered in the action of catalase on H_2O_2 and is shown in Wynne-Jones¹⁰ recent work with ferric catalysed H_2O_2 decomposition in acid solutions. In the latter work the active species is the hydrated ion. In catalase (or in the synthetic complexes)

it is in the form

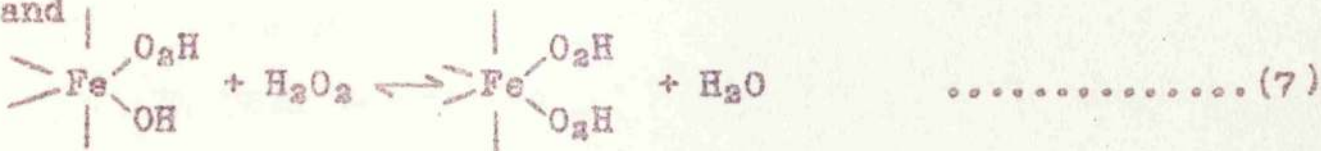


where R_1, R_2 etc. may be amines or part of a protein structure. In all these cases we regard the active essential as the $Fe(OH)_2$ group. In our case it may be the surface of a $Fe(OH)_3, Fe_2O_3,$ or hydrated ferric borate particles. The only essential is that it should be possible to exchange two - OH groups which are attached to the iron - and therefore within range of electron transfer - with H_2O_2 .

Thus



and



To explain the kinetics we need only assume that the total concentration of $\begin{array}{c} | \\ \diagup \\ Fe \\ \diagdown \\ | \end{array}$ remains constant - let it be 'a', and let the fraction of it which appears in the mono- and di-peroxy complex be f_1 and f_2 respectively. Now we must assume, to produce an equation which satisfies the observed form of the kinetics, that the decomposition process itself takes place in the di-peroxy complex by some process involving an electron transfer which is rendered favourable by the nature of the iron atom. Then the rate of decomposition will be:

$$r = kf_2a \dots\dots\dots (8)$$

and we may now relate f_2a to the $[H_2O_2]$, which we here denote as "c", from the equilibrium conditions applying to equations (6) and (7), viz:

$$K_1 = \frac{f_1a}{(1-f_1-f_2)ac} \dots\dots\dots (9)$$

$$K_2 = \frac{f_2a}{f_1ac} \dots\dots\dots (10)$$

from which is obtained

$$r = kf_2a = \frac{kK_1K_2ac^2}{1 + K_1c + K_1K_2c^2} \dots\dots\dots (11)$$

which gives in the limit, $1 \gg (K_1c + K_1K_2c^2)$, the second order process

$$r = kK_1K_2ac^2 \dots\dots\dots (12)$$

and at higher "c" where $K_1K_2c^2 \gg (1 + K_1c)$ the zero order process

$$r = kK_1K_2a \dots\dots\dots (13)$$

In both cases, for a given value of "c", $r \propto a$ as found accurately for the higher concentrations and approximately for the lower.

In the case of copper catalysis we may suppose a similar mechanism, but in this case the limit

$$K_1K_2c^2 \gg (1 + K_1c)$$

applies to much lower concentrations than in the case of iron. This would suggest a much higher value for K_2 for copper than for iron.

It should be noted that the small or even negligible effect of concentration salt solutions or pH on the rate of

decomposition excludes the possibility that (6) or (7) should be written in the form involving HO_2^- ions, thus:



From the results the constants are readily evaluated and an expression obtained which represents the results over the whole of the range of concentrations. Thus we obtain

$$k_a = 0.0505$$

$$K_1 = 1530$$

$$K_2 = 0.65.$$

It may be remarked at this point that it is somewhat surprising that borate has so little inhibiting action on iron and copper catalysts which seem as active on a p.p.m. basis in the presence of borate as in pure aqueous H_2O_2 solutions. It might have been expected that insoluble borate formation would have prevented that catalytic action. One may infer that even in any catalytic ion-borate compounds formed there are still exchangeable $-\text{OH}$ and $-\text{O}_2\text{H}$ groups which can lead to catalysis.

Mg inhibition must, from the evidence already referred to for the relation $[\text{Mg}^{++}][\text{BO}_2^-] = \text{constant}$, at onset of inhibition and from Fig. 26, and also from the observation that cloudiness and eventual precipitation occurs at during, but not before, inhibition, must be explained in terms of an insoluble salt $(\text{Mg})(\text{BO}_2)(\text{BO}_3)$. The expression for the relation between the ionic concentrations at precipitation,

6. General Conclusions.

In outlining the general principles of the decomposition of H_2O_2 in solutions containing borates (and in solid perborates) we may regard as strengthened the general theoretical interpretation applied to all H_2O_2 catalytic decompositions that rupture of the O-O bond is achieved via the formation of a diperoxy attachment to an ion capable of an electron exchange. The formation of this complex from solution at pH values not greater than 11 involves the undissociated H_2O_2 . This general conclusion seems equally valid for a dissolved ion as for a surface anchored ion in the form of a fragment of an oxide of a transition element, e.g. Cu_2O , Mn_2O_3 or indeed Ag_2O .

REFERENCES.PART II

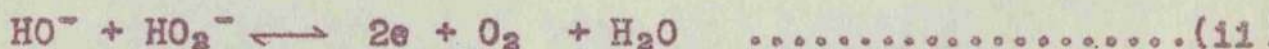
1. Partington and Fathallah, J. Chem. Soc., 1949, 3420.
2. Menzel, Z. anorg. Chem., 1927, 22, 164.
3. idem, Z. phys. Chem., 1923, 402, 105.
3. Kemp, "Chemistry of Borates", Part I, Borax Consolidated Ltd., London 1956.
4. Kemp, D.I.C. Dissertation, London, 1950.
5. Wells, Structural Inorganic Chemistry, Oxford 1945.
6. Carpēni, Bull. Soc. Chim., 1949, 16, 742.
7. Connor and Richards, J. Chem. Soc., 1958, 289.
8. Van Gelder, Rec. Trav. Chim., 1956, 75, 117.
9. Wynne-Jones, Tobe and Jones, Trans. Far Soc., 1959, 55, 91.
10. Wynne-Jones, Tobe, Kitching and Jones, ibid, 1959, 55, 79.

SUMMARY

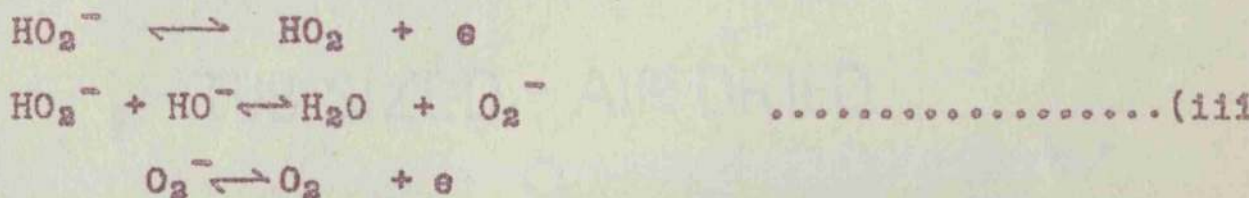
In Part I a detailed study is described of the electrode kinetics of a silver electrode in the presence of H_2O_2 solutions from 0.0003 to 33M and in the pH range 1-13. Special attention is paid to the equilibrium potentials and to their dependence on pH and $[H_2O_2]$. At high pH the results of Berl⁵³ for carbon electrodes are found to apply and the electrode potential is both pH and $[H_2O_2]$ dependent and is given by the equation:

$$E = 0.91 - 0.059 \text{ pH} - 0.03 \log_{10} [H_2O_2] \dots\dots\dots(1)$$

which, following Berl, is consistent with the following reversible electrode reaction



There is always catalysis even in the absence of current flow and this can be explained by breaking down equation (i) into 1-electron steps with HO_2 radicals as intermediates:



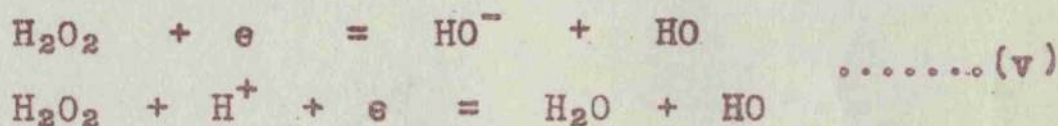
Reaction between HO_2 and H_2O_2 could produce decomposition cycles. At low pH (<6) the e.m.f. becomes independent of $[H_2O_2]$ and is then given by

$$E = 0.85 - 0.059 \text{ pH} \dots\dots\dots(1)$$

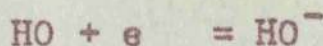
which is the result found by Bockris and Oldfield⁵⁴ for platinum and gold.

Other metals, viz., Cu, Ni, Mn and Fe give identical potentials and it is concluded that the metal plays no direct part in maintaining the steady potential.

A possible scheme is based on one put forward on a wide range of electrode kinetic evidence for platinum by Gerischer and Gerischer.⁵⁵ In the silver case it becomes



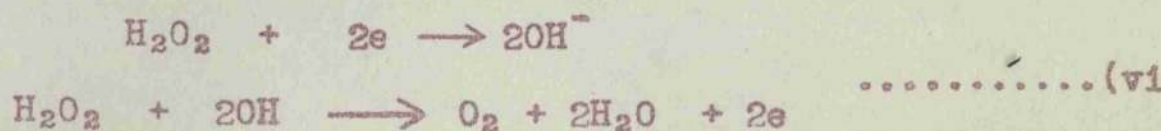
the HO radicals reacting further



or as centres for catalysis.

It is found that, at $[\text{H}_2\text{O}_2]$'s above 1 to 2 M and in the pH range 3-9, an $[\text{H}_2\text{O}_2]$ dependence occurs. This is explained in terms of a separation of anodic and cathodic areas. The anodic areas, once formed, are perpetuated by the fact that a p-n junction would be created at the metal metal oxide boundary and would permit current flow in one direction only. A proposal is made which on this basis links the potential in this zone to $[\text{H}_2\text{O}_2]$.

Experiments with flowing currents introduce the requirement that the anodic and cathodic reactions are 2-electron step processes involving 2 transition complexes per H_2O_2 molecule. Such a process would be written



and the transition complex would indicate that the rate determining step must involve an adsorbed OH radical or ion. Finally we show how these facts can be fitted in a general way to the Hoar⁷¹ scheme for the oxygen electrode. The scheme fits in also with a second order $[H_2O_2]$ dependence found for the rate of decomposition.

Part II describes a detailed account of the kinetics of the loss of oxygen from $NaBO_3 \cdot 4H_2O$ in the solid state, fused state and in dilution solutions, with and without added iron and copper catalysts, and also of the subsequent inhibition by magnesium and zinc compounds.

For the study of the first one per cent of loss of oxygen from the solid perborate a differential tensimetric technique was adopted.

Results obtained from decomposition of the solid perborate showed that a least partial liquefaction must occur before decomposition commences - heating the perborate at $60^\circ C$ in vacuo showed no loss of oxygen at all.

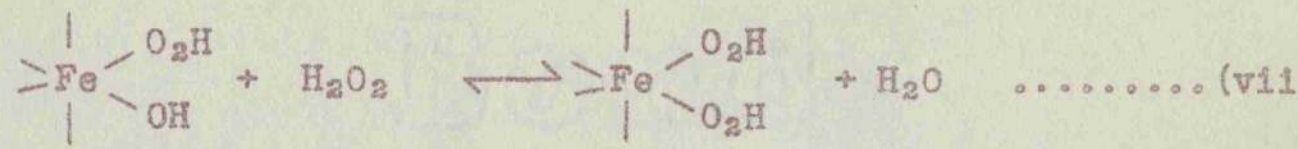
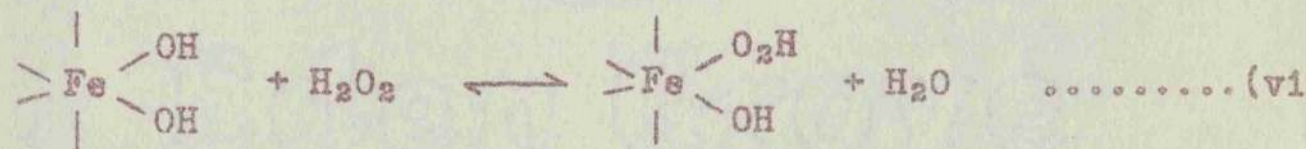
The results obtained from studies of the decomposition in the fused state indicated that the decomposition was entirely due to catalysis and that there was no inherent decomposition in pure perborate. This was confirmed from experiments on a few very pure perborate crystals.

Stabilisation of the fused material by the addition of

magnesium sulphate yielded a relationship with the $[BO_2']$ present, viz., at the onset of inhibition, the product $[Mg^{++}][BO_2'] = \text{constant}$.

Studies in dilute solutions showed clearly that the overall kinetics for the decomposition were identical with those for the fused state, and from the results it was concluded that the decomposition was indeed catalytic and due to iron.

The suggested mechanism which complied with the kinetics of the system studied is as follows.



i.e. a fixed concentration of catalyst forming addition compounds with H_2O_2 , the only essential being that it should be possible to exchange two-OH groups, attached to the iron, and therefore within range of electron transfer — with H_2O_2

From (vii) and (viii) we obtain $r = \frac{kK_2K_2c^2}{1 + K_1c + K_1K_2c^2}$

which gives in the limit $1 \gg (K_1c + K_1K_2c^2)$ second order kinetics and at higher $[H_2O_2]$ where $K_1K_2c^2 \gg (1 + K_1c)$ zero order kinetics apply. These equations agree exactly with the observed experimental results.

Stabilisation is explained in terms of the formation of an insoluble salt $(Mg)(BO_2)(BO_3)$ which both prevents formation of the liquid phase and, at the same time, inhibits the catalysts.

Consideration is also given as to the nature and structure of the metaborate and perborate ions.

been satisfactorily delineated and it was not necessary to measure potentials at the same time as rate of oxygen evolution.

The diagram of the simple apparatus employed is shown in Fig.2. The reaction vessel was immersed in a thermostatically controlled bath at $25^{\circ}\text{C} \pm 0.1^{\circ}$.

The reaction was carried out in a three necked round bottom quickfit flask, V, of 400 ml. capacity. One neck carried the gas funnel off-take which led to the gas measuring apparatus. Another neck incorporated a mercury seal through which a soda glass tube, with the silver catalyst sealed into it, could be inserted. The other neck was used either for stirring or for sweeping the vessel clear of air by passing N_2 through it.

To measure the changes in pressure due to evolved oxygen a gas burette was initially employed, but was found to be unsuitable for measuring small changes in volume over small periods of time. However, a soap film flow meter was found to be convenient for these measurements; it consisted of a calibrated glass tube, along which a soap film was propelled, the tube being attached to a glass mirror scale. The pressure difference across the film was very small and the resistance offered to the film by a clean wet tube was negligible. Hence the volume of gas measured by the film movement could be